Bioanalysis ZONE

Sponsored by

Waters™

Adapting to an evolving drug modality landscape

The need for versatility with performance in bioanalytical laboratories today

Taylor & Francis

Contents

Foreword

Over the past decade, the pharmaceutical industry has witnessed a notable evolution in drug development modalities. Advancements in technology have equipped pharmaceutical companies to efficiently introduce biologics like peptide and protein therapeutics, alongside synthetic oligonucleotides. Simultaneously, traditional small molecules have endured as a mainstay.

Technological progress, organic synthesis enhancements and biopharmaceutical research breakthroughs have paved the way for innovative small molecule drugs, such as proteolysis targeting chimeras (PROTACs) and disease-targeting molecular glues, advancing through discovery and early-stage development. Quantitative bioanalysis technologies are pivotal in new drug development, necessitating adaptation to the unique challenges presented by these diverse modalities. Laboratories must ensure efficiency and quality across multiple assays, demanding versatility in hardware, software, sample preparation and chromatography.

In this eBook, we explore how bioanalytical laboratories, involved from early to late-stage discovery and clinical trials, must remain adaptable to evolving analytical challenges posed by ever-expanding drug modalities.

We hope you enjoy this eBook!

Naamah Maundrell
Editor-in-Chief, Bioanalysis Zone
Naamah.Maundrell@tandf.co.uk

60 seconds with Alderley Analytical's CEO, Paul Holme: navigating the dynamic evolution of bioanalysis

Paul Holme
CEO, Alderley Analytical

Paul's career spans over 34 years, working in both discovery and regulatory environments in large pharma and CROs. Across his career he has gained in-depth knowledge in toxicology, human skin penetration, DMPK and bioanalysis. An experienced scientist and manager, Paul is recognized as a motivational leader and more recently an entrepreneur. Maximizing efficiency, productivity, building and managing high performing teams is something he thrives upon. Paul is now one of three co-founders running and growing their own bioanalytical CRO business supporting clients with their bioanalytical project needs.

A career commencing in toxicology and DMPK studies at ICI (Cheshire, UK) in 1989, Paul later joined AstraZeneca (Cheshire, UK) in 2003, rising to the role of Associate Director of the Regulatory Bioanalysis Unit at Alderley Park. In this position, he led global change to harmonize the bioanalytical services across seven worldwide sites, helping shape AstraZeneca's future bioanalytical strategies. In 2012 Paul gained valuable insight into running a small company where he worked in a management position at a small CRO specializing in human dermal penetration services. In 2014, together with three co-founders a gap in the provision of bioanalytical services to small to mid-sized biotech's was identified and from here Alderley Analytical Limited (Macclesfield, UK) was born. In 2021, Paul became CEO with the goal of establishing Alderley Analytical as a leading provider of bioanalytical services for small to mid-sized biotech's globally. The company has successfully achieved this, sustaining double-digit growth annually, employing over 60 staff and providing services to 200 clients across diverse drug therapies around the world.

Paul holds an honours degree from Manchester Metropolitan University (UK), a Prince II Practitioner certification and is a recognized Member of the Research Quality Association (MRQA) due to extensive experience in GLP and GCP regulated departments.

How has bioanalysis evolved in your laboratory over the last 10 years?

> The bioanalytical needs of industry over the past 10 years have constantly changed and this has led to many challenges for our company, therefore it has been critical for Alderley Analytical to evolve and pivot the strategy along the way. When we opened in 2014, the primary need for our clients was small molecule analysis with a handful of peptides, and typically the levels needed to be quantified were >1ng/mL. The studies we supported were smaller, typically 100–800 samples and for these projects we only needed a couple of standard LC–MS/MS instruments, the odd centrifuge, mixer, evaporator and a few pipettes. Our raw data was paper, and at the time, there was no need for specialized LIMS systems or robotics.

Waters™

However, as the landscape changed so did the types of analyzed molecules. Peptides requiring levels down to single digit pg levels became common and the request to analyze proteins, oligonucleotides or a variety of biomarkers became frequent. The regulatory environment, specifically around data integrity became tighter and naturally, the larger clients and the larger studies started to flow into the laboratory with sample numbers up to 10,000. All of this required us to expand our strategy and evolve.

To support all of the above, new mass spectrometry technology was purchased, LIMS was implemented and raw data was migrated from paper to electronic format. Robotics were implemented into the laboratory and by recruiting identified skill gaps, immunoassay services at Alderley Analytical was born, allowing us to provide a wider service offering to our clients and the wider industry.

What are the most significant high-level challenges presented for bioanalytical laboratories, within CROs, and how do Alderley Analytical successfully overcome these today?

As a CRO the biggest challenge is to make a profit while controlling our costs and meeting the needs of our clients in three key areas of scheduling, science and quality. In this industry we have always strived to do things faster, cheaper and better while delivering the best science and this is only achievable if you get your processes right with these three areas:

Scheduling: Scheduling is an ongoing game of tetris for our LC–MS/MS departments. As the cost of the technology we use is very high, we need to keep those instruments busy all of the time with quick methods, while keeping some contingency for breakdowns! Aligning the use of the instruments with our clients' needs is complicated as their needs can be fluid, especially when working in the clinical environment where study timelines change with short notice and the need for fast turnaround results are necessary. It's very hard to get a long-term line of site for when all our contracted clinical trial analysis will start and sometimes the inevitable clash will occur, this is when we rely on the flexibility of our team of scientists to work out of normal working hours to deliver. Building the number of resources available obviously provides greater flexibility along with bolt on technology like column switching and batch plate hotels to allow many different methodologies and more plates to be run in an overnight period. The development of quick robust methods is also key when possible to do so. A key investment for Alderley Analytical was the Waters ACQUITY Premier UPLC systems used alongside their Premier UPLC columns. These systems remove the need for long passivation periods needed for certain oligonucleotide analysis allowing more flexible use of those systems.

Waters™

Science: Good science is critical to success. We need to develop solid robust methods that validate well and minimize batch failures during sample analysis. It is critical to use the best technology to allow us to achieve this goal. As mentioned above, the purchase of the Waters TQ Absolute LC–MS/MS instruments with ACQUITY Premier UPLC Systems has been a game changer to improve assay robustness. Good science also comes from the knowledge and expertise of our staff and without doubt the biggest challenge we are facing is the recruitment of experienced bioanalytical scientists. Historically, we had big pharma with lots of internal bioanalytical scientists working for them, many of whom would eventually end up in senior positions in the large CRO's where they would mentor the less experienced scientists. The number of experts on the market open to recruitment seems to have dropped, meaning the only way forward is to recruit less experienced individuals and train from within.

While this process does work it can take many years for staff to build all the knowledge and experience needed to become an expert. Alderley Analytical is developing its own internal training program and has started a degree apprenticeship scheme to hopefully create the experts of the future.

Quality: This is linked to performing good science, but human error does and will always occur. While process can be implemented to minimize mistakes, we can also use technology. The wider use of LIMS is now being adopted at Alderley Analytical and we are in the process of looking to minimize human error by using the Waters Andrew+ robotics systems to perform key steps of our bioanalytical assays to reduce mistakes and analyst-to-analyst variation. Future e-notebooks options are also in the planning. Our team of quality professionals is growing to ensure that we have a good quality oversight for all our studies, procedures and processes and that we maintain our regulatory compliance and meet the needs of the guidelines we adhere to.

Could you share the analytical challenges presented across the specific modality types of small molecules, peptides and oligonucleotides and how Alderley Analytical have overcome these challenges?

The main challenge we have with many projects relating to small molecules, peptides and oligonucleotides is the 'sticky' nature of the molecules; non-specific binding (NSB). This can be a barrier to achieving the required LLOQ and can make the assays longer due to extensive injector and column washes that are sometimes required. Assays do not perform well if we do not control these NSB issues, these can be controlled by using good science and the correct consumables and technology. Specific low-bind tubes and plates can be purchased, the Waters Premier UPLC columns typically a good choice and again the ACQUITY Premier UPLC systems provide benefit. We are lucky that our technology suppliers understand the challenges and provide an array of solutions to help.

What do you expect to see in the coming years in terms of requirements in bioanalysis and how will your teams and laboratories prepare for this?

As a company we tend to pivot our strategy depending on the inward requests and also the make-up of our client pipelines. We have recently seen an increase in the oligonucleotide pipelines and have now tooled up to provide expert support in this area by bringing in the most suitable technology and experts. We have also seen an upward trend in the need for immunoassay techniques whether that is for developing stand-alone immunoassays or for sample clean-up prior to LC–MS/MS of protein-based molecules, again we have ensured we have the best tools. We keep a close eye on the industry trends and new molecule types like PROTACs or molecular glue technologies and if we see or feel there is a growing demand there, we will then focus our purchasing and recruitment strategy appropriately.

What other considerations are there for bioanalytical laboratories today and in the future?

When we bring new clients, on-board there is a process to go through called a request for information (RFI). They check we have the correct infrastructure in terms of expertise, technology and quality standards but we are now seeing additional requirements in terms of sustainability and environmental policies. While recycling is a given these days we now also have to consider green credentials of our purchasing strategy and our clients expect this. We have to establish that our consumable and technology suppliers have the correct sustainability and environmental policies of their own but also for the technology we need to purchase, being mindful of how the purchase will impact our own policies and the environment. The purchase of our WATERS TQ Absolute LC–MS/MS instruments was based not only on the technology advantages but also on the systems green credentials. These systems use less energy to run and have a lower heat output than other systems, which in turn leads to lower cooling needs of the laboratory and a lower company energy usage. We have a suite of -80oC freezers, which use an incredible amount of energy to run, we are now looking at alternative lower energy freezers for future use. These considerations will certainly drive the direction of our future purchasing decisions.

Xenobiotica
the fate of foreign compounds in biological systems

ISSN: (Print) (Online) Journal homepage: www.tandfonline.com/journals/ixen20

Investigation of the pharmacokinetics and metabolic fate of Fasiglifam (TAK-875) in male and female rats following oral and intravenous administration

Billy J. Molloy, Adam King, Lee A. Gethings, Robert S. Plumb, Russell J. Mortishire-Smith & Ian D. Wilson

To cite this article: Billy J. Molloy, Adam King, Lee A. Gethings, Robert S. Plumb, Russell J. Mortishire-Smith & Ian D. Wilson (2023) Investigation of the pharmacokinetics and metabolic fate of Fasiglifam (TAK-875) in male and female rats following oral and intravenous administration, Xenobiotica, 53:2, 93-105, DOI: 10.1080/00498254.2023.2179952

To link to this article: https://doi.org/10.1080/00498254.2023.2179952

XENOBIOTICA
2023, VOL. 53, NO. 2, 93–105
https://doi.org/10.1080/00498254.2023.2179952

Taylor & Francis
Taylor & Francis Group

RESEARCH ARTICLE

OPEN ACCESS Check for updates

Investigation of the pharmacokinetics and metabolic fate of Fasiglifam (TAK-875) in male and female rats following oral and intravenous administration

Billy J. Molloy[a], Adam King[a], Lee A. Gethings[a], Robert S. Plumb[b], Russell J. Mortishire-Smith[a] and Ian D. Wilson[c]

[a]Waters Corporation, Wilmslow, UK; [b]Waters Corporation, Milford, MA, USA; [c]Division of Systems Medicine, Department of Metabolism, Digestion and Reproduction, Imperial College, London, UK

ABSTRACT

1. The metabolism and pharmacokinetics of fasiglifam (TAK-875, 2-[(3*S*)-6-[[3-[2,6-dimethyl-4-(3-methylsulfonylpropoxy)phenyl]phenyl]methoxy]-2,3-dihydro-1-benzofuran-3-yl]acetic acid), a selective free fatty acid receptor 1 (FFAR1)/GPR40 agonist, were studied following intravenous (5 mg/kg) and oral administration (10 and 50 mg/kg) to male and female Sprague Dawley rats.
2. Following intravenous dosing at 5 mg/kg, peak observed plasma concentrations of 8.8/9.2 μg/ml were seen in male and female rats respectively.
3. Following oral dosing, peak plasma concentrations at 1 h of ca. 12.4/12.9 μg/ml for 10 mg/kg and 76.2/83.7 μg/ml for 50 mg/kg doses were obtained for male and female rats respectively. Drug concentrations then declined in the plasma of both sexes with $t_{1/2}$'s of 12.4 (male) and 11.2 h (female). Oral bioavailability was estimated to be 85-120% in males and females at both dose levels.
4. Urinary excretion was low, but in a significant sex-related difference, female rats eliminated ca. 10-fold more drug-related material by this route.
5. Fasiglifam was the principal drug-related compound in plasma, with 15 metabolites, including the acyl glucuronide, also detected. In addition to previously identified metabolites, a novel biotransformation, that produced a side-chain shortened metabolite via elimination of CH_2 from the acetyl side chain was noted with implications for drug toxicity.

ARTICLE HISTORY
Received 8 December 2022
Revised 9 February 2023
Accepted 9 February 2023

KEYWORDS
Fasiglifam; pharmacokinetics; metabolite profiling; novel metabolites; oxidative decarboxylaton; sex differences

Introduction

Fasiglifam (TAK-875, 2-[(3*S*)-6-[[3-[2,6-dimethyl-4-(3-methylsulfonylpropoxy)phenyl]phenyl] -methoxy]-2,3-dihydro-1-benzofuran-3-yl]acetic acid, Figure 1) was designed as a selective free fatty acid receptor 1 (FFAR1)/GPR40 agonist for use in the treatment of diabetes (Kaku 2013). However, it was withdrawn from late stage development due to hepatotoxicity (Kaku et al. 2015, 2016). Previous studies in the rat have shown that fasiglifam was well absorbed after PO dosing, with good bioavailability following which drug and metabolites were then excreted mainly *via* the faeces following biliary elimination (Kogame et al. 2019a, 2019b). In the rat the observed biotransformations involved formation of the acyl glucuronide (fasiglifam-G) as the major metabolite of fasiglifam, together with smaller quantities of the taurine conjugate. Fasiglifam and these 2 conjugates formed the majority of the drug-related material in rat bile (accounting for 46.3, 27.0 and 6.7% of the dose respectively) (Kogame et al. 2019a). Indeed, acyl glucuronidation was found to be the predominant elimination pathway for fasiglifam, not only in the rat but in all species tested, including humans (Kogame et al. 2019a).

With respect to the circulation of drug-related material, fasiglifam itself formed the major component in the plasma of all species. A minor oxidative cleavage metabolite (M-I) was observed in both rat and human plasma (<10% of plasma radioactivity). In human plasma, hydroxylated fasiglifam (T-1676427), fasiglifam-G, and the glucuronide of M-I were also detected as additional minor metabolites (<2% of plasma radioactivity) (Kogame et al. 2019a). Fasiglifam and its acyl glucuronide were shown to be substrates of BCRP and Mrp2/MRP2 in the same study, respectively (Kogame et al. 2019a).

Here, we describe studies on fasiglifam following administration to male and female rats at doses of 5 mg/kg IV and 10 or 50 mg/kg PO. The study was designed in part to investigate the use of microsampling and rapid UHPLC analysis,

CONTACT Ian D. Wilson i.wilson@imperial.ac.uk Division of Systems Medicine, Department of Metabolism, Digestion and Reproduction, Imperial College, London, UK

Supplemental data for this article can be accessed online at https://doi.org/10.1080/00498254.2023.2179952.

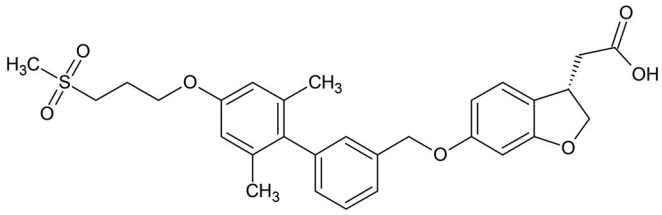

Figure 1. Fasiglifam (TAK-875), a GPR40 agonist withdrawn from phase III trials after the observation of elevated liver enzymes.

coupled with advanced MS and ion mobility (IM), to provide comprehensive pharmacokinetic and metabolic profiles on target compounds. However, we also hope that the use of both these and, subsequently, 'omic' tools might cast further light on the biochemical effects of fasiglifam.

Materials and methods

Solvents and chemicals

Solvents (LC/MS grade water, acetonitrile (ACN) 0.1% formic acid (FA) in water and 0.1% formic acid in ACN) and ammonium acetate were obtained from Sigma Aldrich (Dorset, UK). Instrument calibration used the 'Waters Major Mix IMS/ToF Calibration Kit for IMS' (Waters Corp., Milford, USA). Leucine-enkephalin (Sigma Aldrich) was used to provide a lockmass for mass spectrometry (MS). Fasiglifam was purchased from Cambridge Isotopes (Cambridge, UK).

Study conduct

The study was performed using 15 male and 9 female Sprague Dawley rats, 7 weeks of age and weighing between 170.3 and 260.5 g (Janvier Laboratories, Toulouse, France) with animals housed at the Evotec France SAS animal facility. The rats were housed, by group, for an acclimatisation period (3 days, $n = 2$ per cage) and then individually in metabowls for the 96 h of the study. The Evotec facility is accredited by both the French Ministry of Agriculture (D 31 555 09) and the Association for Assessment and Accreditation of Laboratory Animal Care International (AAALAC# 001433). This study complied with the corresponding project APAFIS#04.932.02 and was reviewed by the Evotec France Ethical Committee (identified below as CEPAL: CE 029) and authorised by the French Ministry of Education, Advanced Studies and Research prior to commenncement. In addition, the study was reviewed by the SBEA (internal Animal Welfare Body) (Evotec, Tolouse, France). The doses and formulations used for both oral (PO) and intravenous (IV) administration were based on those previously used by Kogame et al. (2019a).

Intravenous administration of fasiglifam (5 mg/kg)

For IV administration fasiglifam was formulated as a clear and colourless solution in N-methyl-2-pyrrolidone (NMP)/50 mM phosphate buffer (pH 7.4), 10:90 v/v at 1.0 mg/mL and administered (5 mL/kg), *via* the tail vein, to 3 male and 3 female Sprague Dawley rats as a single 5 mg/kg (1 mg/mL, 10 mL/kg) dose. A further 3 male rats were administered the drug-free vehicle as a control group.

Rats were housed individually in metabowls for the collection of urine and faeces. Blood samples were obtained at pre-dose, 1, 3, 6, 12, 24, 48 and 96 h post-dose. At each time point 100 μL of blood was collected (2×50 μL) from the *saphenous* vein into Minivette POCT K2-EDTA coated capillaries. At the terminal point (96 h post-dose) an additional 0.5 mL of blood was collected by exsanguination *via* the *vena cava*. Plasma was then prepared from the blood, which was transferred into 1.5 ml microcentrifuge tubes for centrifugation at 8,000 g (3 min, 4 °C). Aliquots of the resulting plasma (up to 40 μL/sample) were transferred to a 96-well plate and an equivalent volume of 0.5 M ammonium formate buffer, pH 3.0 (30%, v/v) was added to each well to stabilise acyl glucuronides. The 96 well plates were stored at −80 °C until shipment and analysis.

In addition to blood, urine was collected predose (overnight before dosing) and over the periods 0–24, 24–48 and 48–96 h post-administration. Samples (both IV and PO routes) were transferred from the study site to Waters Corp., (Wilmslow, UK) on solid carbon dioxide. All samples were stored on receipt at −80°C until analysis as described below.

Oral (PO) administration of Fasiglifam

For PO administration 15 rats were randomly allocated into two treatment groups and dosed orally by gavage at either 10 or 50 mg/kg ($n = 3$ males and 3 females per dose level) with fasiglifam as a suspension in methylcellulose/water (0.5/99.5 w/v) or with drug-free vehicle in the control group (3 males). Fasiglifam was formulated as 5 or 10 mg/mL suspensions (depending upon the dose) and administered at 10 mL/kg. Blood, urine and faeces sampling and storage were as for the IV route.

Sample preparation for the bioanalysis of Fasiglifam in rat plasma

Rat plasma samples (10 μL) were prepared for analysis by precipitating protein with 40 μL of ACN, vortex mixing and centrifugation 25,000 g for 5 min. The supernatant was diluted 1:100 v/v with 25% ACN. An external calibration curve, prepared in drug-free control rat plasma, over the range 0 to 10,000 ng/mL and comprising a solvent blank (1:3 v/v ACN:H_2O) a blank (extracted matrix blank) and 7 concentrations of fasiglifam (0, 10, 50, 100, 500, 2000, 5000 and 10,000 ng/mL). Quality control (QC) samples containing fasiglifam were prepared with concentrations of 25, 2000 and 8000 ng/mL. Samples were analysed in the following order; solvent blank; blank; QCs (25, 2000, 8000 ng/mL); blank; calibration curve (0, 10, 50, 100, 500, 2000, 5000 and 10,000 ng/mL) samples; blank; extracted plasma samples; blank; calibration curve (0, 10, 50, 100, 500, 2000, 5000 and 10,000 ng/mL); matrix blank; QCs (25, 2000, 8000 ng/ml); blank. To be accepted, the batch QC samples had to be

within ±15% of the nominal value with a minimum of 2/3 achieving this, and with no more than one failure at each concentration.

Urine analysis

Urine samples were analysed for fasiglifam using the same sample preparation approach as that employed for the analysis of plasma. Urine calibration curves and QCs were prepared in control rat urine produced by the pooling of urine from the vehicle-only samples. A standard calibration line was prepared at concentrations of 0, 0.1, 0.5, 1, 5, 10, 50 and 100 ng/mL with QCs made at 2, 40 and 80 ng/mL.

In some cases where the measured concentrations in the samples were found to be above the ULOQ (the top standard in the calibration curve) re-analysis was performed following a 1:10 dilution with control urine and using a new calibration line and QC's.

U(H)PLC/MS/MS Sample analysis for fasiglifam determination

Plasma extracts (10 μL) and urine were analysed using an ACQUITY™ UPLC™ I-Class System connected to a Xevo™ TQ-S Micro tandem quadrupole mass spectrometer (Waters Corp., Wilmslow, UK). UPLC used a 2.1 × 50 mm BEH™ C18 1.7 μm column (Waters Corp, Milford, USA) maintained at 60 °C at a flow rate of 500 μL/min. A linear reversed-phase (RP) solvent gradient, formed from 0.1% FA (v/v) in 10 mM aqueous ammonium formate (solvent A) and 0.1% FA (v/v) in ACN (solvent B) was used for analysis. The gradient composition ranged from from 50 to 60% solvent B over 0.9 min and was followed by a column flush using 95% solvent B for 1 min, and then re-equilibration for 0.6 min prior to the next injection. MS analysis was performed at unit mass resolution using positive electrospray ionisation (+ve ESI) at a capillary voltage of 2.2 kV, and a source temperature of 150 °C. The cone gas flow was 50 L/h and the gas used was nitrogen. The desolvation gas temperature was 650 °C, the desolvation gas flow was 1000 L/h. The data were collected using MassLynx™ V 4.1 (Waters Corp., Milford, USA). MRM (Multiple Reaction Monitoring) transitions were monitored for the MS quantification and confirmation of fasiglifam using various collision energies (CE) and cone voltages (CV) as indicated in brackets after the monitored transition. For the quantification of fasiglifam *m/z* 525.14 > 121.0 (CV = 60 V, CE = 33 eV) was used whilst the ions m/z 525.14 > 331.1 (CV = 60 V, CE = 18 eV) and 525.14 > 465.1 (CV = 60 V, CE = 8 eV) were used for the confirmation of peak identity.

Metabolite profiling and identification of fasiglifam metabolites in plasma

Samples for metabolite detection and identification were prepared by pooling equal amounts (2 μL/sample) for both the PO and IV routes from all of the samples from 1–96 h post dose for each route of administration. These samples were then mixed with 4 volumes of ACN to precipitate plasma proteins. After vortex mixing and centrifugation at 25000 g for 5 mins, 10 μL of the resulting supernatants were diluted to 500 μL with 490 μL of 1:1 v/v ACN:H_2O to provide a sample suitable for analysis. The extracted rat plasma samples were analysed using reversed-phase (RP) liquid chromatography using an ACQUITY UPLC I-Class System connected to a SELECT SERIES™ Cyclic™ IMS/MS (Waters Corp., Wilmslow, UK) (Giles et al. 2019) operating in single pass, resolution (V optics) mode. Briefly, a 2 μL aliquot of the sample was loaded onto a 2.1 × 100 mm ACQUITY™ HSS T3 1.7 μm C18 column (Waters Corp., Milford, USA). The column was maintained at 40 °C and eluted with a linear solvent gradient of 40–70% 0.1% aqueous formic acid: acetonitrile over 10 min at a flow rate of 600 μL/min.

IM and MS data were collected in both positive and negative electrospray ionisation (ESI) modes. The capillary voltage was 3.0 kV (ESI+) or 2.0 kV (ESI-), cone voltage was 25 V, source temperature was set at 120 °C with a cone gas (nitrogen) flow rate of 50 L/h, desolvation gas (nitrogen) temperature of 600 °C and nebulisation gas (nitrogen) flow of 800 L/h. Ion mobility settings for a single pass consisted of cIM pressure at 2.3 mbar (nitrogen), IM travelling wave height at 35 V and constant velocity of 375 m/s. Following ionisation the ions were passed into the ion mobility cell. The helium cell (situated at the front of the drift cell) gas flow was fixed at 180 mL/min, and the IMS gas was nitrogen with a flow fixed at 90 mL/min. A wave velocity of 650 m/s, with a wave height of 40 V, an EDC delay coefficient of 1.54 V, a bias of 3, a mobility RF offset of 250, an RF offset of 300 V, an IMS wave delay of 1000 μs and a DC entrance of 20 V were applied. The IMS device was calibrated using the Waters Major Mix IMS/ToF Calibration Kit for IMS over the CCS range = 130–306 $Å^2$ to allow for CCS values to be determined in nitrogen. Following IM separation, the ions were subjected to MS^E data acquisition over the *m/z* range 50–1200. Continuum mode was used for the experiment with a low collision energy of 20 eV and a collision energy ramp from 20–40 eV. Leucine encephalin (MW = 55.62771 (ESI+): 554.2615 (ESI-) was used as a lock mass with a scan collected every 30 s and a cone voltage fixed at 40 V. cIM-MS data were collected using a web-based user interface which is based on existing MassLynx Software (Waters Corp., Wilmslow, UK).

Metabolite profiling and identification for fasiglifam metabolites in urine

Reversed-phase profiling of urine for fasiglifam and its metabolites was performed using 20 μL of individual urine samples to which 20 μL of LCMS grade water was added (in 1.5 mL centrifuge tubes). A further 350 μL of LCMS grade ACN was then added to each sample, with vortex mixing. After 10 min (at 2–8 °C) the mixture was centrifuged (13,000 rcf, 10 min.) and 100 μL of the supernatant was further diluted 1:1 with LCMS grade water to increase the aqueous composition of the sample prior to RP-U(H)PLC/MS analysis.

Pharmacokinetic analysis

Basic, non-compartmental pharmacokinetic analysis was performed using the freeware program PKSolver (Zhang et al. 2010) to calculate $T_{1/2}$, AUC, oral bioavailability, volume of distribution, etc. (All of the individual plasma concentration data used for calculating these properties are provided in Supplementary Tables S3–S8).

Data analysis for drug metabolite identification

UHPLC-MS data were imported into waters_connect™ (Waters, Wilmslow UK) and processed using UNIFI™ 1.9.13 (Waters, Wilmslow UK). Fasiglifam and its metabolites were identified using an IMS-enabled pathway profiling method. Previously reported metabolite structures were included for targeted analysis, and a virtual library of putative metabolite structures was generated by combining likely cleavages with standard phase functionalisation and conjugation biotransformations (Mortishire-Smith et al. 2009). Potential matches were evaluated for drug-related likelihood on the basis of a variety of mass spectral features including whether or not they had product ions or neutral losses in common with the parent drug. This could be explained by a combination of likely biotransformations, which were inside plausible mass defect space (Mortishire-Smith et al. 2009), and had substantially higher intensity in analyte samples compared with control samples. Assignment of metabolite identities and tracking of each metabolite across samples was achieved on the basis of retention time, *m/z* and CCS values.

Results and discussion

Clinical observations

No adverse reactions were observed following IV (5 mg/kg) or PO (10 & 50 mg/kg) administration of fasiglifam (TAK-875) in this study.

Drug and metabolite bioanalysis

Several methods for the determination of fasiglifam concentrations in plasma have been described (e.g. Kogame et al. 2019 a, 2019b; Naik et al. 2012). Here the bioanalysis of fasiglifam in the plasma of male and female rats administered with the drug by either IV or PO routes was undertaken using a rapid UHPLC-MS/MS method. Plasma concentrations of fasiglifam were obtained using a 'fit for purpose' assay using 10 μL samples. In the absence of a suitable stable isotopically labelled internal standard being available fasiglifam was quantified *via* an external calibration curve using the drug itself in control rat plasma. The method, involving simple protein precipitation and dilution with water, produced a linear response in rat plasma ($r^2 = 0.9994$) over the concentration range of 10–10,000 ng/mL (using 1/x weighting). Whilst fasiglifam was undetectable in plasma samples from the vehicle-dosed controls, or predose samples, it was quantifiable over the entire 96 h of the study in both male and female rats following either IV or PO administration. All of the QC samples used to monitor the assay were within the acceptance criteria of ±15% of their nominal values.

Pharmacokinetic analysis

Following IV administration of fasiglifam at 5 mg/kg plasma concentrations, as determined by UHPLC/MS/MS, peaked at 8.8 ± 0.9 μg/mL (male) and 9.2 ± 1.2 μg/mL (female) then declined bi-exponentially in both male and female animals with an estimated clearance of 1.7−1.4 L/h. The volume of distribution at steady-state was calculated as 542 and 528 mL/kg and the terminal half-life was 12.4 h for male and 11.2 h for female rats respectively. There was also evidence of a transient increase in plasma concentrations at 24 h However, all animals were very similar in profile, and both sexes gave similar PK data. By 96 h most of the fasiglifam had been eliminated from the plasma with concentrations of less than 20 ng/mL.

The maximum observed plasma concentrations of fasiglifam after PO dosing at 10 mg/kg were 12.4 ± 2.6 and 12.9 ± 3.5 μg/ml for male and female animals respectively and were reached 1 h after administration. Following PO administration at the higher dose of 50 mg/kg the maximum observed mean plasma concentrations were 76.2 ± 3.7 and 83.7 ± 13.2 μg/ml for the male and female rats respectively and, as seen for the 10 mg/kg dose, these were achieved at 1 h postdose (Tables S3–S8). Bioavailability was estimated at between 85–120% for male animals and 91–108% for female animals (using AUC-t). Estimations of the oral half-life of fasiglifam in the rat were 11.1 h for males and 11.6 h for females at the 10 mg/kg dose and 10.3 and 9.8 h for male and female rats respectively for the 50 mg/kg dose. A slight increase in the fasiglifam plasma concentrations was noted at the 24 h post-dose time point in male and female animals at the 10 mg/kg dose and this phenomenon was also observed at 24 h and 48 h after administration of the 50 mg/kg dose to male and females animals respectively. While several phenomena may be responsible for this, the most likely of which is entero-hepatic circulation, perhaps following hydrolysis of the acyl glucuronide, which is known to be excreted as the major fasiglifam metabolite in rat bile (Kogame et al. 2019a), further studies would be required to determine the cause of this effect, and care should be exercised not to over-interpret this observation.

The results for the plasma pharmacokinetics are summarised in Table 1, and illustrated in Figure 2 for the 50 mg/kg dose for both male and female rats (profiles for the 5.0 mg/kg IV and 10 mg/kg PO doses are provided in Figures S1 and S2, respectively).

Urine analysis

As described in the experimental section, urine samples, were collected predose, 0–24, 24–48, and 48–96 h after administration of fasiglifam and were subsequently analysed using the same method employed for plasma analysis. The resulting data are summarised in Table 2. For both male and female-derived samples the highest quantities of fasiglifam

Table 1. Mean Summary Plasma Pharmacokinetic Data for Male and Female Rats following the administration of Fasiglifam at 5 (IV) 10 and 50 (PO) mg/kg.

	Units	5mg/kg IV Male	5mg/kg IV Female	10m/kg Oral Male	10mg/kg Oral Female	50mg/kg Oral Male	50mg/kg Oral Female
T max_obs	h	1	1	1	1	1	1
C max	(μg/mL)	8.8	9.2	12.4	12.9	76.2	83.7
Vd	L	0.56	0.47	0.61	0.67	0.56	0.53
t 1/2	Hr	12.4	11.2	11.1	11.6	10.3	9.8
Cl	L/hr	1.70	1.40	1.71	1.51	1.14	0.83
AUC 0-96 h	mg/ml*h	0.10	0.11	0.17	0.20	1199	1189
Vd (derived)	mL/kg	542.4	528.3	326.8	359.4	68.5	88.9
Oral bioavailability (%)	F	–	–	85.0	90.9	119.9	108.1

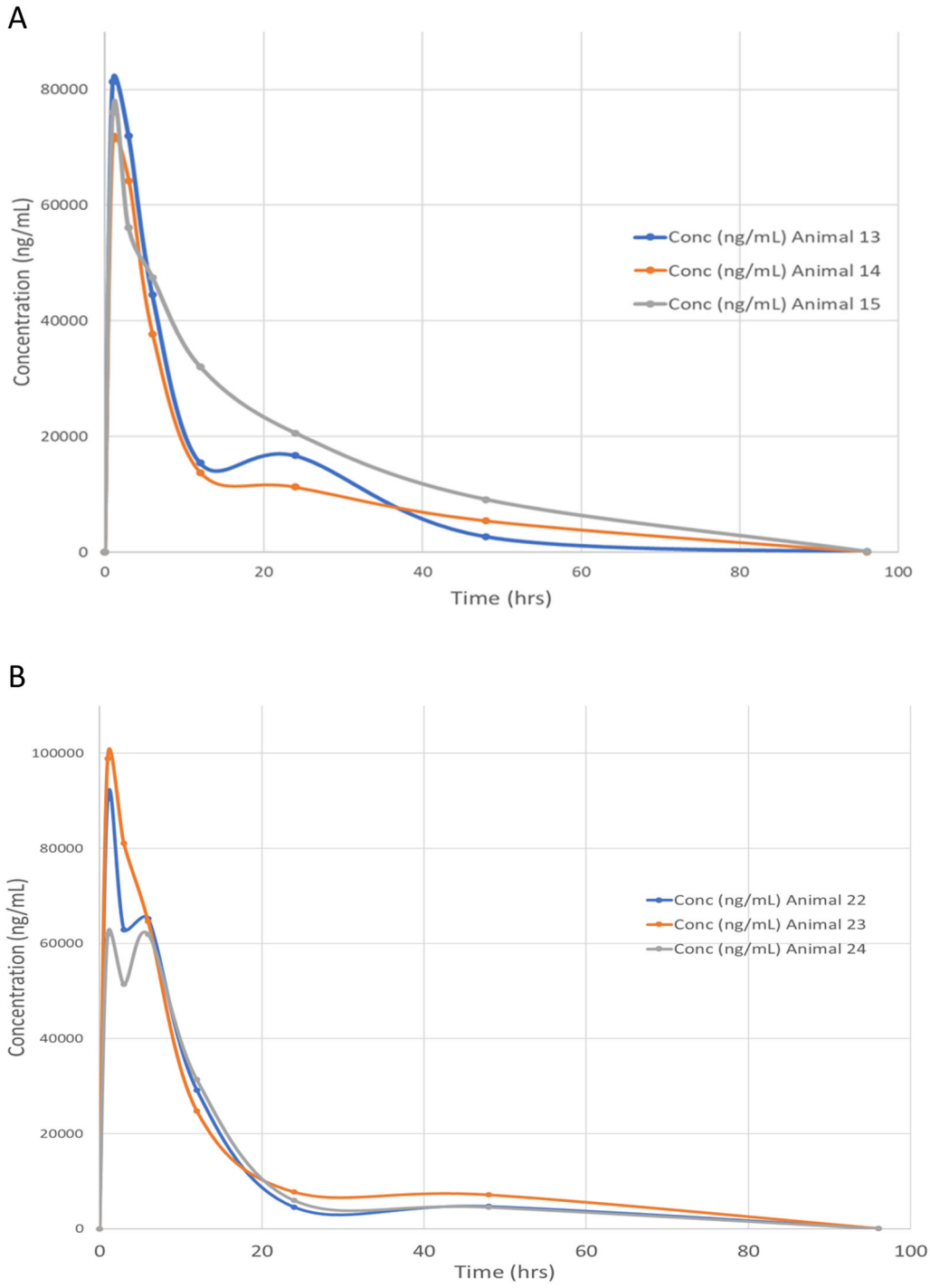

Figure 2. Plasma concentration vs time profiles (0–96 h) for fasiglifam dosed orally at 50 mg/kg to A) male and B) female rats respectively.

Table 2. Mean Fasiglifam Urinary Excretion Following IV and PO dosing at 5 mg/kg, 10 mg/kg, 50 mg/kg at Predose, 0–24, 24–48 and 48–96hr Post-Administration.

	Mean Fasiglifam Total Amounts in Urine (μg /sample/route)							
Sample Occasion	Vehicle	Vehicle	IV 5mg/kg	IV 5mg/kg	PO 10mg/kg	PO 10mg/kg	PO 50mg/kg	PO 50mg/kg
Sex	M	F	M	F	M	F	M	F
Predose	ND	ND	BLLoQ	BLLoQ	BLLoQ	BLLoQ	BLLoQ	BLLoQ
0–24 h	ND	ND	0.03	1.0	0.06	0.73	0.30	2.44
24–48 h	ND	ND	0.05	0.23	0.05	1.29	0.42	1.91
48–96 h	ND	ND	0.00	0.01	0.02	0.03	0.04	0.20
Total 0-96 h (mg)	N/A	N/A	0.08	1.24	0.13	2.05	0.75	4.54
Renal Clearance (mL/h)	N/A	N/A	0.78	1.22	4.51	3.09	1.78	3.98

M: Male; F: Female; ND: None detected; BLLoQ: Below lower limit of quantification; N/A: not applicable.

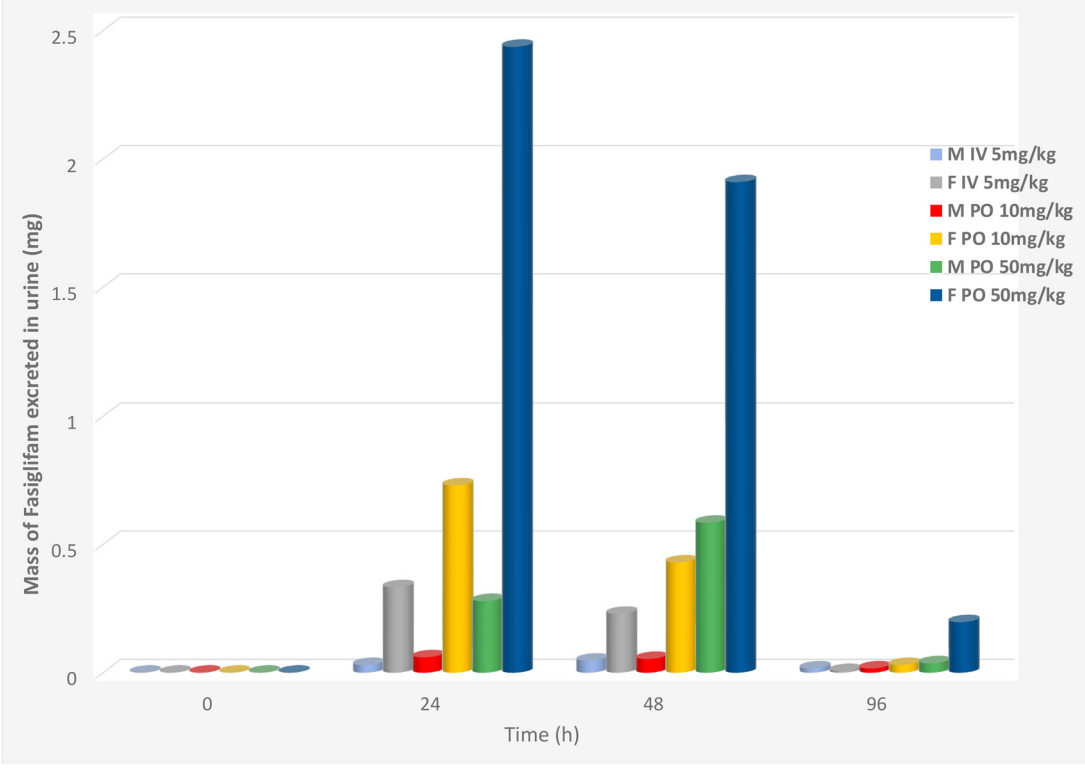

Figure 3. Urinary excretion of fasiglifam by male and female rats following IV (5 mg/kg) and PO (10 and 50 mg/kg) administration. Key in inset to Figure.

excreted in the urine were observed in the 0–24 h samples, irrespective of dose or route of administration. By 24–48 h post dose the amounts present in urine had fallen markedly. In the final 48–96 h collections, whilst fasiglifam was still present in the urine of orally dosed rats (with female 50 mg/kg PO samples having the highest concentrations) it was barely detectable in the urine of the IV dosed male rats. From the mean urinary drug excretion data provided in Table 2 (see Tables S9 – 12 for individual animal data) a clear sex difference can be seen between the male and female-derived samples. Thus, female animals consistently excreted greater amounts of fasiglifam, irrespective of dose or route, with e.g. the 0–24 h urine samples from females containing ca. 10 fold more of the drug. For example, mean totals of fasiglifam of 0.3, 0.73 and 2.44 μg were detected for the female-derived 0–24h urines following dosing at 5 mg/kg IV and 10 mg/kg PO and 50 mg/kg, whilst the equivalent male urine samples contained only 0.03, 0.06 and 0.3 μg respectively. A visual comparison of the changes in fasiglifam concentration with time is given in Figure 3.

The urine was also examined for evidence of the excretion of the metabolites of the drug detected in plasma and for any additional biotransformation products such as (sulfate and glucuronide conjugates. etc.). After careful examination of the urinary data only metabolite M-I, a product of the oxidative cleavage of the ether linkage of fasiglifam (Kogame et al. 2019a), was detected. This metabolite was found in urine, with signal intensities similar to those of the parent compound. However, in the absence of an authentic standard, no attempt to quantify M-I was made.

Whilst interesting, the significance of the sex differences in the urinary excretion of fasiglifam, which represents only

a minor route for the elimination of the drug and it's metabolites, (Kogame et al. 2019a) by male and female rats is not clear.

Fasiglifam metabolite profiling and identification in plasma

As indicated in the introduction, the metabolic fate of fasiglifam in rat, and other species, has previously been described (Kogame et al. 2019a, 2019b). The major reported biotransformation of fasiglifam is the formation of the acyl glucuronide (designated fasiglifam-G). Other, minor, routes of metabolism were noted, including taurine conjugation (fasiglifam-Tau), oxidative cleavage of the ether linkage to form the acid M-I and its subsequent glucuronidation to form M-I-G. In addition, oxidation of one of the aryl methyl groups was observed to form the alcohol T-1676427.

Here, in the absence of a radiolabelled form of the drug to act as a specific tracer, the metabolites of fasiglifam present in both plasma and urine were characterised using a combination of both targeted and untargeted screening. The targeted approach was based on including the previously identified biotransformation products of fasiglifam as 'expected metabolites', with defined structures and known *m/z* values, and during data processing their presence was explicitly sought. Untargeted screening was undertaken in order to find and characterise other drug-related components in the samples. These were identified on the following basis

At least one of the following criteria had to be met: -

1. The component could be rationalised on the basis of a combination of plausible biotransformations.
2. The component had at least one product ion in common with the parent compound.
3. The component had at least one neutral loss in common with the parent.

Each candidate metabolite passing these filtration steps was then further evaluated for compliance with all of the following criteria:-

1. The component must not have been present in the control sample
2. The component must have had a response of greater than 400 response units (corresponding to ca 0.05% of the response of the parent compound in the 1 hour plasma sample).
3. The component must have had a retention time between 2 min and 8 min (to eliminate false positives in the injection front and high organic wash)
4. The component had a *m/z* value which was inside the allowed mass defect region for likely metabolites

These filtration steps were applied automatically by the software after creation of the filter. Additional curation of likely drug-related material was done by reviewing the response/timepoint summary plot, since drug metabolites are expected to have a sensible relationship between response and timepoint (i.e. metabolites are unlikely to be present at 1 h, absent at 3 h, but present again at 6 h).

Although both positive and negative ESI data were obtained on these samples, metabolite identification was primarily undertaken using the negative ion data obtained on the 50 mg/kg plasma samples. The product ion spectra were isolated from the sample in which a given metabolite was most intense. On this basis, a total of 15 metabolites were determined as being present in the plasma samples of the 50 mg/kg dose group in samples from at least one timepoint (Figures S3–S18) and these were numbered from M1 to M15 on the basis of their retention time (see Table 3). The product ion spectrum of fasiglifam is shown in Figure 4, together with the assignments of the 6 most intense product ions (corrected for the theoretical m/z values of the assigned elemental composition). All product ion assignments were within 0.5 mDa of the theoretical *m/z* values. Single bond cleavage between C10-and C11 (decarboxylation) lead to *m/z* 479.1892, between O29 and C30 to *m/z* 403.1552 and between O13 and C14 to *m/z* 192.0428. The two remaining major product ions involved two concomitant bond cleavages (O29/C30 with C10/C11 to form *m/z* 359.1653 and O13/C14 with C10/C11 to form *m/z* 148.0524).

In addition to mass spectrometry, we also employed an ion mobility (IM) step in this investigation. IM performed following UHPLC provides another, orthogonal, separation step that can result in the resolution of the ions of interest from coeluting components. The ability to discriminate ions belonging to the target compound from these coeluting components can result in significant improvements in the resulting mass spectra obtained as shown in Figure 5. This figure shows a direct comparison of the results obtained for metabolite M12 (M-2H + O) (discussed in more detail below) both with, and without, IM enabled. As can easily be seen, in the absence of IM there are a number of interferences, some of which are similar in intensity to M12 (m/z 537.1583). With the extra resolution provided when IM is applied, interfering ions were filtered out of the data and the product ion spectrum for M12 was no longer subject to their interference, greatly simplifying interpretation and metabolite characterisation.

In addition to improving the quality of the mass spectra, the IM data can be used to determine the collision cross section (CCS) of metabolites, which like retention time (t_R) is characteristic of the compound under these conditions and can be used to help 'track' metabolites across different analyses where perhaps there have been small changes in t_R . The mass spectral, t_R and CCS values for fasiglifam and its metabolites in rat plasma are summarised in Table 3.

As can be seen from Table 3, the CCS values for those metabolites subject to biotransformations such as hydroxylation all fall within a relatively narrow range from 219–222.9 $Å^2$ (fasiglifam itself had a CCS value of 219.0 $Å^2$) However, as might be expected, where biotransformations gave rise to major structural differences being introduced into the metabolite compared to fasiglifam itself large changes in CCS were seen, as noted below. All of these properties, but notably

Table 3. Mass spectral, t_R, CCS and intensity values for fasiglifam and its metabolites in rat plasma.

Label	Component Name	Formula	Observed m/z	Mass error (ppm)	Observed CCS (Å^2)	Observed tR (min)	Common Neutral Losses	Common Fragment Ions	Total Fragments Found	Response
M1	Tak875 M-I	C19H22O5S	361.1111	−1.2	199.7	6.03	TRUE	FALSE	1	1908
M2	Tak875 + O	C29H32O8S	539.1739	−1.1	219.8	6.22	TRUE	TRUE	6	6020
M3	Tak875-G	C35H40O13S	699.2113	−0.5	246.3	6.26	FALSE	FALSE	1	2523
M4	Tak875 + O2	C29H32O9S	555.1687	−1.2	222.9	6.32	FALSE	TRUE	4	4281
M5	Tak875 + O-H2	C29H30O8S	537.1585	−0.7	220.2	6.34	TRUE	FALSE	3	1036
M6	Tak875 + O2	C29H32O9S	555.1688	−1.1	224.3	6.41	TRUE	FALSE	1	787
M7	Tak875-tau	C31H37NO9S2	630.1836	−0.2	238.4	6.44	TRUE	FALSE	1	3834
M8	Tak875 + O	C29H32O8S	539.1743	−0.3	220.8	6.46	TRUE	FALSE	5	3812
M9	Tak875 + O2	C29H32O9S	555.1690	−0.7	221.1	6.53	FALSE	FALSE	12	19155
M10	Tak875 + O	C29H32O8S	539.1738	−1.2	220.3	6.54	FALSE	FALSE	7	1162
M11	Tak875 + O-H2	C29H30O8S	537.1586	−0.5	220.0	6.6	TRUE	FALSE	5	3173
M12	Tak875 + O-H2	C29H30O8S	537.1583	−1.1	219.0	6.83	TRUE	FALSE	5	12403
M13	Tak875-CH2 (from side chain)	C28H30O7S	509.1636	−0.8	214.8	6.83	TRUE	FALSE	4	2277
M14	Tak875-H2	C29H30O7S	521.1636	−0.6	217.8	6.98	TRUE	TRUE	8	19205
M15	Tak875-H2	C29H30O7S	521.1638	−0.3	218.1	7.06	TRUE	TRUE	7	6973

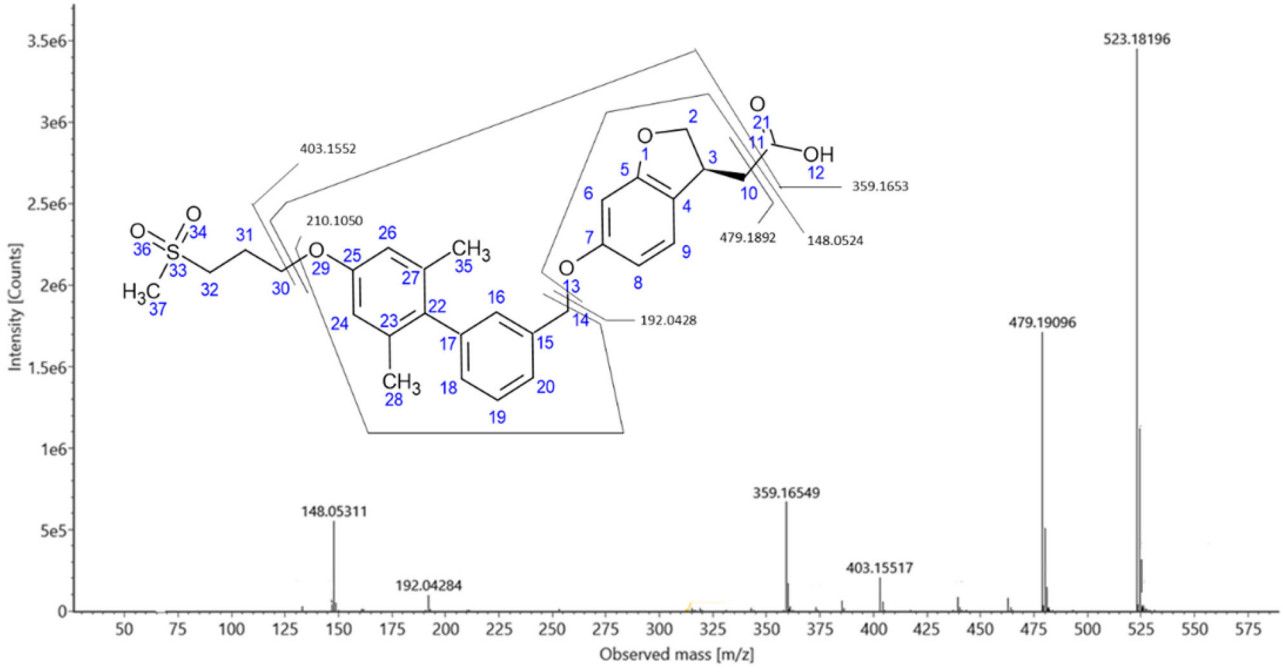

Figure 4. Product ion spectrum and structural assignment of observed major fragment ions for fasiglifam.

the improvement in spectra clarity have been used here (see Figure 5 for an example).

The acyl glucuronide (M + Gluc, M3), taurine conjugate (M + Tau, M7) and cleavage metabolite (M-I, M1) previously reported by Kogame et al. (2019a) were all determined to be present on the basis of unique *m/z* values and fragment ions. In addition, these three metabolites showed large differences in CCS value compared to fasiglifam itself, with the glucuronide and taurine conjugates increasing to 246.3 and 238.4 Å^2 respectively whilst the cleavage product M1 fell to 199.7 Å^2 (see Table 3). The glucuronide of TAK-875 MI was not observed. A number of other oxidative metabolites, some of which have not, to our knowledge, been previously reported were also present. Of the detected metaboliotes, two (M2, M8) corresponded to simple oxidations (M + O) and presumably included the major M + O metabolite reported by Kogame et al. (2019a) in which oxidation was localised to the dimethylphenyl ring system.

Analysis of product ions for these species allowed some degree of localisation, with the oxidation on M2 localised to the central biphenyl moiety. Two double oxidations (M + 2O, M4 and M9) were also identified. In the case of M4, both oxidations were localised to the left-hand half of the molecule, while in M9, both oxidations were localised to the dihydrobenzofuranylacetic acid. Three M-2H + O metabolites were identified (M5, M11 and M13). The site of metabolism in both M5 and M11 excluded the alkylsulphone.

Localisation of the biotransformation in M13 to the dihydrobenzofuranylacetic acid moiety can be made on the basis of the following product ion assignments. The ion at m/z 373.144 corresponds to the addition of 14 Da to *m/z* 359.165 which excludes the alkylsulfone. A new product ion at *m/z* 329.1550 is consistent with an elemental composition of $C_{23}H_{21}O_2$, and is most easily explained by cleavages of C25–O29 and C3-C10, meaning that the biotransformation is not

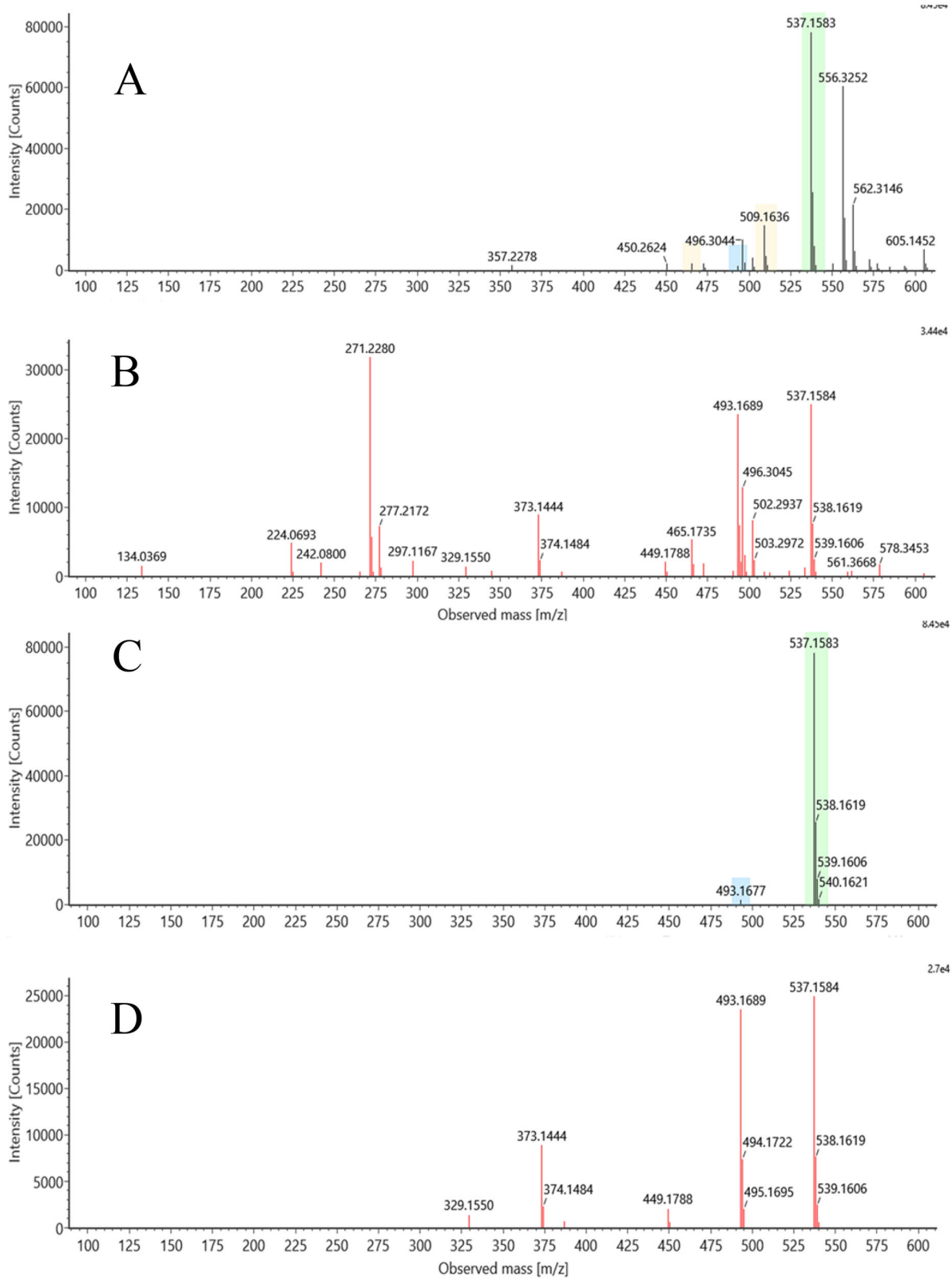

Figure 5. Effect of ion mobility on mass spectral quality: The upper two panels (A: low energy spectrum, B: high energy spectrum) show precursor and product ion spectra for metabolite M12 of fasiglifam generated without drift time correlation. The lower two panels (C: low energy spectrum, D: high energy spectrum) show the same data after drift time correlation has been applied.

present in this fragment, and making C10 the most plausible site of the biotransformation.

The biotransformation in M14 (loss of 2H) can also be localised to the 2-position of the dihydrobenzopyran, or the adjacent methylene (C2–C3 or C3–C10), on the following basis. *m/z* 359.165 and 479.189 are shifted down by 2 Da, eliminating the alkylsulfone as the site of biotransformation. A minor ion in the product ion spectrum of fasiglifam, *m/z*

210.015, is a more pronounced product ion in the spectrum of M14 and can be assigned to the central biaryl moiety whose structure is conserved in M14. m/z 148.053 is shifted by 1 Da to m/z 147.044, indicating a change in the ion form and consistent with biotransformation of the dihydrobenzopyranomethyl group.

Rationalisation of a structure for M12 was made easier by the assignments of the previously unreported metabolites (M13, M-2H + O and M14 (M-H_2). On first inspection, there appears to be no obvious simple way for fasiglifam to undergo demethylation, which is the most common mechanism for formation of a M-CH_2 metabolite. On closer examination of the product ion spectrum for M13 however, it is apparent that the most likely explanation is chain shortening of the terminal acetic acid (mass spectra shown in Figure 6) (all 3 observed product ions are shifted by 14 Da from the parent product ion spectrum (148.053 > 134.037, 359.165 > 345.149, 479.191 > 465.174), together localising the loss of CH_2 to the dihydrobenzofuranyl region of the molecule. Loss of CH_2 internally from the dihydrobenzofuran is intrinsically less likely (metabolically) than oxidative chain shortening.

Based on the MS data, and supported by the CCS values obtained during the course of this investigation, the metabolic fate of fasiglifam in the rat, as determined in this study is summarised and illustrated in Figure 7 whilst the mass, t_R and CCS values for fasiglifam and its metabolites are given in Table 3.

The loss of CH_2 and the subsequent appearance of side chain-shortened carboxylic acid metabolites is however, not unprecedented and indeed this type of biotransformation was originally observed in *in vitro* studies on diclofenac (2-[2-(2,6-dichlorophenyl)aminophenyl] ethanoic acid) by Grillo et al. (2008) and subsequently confirmed *in vivo* (Sarda et al. 2012). Grillo et al. (2008) concluded that this reaction was the result of a CYP450 3A4-mediated oxidative decarboxylation leading to a further, novel, bioactivation pathway. From their experiments they posited that the decarboxylation of diclofenac was through an intermediate benzylic carbon-centred free radical that underwent either elimination through an *O*-imine methide that then reacted with GSH, or recombination to form a benzyl alcohol that could be dehydrated to a reactive *O*-imine methide that could also react with GSH. Whilst we did not see evidence of a glutathione conjugate of the type observed by Grillo et al. (2008) the evidence for metabolism of the carboxylic acid-containing side chain of fasiglifam was clear, and suggestive of the formation of a hydroxylated intermediate (which we did not observe) leading to the production of M12 (*via* decarboxylation and formation of a carboxylic acid), M13 (oxidation of the putative hydroxylated metabolite to a ketone) and dehydration to M14 (see Figure S18).

Such modifications to ethanoic acid side chains, leading to side chain shortening and a variety of other outcomes, do not appear to be confined to diclofenac, and similar biotransformations have also been detected for the NSAIDS lumiracoxib (Dickie et al. 2017) and fenclozic acid (Ekdahl et al. 2018). As Grillo et al. (2008) noted in their conclusions, such reactions may have 'implications with respect to the CYP450-mediated metabolism of structurally related carboxylic acid-containing drugs that may be able to undergo decarboxylation and subsequent elimination- or dehydration-type reactions leading to (for example) imine-, quinone-, or

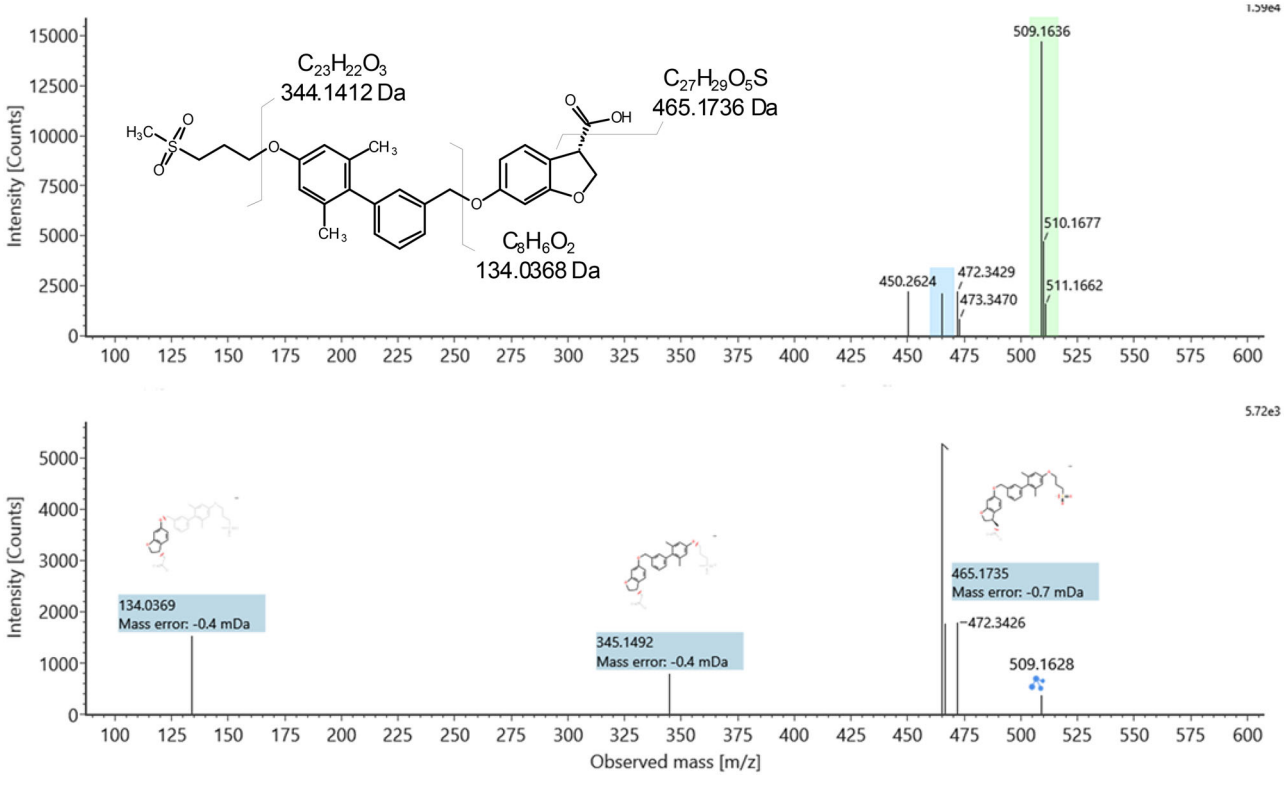

Figure 6. Precursor and product ion spectra for the side chain-shortened fasiglifam metabolite M13.

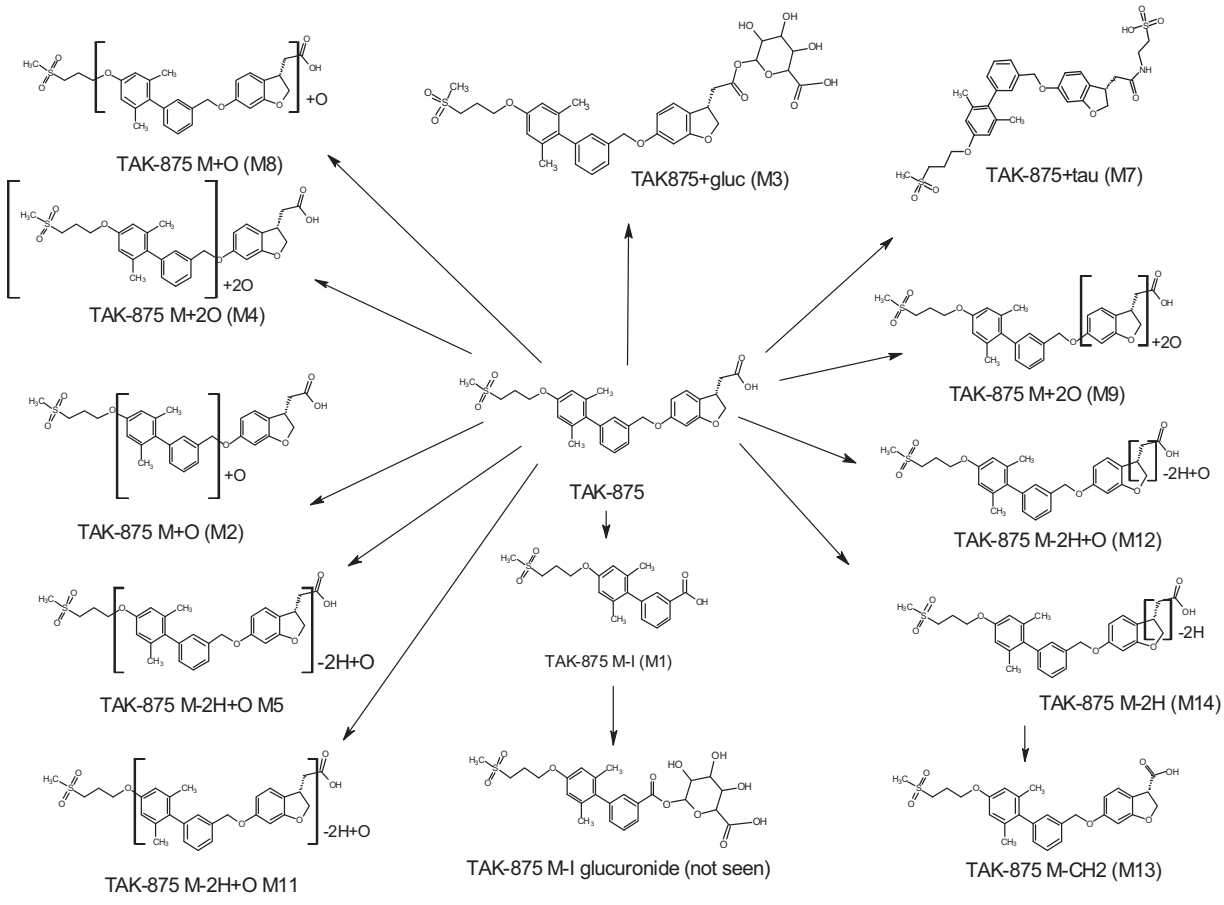

Figure 7. The circulating metabolites of fasiglifam (TAK875), shown as semi-localised structures indicating the likely sites of metabolism where these could not be determined with confidence based on MSMS data alone.

thioquinone-methide chemically reactive, and potentially toxic, intermediates.'

Since the withdrawal of fasiglifam there have been a number of efforts to uncover the mechanism(s) responsible for its toxicity with transporter interactions, reactive metabolites and mitochondrial dysfunction all suggested as being involved (e.g. see. Li et al. 2015; Wolenski et al. 2017; Otieno et al. 2018; Kogame et al. 2019b). In repeat dose toxicology studies in rat and dog (Kogame et al. 2019b), observed drug-related liver toxicity (granulomatous inflammation and crystal formation in liver tissue and bile ducts) only in dogs. MALDI/MS on dog liver sections identified both fasiglifam and fasiglifam-G in these crystals. They also found that, after 14 days of PO administration to dogs (200 mg/kg/day), concentrations of both drug and glucuronide had greatly exceeded the solubility limit of these compounds (ca. 3000 μg/ml) in the bile and were much higher than those seen in rat. The authors conjectured that this 'when taken together with lower bile flow rate could cause crystal formation in dog bile' suggesting that the liver toxicity seen in rat and dog was due to different mechanisms, and its relevance to humans is not clear.

In the case of transporter interactions, Li et al. (2015) demonstrated that fasiglifam inhibited a range of rat transporters (including the efflux transporter MRP/Mrp 2 and the uptake transporters OATP/Oatp and Ntcp) providing a possibly mechanism affecting bile acid and bilirubin homeostasis. Similarly, others have shown effects on transporters in rats and dogs (Wolenski et al. 2017) which the authors pointed out had potential consequences for bile acid transport (elevated serum total bile concentrations were one result) and bilirubin homeostasis, etc. Fasiglifam also showed extensive inhibition of transporters in *in vitro* and *in vivo* studies in rat, dog and cynomolgus monkeys as well as *in vitro* experiments using human transporters (Otieno et al. 2018). It also appeared that, in addition to the parent drug, the acyl glucuronide was also a transporter inhibitor and exceptionally potent against MRP3. Studies in rat and dog hepatocytes by Kogame et al. (2019b) also showed transport of both fasiglifam and fasiglifam G by MRP 2 and BSEP but suggested, on the basis of inhibitor studies, that passive diffusion was more important for hepatic uptake than transporters.

In addition to its effects on transporters fasiglifam was also shown to inhibit mitochondrial respiration in HepG2 cells and also affected the activities of mitochondrial Complexes 1 and 2 present in mitochondria isolated from rats (Otieno et al. 2018).

Apart from the established transporter interactions and effects on mitochondrial function, described above, another potential cause of toxicity is the formation of reactive metabolites and fasiglifam-G, in addition to its transported effects, is a clear candidate for this role. Thus, the well-established reactivity of acyl glucuronides (AG) *via* transacylation means

that these conjugates have long been associated with hepatic toxicity (although establishing a direct relationship has proved elusive). However, even if it should emerge that the acyl glucuronides themselves are not especially toxic but only represent a 'canary in the coal mine', the relationship that has been established between the degradaton rate of AG's and the observation of toxicity is clear (e.g. Sawamura et al. 2010; Iwamura et al. 2017; Bradshaw et al. 2020). By incubating ^{14}C-fasiglifam with hepatocytes it has been possible to demonstrate that covalent binding was reduced by 40% *via* the use of borneol, but not aminobenzotriazole (ABT), suggesting that glucuronidation rather than P450-related oxidation was responsible (Otieno et al. 2018). In addition, they were also able to determine a covalent body burden of 2.0 mg/day. Another type of reactive metabolite formation that is commonly observed for carboxylic acid-containing drugs involves the biosynthesis of acyl-CoA conjugates. These acyl-CoA conjugates are known to be very reactive (Darnell and Weidolf 2013), and whilst these can be difficult to detect, due to their relative instability, their downstream products, amino acid conjugates with glycine and taurine, for example, are stable. Fasiglifam-Tau is a known metabolite of fasiglifam and therefore the production of CoA conjugates can be inferred and indeed these were also detected by Otieno et al. (2018) (although the data were not shown). The authors postulated that the incomplete suppression of the covalent binding of fasiglifam-G (despite a 90% fall in its production) might be due in fact to covalent binding *via* the CoA conjugate. To these two possible mechanisms for covalent binding we can now add a third, given the MS evidence, for the production of reactive metabolites via the oxidative decarboxylation of fasiglifam (empirically resulting in the loss of CH_2) shown by the presence of the proposed side chain shortened M13 metabolite.

It therefore seems, from the studies described above, that it would not be unreasonable to ask the question 'could the ADRs that led to the discontinuation of fasiglifam in the clinic have been predicted from preclinical data?'.

It is widely accepted that metabolic activation to reactive metabolites is a reasonable explanation for the the toxicity of many compounds, but it is increasingly accepted that, particularly for idiosyncratic adverse drug reactions (IADRs), more complex mechanisms exist that depend on several different types of toxicity and which are a function of combinations of these and the individual susceptibilities of the patients themselves. In an attempt to better quantify and predict this, risk factors such as the daily or covalent body burden (CVB) have been suggested for reactive species. When added to a further panel of *in vitro* tests covering transporter inhibition (Bsep, Mrp 2), mitochondrial toxicity (in HepG2 cells) and cytotoxicity, Thompson et al. (2012), provided a scoring system, based on aggregating the results (as Yes/No outcomes) to provide a risk assessment for compounds. Based on their *in vitro* hepatocyte study, Otieno et al. (2018) were able to calculate a CVB of 2.0 mg/day, which is well within the zone of concern defined by Thompson et al. (2012). If the results for transporter inhibition (seen in several studies), and effects on mitochondria are combined with the CVB data then it seems clear, as also noted by Otieno et al. (2018), that fasiglifam could be seen to be a moderately high-risk compound. With this information could the risk have been mitigated? Whilst it is difficult to suggest any structural changes that would change the properties of transporter inhibition and mitochondrial effects it does seems possible that 2 of the 3 potential routes for reactive metabolite formation could be either eliminated altogether or reduced. Factors that reduce the transacylation rates of acyl glucuronides are associated with reduced toxicity. So, ibufenac (4-isobutylphenyl)acetic acid), which like fasiglifam has an acetic acid side chain, and was withdrawn because of liver toxicity, forms an acyl glucuronide that has a fast tranacylation rate (Johnson et al. 2010). It was replaced by ibuprofen (2-(4-isobutylphenyl)propanoic acid), where the side chain has been modified by methylation of the alpha carbon, adjacent to the carboylic acid moiety. Ibuprofen is relatively non toxic and, although it also forms an acyl glucuronide, has a much slower transacylation rate (particularly the S enantiomer) than ibufenac (e.g. see Johnson et al. 2013). This ability to change transacylation rates by using steric hindrance is a general observation, and modification of fasiglifam in this way would almost certainly have considerably slowed this. In addition, the introduction of a methyl group at this position would also block the oxidative decarboxylation seen for fasiglifam. Whilst representing what would appear, at first sight, to be a minor change to the structure of fasiglifam, with clear benefits to reducing chemical reactivity, the effect of such a change on potency towards GPR40 would clearly require evaluation. reaction

Conclusions

This study has established that the pharmacokinetics of fasiglifam in male and female rats was similar but that there was a clear sex difference in the urinary excretion of fasiglifam. However, in line with previously published data (Kogame et al. 2019a) urine was a minor route of excretion. Thus up to10-fold higher drug concentrations were detected in urine samples obtained from females compared to males administered the same dose. The investigation of the plasma for biotransformation products of fasiglifam using UHPLC/cIM/MS identified a number of novel metabolites of the drug. Several of these previously undescribed metabolites, indicative of a novel route of oxidative decarboxylation for the drug, provide evidence for a third pathway for the production of reactive metabolites (in addition to the production of acylCoA- and acylglucuronide conjugates) with potential implications for toxicity. However, in the absence of a more in-depth quantitative of the exposure of the rat to this additional reactive metabolite-producing pathway it is difficult to estimate its importance, if any, to the well-established DILI resulting from the administration of fasiglifam.

Disclosure statement

ID Wilson provides consultancy to a number of organisations including Waters Corp. The other authors report no competing interests.

Funding

The author(s) reported there is no funding associated with the work featured in this article.

ORCID

Adam King http://orcid.org/0000-0002-0819-2874
Lee A. Gethings http://orcid.org/0000-0003-3513-364X
Robert S. Plumb http://orcid.org/0000-0001-8135-3972
Ian D. Wilson http://orcid.org/0000-0002-8558-7394

References

Bradshaw PR, Athersuch TJ, Stachulski AV, Wilson ID. 2020. Acyl glucuronide reactivity in perspective. Drug Discov Today. 25(9):1639–1650.

Darnell M, Weidolf L. 2013. Metabolism of xenobiotic carboxylic acids: focus on coenzyme A conjugation, reactivity, and interference with lipid metabolism. Chem Res Toxicol. 26(8):1139–1155.

Dickie AP, Wilson CE, Schreiter K, Wehr R, Wilson EM, Bial J, Scheer N, Wilson ID, Riley RJ. 2017. The pharmacokinetics and metabolism of lumiracoxib in chimeric humanized and murinized FRG mice. Biochem Pharmacol. 135:139–150.

Ekdahl A, Weidolf L, Baginski M, Morikawa Y, Thompson RA, Wilson ID. 2018. The metabolic fate of fenclozic acid in chimeric mice with a humanized liver. Arch Toxicol. 92(9):2819–2828. 2018,

Giles K, Ujma J, Wildgoose J, Pringle S, Richardson K, Langridge D, Green M. 2019. A cyclic ion mobility-mass spectrometry system. Anal. Chem. 91(13):8564–8573.

Grillo MP, Ma J, Teffera Y, Waldon DJ. 2008. A novel bioactivation pathway for 2-[2-(2,6-dichlorophenyl)aminophenyl]ethanoic acid (diclofenac) initiated by cytochrome P450-mediated oxidative decarboxylation. Drug Metab Dispos. 36(9):1740–1744.

Iwamura A, Nakajima M, Oda S, Yokoi T. 2017. Toxicological potential of acyl glucuronides and its assessment. Drug Metab Pharmacokinetics. 32(1):2–11.

Johnson CH, Karlsson E, Sarda S, Iddon L, Iqbal M, Meng X, Harding JR, Stachulski AV, Nicholson JK, Wilson ID, et al. 2010. Integrated HPLC-MS and 1 H-NMR spectroscopic studies on acyl migration reaction kinetics of model drug ester glucuronides. Xenobiotica. 40(1):9–23.

Kaku K. 2013. Fasiglifam as a new potential treatment option for patients with type 2 diabetes. Expert Opin Pharmacother. 14(18):2591–2600.

Kaku K, Enya K, Nakaya R, Ohira T, Matsuno R. 2015. Efficacy and safety of fasiglifam (TAK-875), a G protein-coupled receptor 40 agonist, in Japanese patients with type 2 diabetes inadequately controlled by diet and exercise: a randomized, double-blind, placebo-controlled, phase III trial. Diabetes Obes Metab. 17(7):675–681.

Kaku K, Enya K, Nakaya R, Ohira T, Matsuno R. 2016. Long-term safety and efficacy of fasiglifam (TAK-875), a G-protein-coupled receptor 40 agonist, as monotherapy and combination therapy in Japanese patients with type 2 diabetes: a 52-week open-label phase III study. Diabetes Obes Metab. 18(9):925–929.

Kogame A, Lee R, Pan L, Sudo M, Nonaka M, Moriya Y, Higuchi T, Tagawa Y. 2019a. Disposition and metabolism of the G protein coupled receptor 40 agonist TAK-875 (Fasiglifam) in rats, dogs, and humans. Xenobiotica. 49(4):433–445.

Kogame A, Moriya Y, Mori I, Pan L, Morohashi A, Ebihara T, Fukui H, Tagawa Y, Benet LZ. 2019b. Characterization of fasiglifam-related liver toxicity in dogs. Drug Metab Dispos. 47(5):525–534.

Li X, Zhong K, Guo Z, Zhong D, Chen X. 2015. Fasiglifam (TAK-875) inhibits hepatobiliary transporters: a possible factor contributing to fasiglifam-induced liver injury. Drug Metab Dispos. 43(11):1751–1759.

Mortishire-Smith RJ, Castro-Perez JM, Yu K, Shockcor JP, Goshawk J, Hartshorn MJ, Hill A. 2009. Generic dealkylation: a tool for increasing the hit-rate ofmetabolite rationalization, and automatic customizationof mass defect filters. Rapid Commun Mass Spectrom. 23(7):939–948.

Naik H, Vakilynejad M, Wu J, Viswanathan P, Dote N, Higuchi T, Leifke E. 2012. Safety, tolerability, pharmacokinetics, and pharmacodynamic properties of the GPR40 agonist TAK-875: results from a double-blind, placebo-controlled single oral dose rising study in healthy volunteers. J Clin Pharmacol. 52(7):1007–1016.

Otieno MA, Snoeys J, Lam W, Ghosh A, Player MR, Pocai A, Salter R, Simic D, Skaggs H, Singh B, et al. 2018. Fasiglifam (TAK-875): mechanistic investigation and retrospective identification of hazards for drug induced liver injury. Toxicological Sciences. 163(2):374–384.

Sarda S, Page C, Pickup K, Schulz-Utermoehl T, Wilson I. 2012. Diclofenac metabolism in the mouse: novel in vivo metabolites identified by high performance liquid chromatography coupled to linear ion trap mass spectrometry. Xenobiotica. 42(2):179–194.

Sawamura R, Okudaira N, Watanabe K, Murai T, Kobayashi Y, Tachibana M, Ohnuki T, Masuda K, Honma H, Kurihara A, et al. 2010. Predictability of idiosyncratic drug toxicity risk for carboxylic acid-containing drugs based on the chemical stability of acyl glucuronide. Drug Metab Dispos. 38(10):1857–1864.

Thompson RA, Isin EM, Li Y, Weidolf L, Page K, Wilson I, Swallow S, Middleton B, Stahl S, Foster AJ, et al. 2012. In vitro approach to assess the potential for risk of idiosyncratic adverse reactions caused by candidate drugs. Chem Res Toxicol. 25(8):1616–1632.

Wolenski FS, Zhu AZX, Johnson M, Yu S, Moriya Y, Ebihara T, Csizmadia V, Grieves J, Paton M, Liao M, et al. 2017. Fasiglifam (TAK-875) alters bile acid homeostasis in rats and dogs: a potential cause of drug induced liver injury. Toxicol Sci. 157:50–61.

Zhang Y, Huo M, Zhou J, Xie S. 2010. PKSolver: An add-in program for pharmacokinetic and pharmacodynamic data analysis in Microsoft Excel. Comput Methods Programs Biomed. 99(3):306–314.

Waters™

Application Note

An Automated, Standardized, Kit-Based Sample Preparation Workflow for Bioanalytical Quantification of Therapeutic Oligonucleotides

Nikunj Tanna, Mary Trudeau, Margot Lee

Waters Corporation

Abstract

Oligonucleotide Therapeutics (ONTs) are a key focus area for many drug developers today given their powerful ability to address disease biology at the level of gene transcription and translation, and for their high target specificity and low toxicity. As the pipeline for this therapeutic class of drugs continues to expand, so does the need for sensitive, accurate, and robust bioanalytical assays to support this drug discovery and development pipeline. LC-MS detection and quantification is a widely accepted technology for bioanalytical studies, for the many benefits it affords (*i.e.*, broad drug applicability, sensitivity, selectivity, and broad linear dynamic range). However, achieving reproducible performance with LC-MS based bioanalytical assays can be challenging. In general, the greatest source of variability for these assays arises from the sample preparation needed to extract the drug and its metabolites from biofluids, and this is especially true for oligonucleotide extractions. Liquid-Liquid Extraction (LLE) and Solid Phase Extraction (SPE) are the two most widely used techniques for the extraction of ONTs from biofluids for LC-MS based quantification. LLE is a low throughput, difficult to automate technique which skilled and experienced scientists to develop, optimize, and implement these methods within a lab or across an organization. SPE is a more automation friendly, higher throughput assay, but may require

systematic optimization of every step to achieve desired recovery, reproducibility, and sensitivity. To this end, a simple, broadly applicable sample preparation workflow for ONTs that reduces the need for method development and brings greater consistency and reproducibility to LC-MS bioanalytical results is therefore highly desired. The OligoWorks™ SPE Microplate Kit (OligoWorks Kit) from Waters has been designed with this in mind. It utilizes standardized, detergent free reagents, and a robust optimized protocol that works across a diverse range of ONTs with little to no method development needed. The automation friendly reagents and SPE devices provided in each kit make it easy to automate the sample preparation procedure on an automated liquid handler, like the Andrew+™ Pipetting Robot, which can further enhance analytical performance and productivity and reduce human error/variability.

This work uses the OligoWorks Kit components and standard protocol (Figure 1) automated on the Andrew+ Pipetting Robot to successfully extract a diverse range of ONTs from plasma and achieve accurate, robust, and reproducible bioanalytical performance, with little to no need for method development.

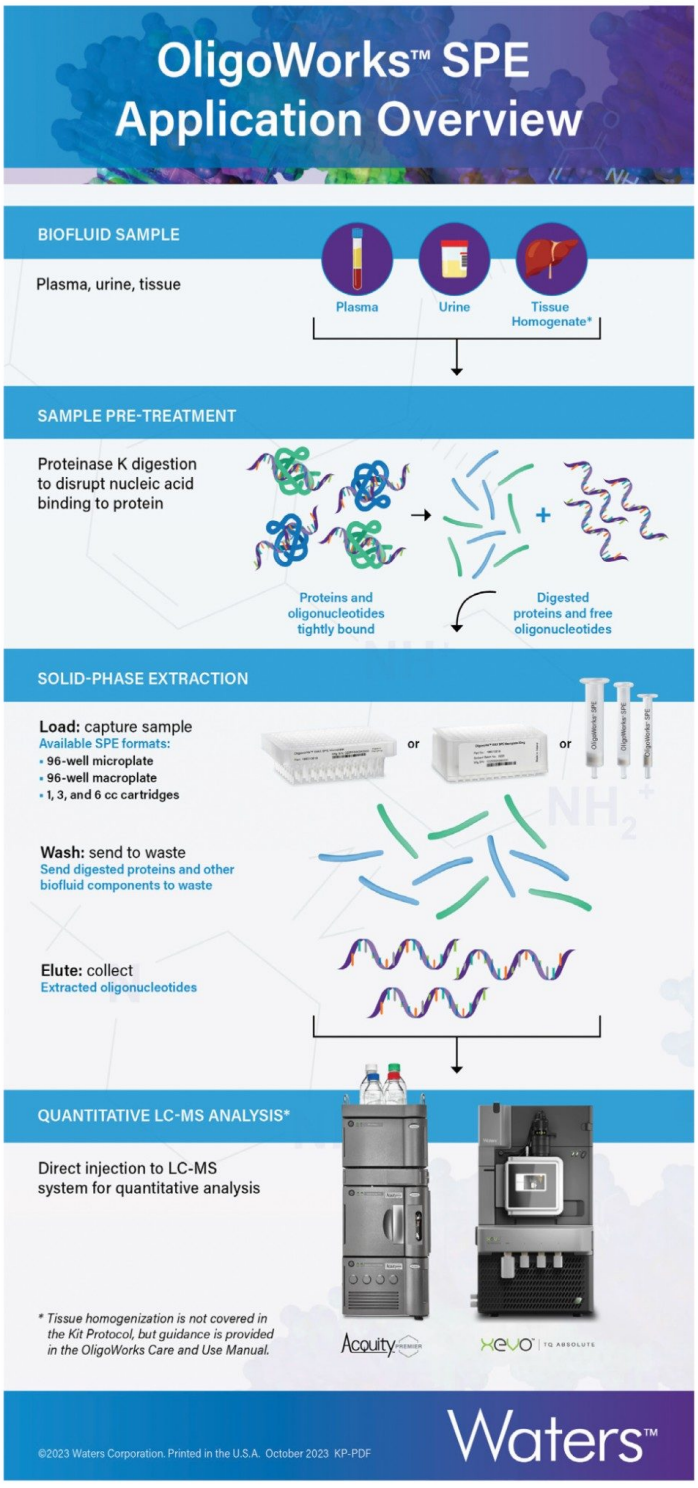

Figure 1. Graphical illustration of oligonucleotide bioanalytical quantification sample

preparation, extraction and LC-MS workflow.

Benefits

- A standardized, detergent free, kit-based solution for the extraction and LC-MS quantification of therapeutic oligonucleotides from biomatrices that requires little to no method development
- Achieve excellent recoveries (>80%) with low %CV (<15%) across a diverse range of ONTs
- Automation friendly workflow as demonstrated with the Andrew+ Pipetting Robot, with Click & Execute OneLab™ Software Library Methods that make implementation easy and improve assay performance
- Accurate, sensitive, and reproducible quantification across a diverse set of therapeutic oligonucleotides from extracted plasma samples

Introduction

The Solution

OligoWorks Kits are simple, standardized, flexible, and automation friendly sample preparation kits designed to enable accurate and robust LC-MS based bioanalytical quantitation across a diversity of oligonucleotides. The kits use an effective enzyme-based digestion sample pretreatment step with RapiZyme™ Proteinase K Digestion module to effectively disrupt oligonucleotide-biomatrix protein binding followed by selective purification using the OligoWorks SPE device, which contains a mixed-mode anion exchange SPE sorbent, designed, and QC verified for oligonucleotide performance. Each kit contains pre-measured, lot traceable, detergent free reagents, and a universal protocol to streamline the oligonucleotide sample preparation workflow and facilitate implementation by users at all experience levels.

The goals of this work were to demonstrate efficient extraction and accurate quantification of oligonucleotides from plasma using the OligoWorks Microplate Kit, automated on the Andrew+ Pipetting Robot. For this evaluation, gene-expression modulator 91 (GEM91), a 25-mer phosphorothioated antisense oligonucleotide (MWT 7771), GEM 132, a 20-mer phosphorothioated antisense oligonucleotide with 2′ methoxy caps (MWT 6600), a N-Acetylalactoseamine (GalNAc) conjugated siRNA (MWT 8590), and a 20-mer single-stranded DNA (ssDNA)

oligonucleotide (MWT 6122) were used.

Experimental

LC-MS Chromatographic Separation and Experimental Conditions

LC system:	ACQUITY™ Premier UPLC System with FTN
Column:	ACQUITY Premier Oligonucleotide C_{18} Column, 130 Å, 1.7 µm, 2.1 x 50 mm, 1/pk (p/n: 186009484)
Column temperature (°C):	55 °C
Sample temperature (°C):	10 °C
Mobile phase A:	1% HFIP (Hexafluoro-2-propanol) 0.1% DIPEA (N, N-Diisopropylethylamine) in H_2O
Mobile phase B:	0.75% HFIP (Hexafluoro-2-propanol), 0.0375% DIPEA (N, N-Diisopropylethylamine, 65% ACN 35% H_2O
Purge solvent:	25:25:25:25 Methanol:Acetonitrile:Isopropanol:Water
Injection volume (µL):	10 µL

LC Gradient table

Time (min)	Flow (mL/min)	%A	%B	Curve
Initial	0.600	95	5	6
3.25	0.600	77	23	6
3.75	0.600	10	90	6
4.10	0.600	10	90	6
4.25	0.600	95	5	6

MS System Conditions

MS system:	Xevo™ TQ Absolute MS
Ionisation mode:	ESI Negative
Acquisition mode:	MRM
Capillary voltage (kV):	3
Desolvation temperature (°C):	600
Desolvation gas flow (L/Hr):	1000
Cone gas flow (L/Hr):	150
Collision gas flow (L/Hr):	0.2
Nebulizer (Bar):	7

MRM Transitions

MRM transitions				
Oligonucleotide	**Precursor (*m/z*)**	**Product (*m/z*)**	**Cone voltage (V)**	**Collison energy (eV)**
GEM91	646.6	95.0	40	30
GEM132	824.5	94.9	40	40
GalNAc	714.6	227.4	40	20
ss DNA (20-mer)	764.3	125.1	40	30

Data Management

Instrument control software:	MassLynx™ (v4.2)
Quantification software:	TargetLynx™ (v4.2)
Automation software:	OneLab (1.19.2)

Chemicals, reagents, materials and solvents

GEM91 and GEM132 were sourced from Avecia Nitto Denko (MA, USA), GalNAc conjugated siRNA was kindly donated by Alnylam Pharmaceuticals (Cambridge, MA). The ssDNA 20-mer oligonucleotide was sourced from Waters Corporation (Milford, MA).

MS grade Methanol, water, acetonitrile, isopropanol, Hexafluoro-2-propanol (HFIP), N,N-Diisopropylethylamine (DIPEA) and ammonium acetate were purchased from Sigma Aldrich (St. Louis, MO, USA). K_2 EDTA rat plasma was procured from BioIVT (Westbury, NY, USA). DNase/RNase-free distilled water was purchased from ThermoFisher Scientific (p/n: 10977015) and was used for oligonucleotide standard preparation and SPE sample eluate dilution. OligoWorks Kit (p/n: 186010614 <https://prod1-author.waters.com/nextgen/global/shop/application-kits/186010614-oligoworks-spe-microplate-kit.html>) was procured from Waters Corporation (Milford, MA, USA).

OligoWorks Kit Wash Reagent Preparation

OligoWorks Kit SPE Wash 1: 50 mM Ammonium Acetate buffer, pH 5.5 was prepared by weighing out 3.84 g ammonium acetate and bringing to 1 Liter volume and adjusting pH to 5.5.

OligoWorks Kit SPE Wash 2: 30% Methanol/70% Water solution was prepared by adding 300 mL of methanol to 700 mLs of water.

Stock solutions, Calibration Curve, and QC Sample Preparation

GEM91, GEM132, GalNAc conjugated siRNA, and ssDNA were reconstituted in RNase/DNase-free distilled Water to provide a 1 mg/mL stock solution using Eppendorf DNA LoBind™ Tubes (p/n: 022431021 and 022431005). A combined working stock solution for all four oligonucleotides at 10 µg/mL each was created by adding 10 µL of each of the 1 mg/mL stock solution to 960 µL of water in DNA LoBind tubes. Calibration curve (0.25–1000 ng/mL) and quality control (QC) samples (LQC-0.75 ng/mL, MQC-50 ng/mL and HQC-750 ng/mL) in plasma were prepared using the Andrew+ Pipetting Robot.

Sample Pretreatment and SPE Extraction using the OligoWorks Microplate Kit

Prepared calibration curve and QC samples (100 µL) were added to an Eppendorf 1mL deep well plate and digested using the reagents and protocol supplied in the RapiZyme Proteinase K Digestion Module and subsequently extracted using the OligoWorks Kit SPE Microplate and eluent, following the protocol provided in the OligoWorks Kit and OligoWorks care and use manual (720008066 < https://www.waters.com/waters/support.htm?lid=135127508>). This protocol is illustrated in Figure 2. (Note: reagent volume of Proteinase K in the OligoWorks kit is sufficient to automate a full plate of 96 samples with 10% overage. If higher overage is desired, additional RapiZyme Proteinase K Digestion Module (p/n: 186010601 < https://www.waters.com/nextgen/global/shop/standards--reagents/186010601-rapizyme-proteinase-k-digestion-module.html>) can be procured separately.)

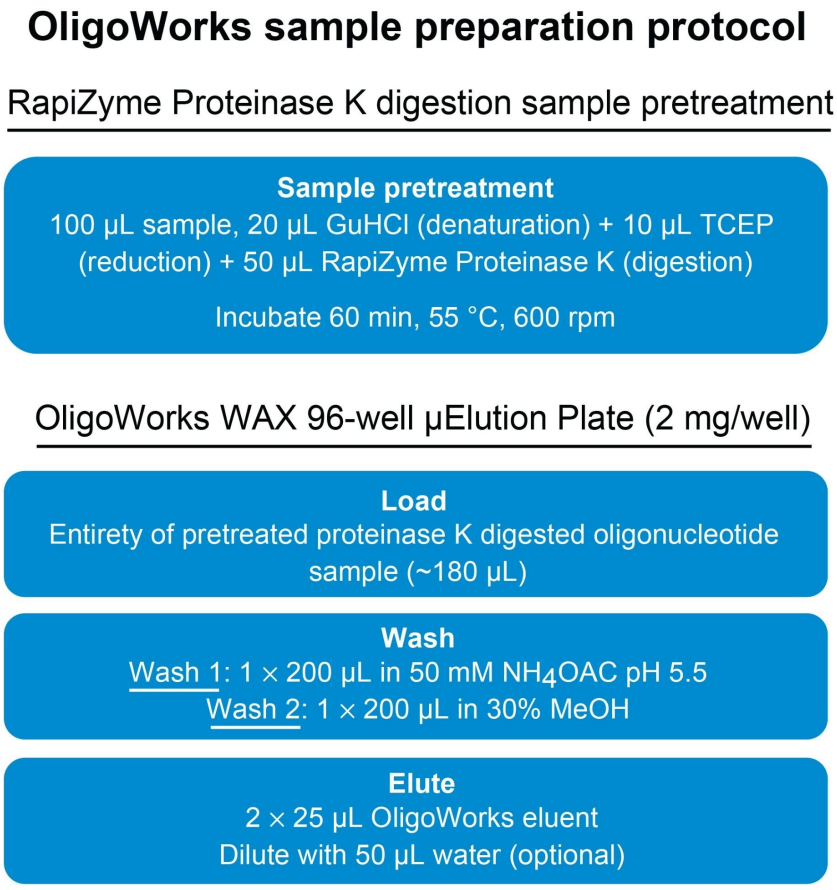

Figure 2. Graphical representation of the OligoWorks Kit Protocol (p/n: 186010614), optimized for 100 µL starting plasma/sera sample.

Automation platform

Andrew+ Pipetting Robot was used to generate calibration curves and QC's of plasma samples in a Waters QuanRecovery 700 µL plate by downloading and modifying the Simple Serial Dilution Preparation < https://onelab.andrewalliance.com/app/lab/GK6ovDkA/library/simple-serial-dilution-preparation-9jn2GGwa> method from the OneLab Software Library. All calibration curves and QC's were then extracted in triplicate by downloading the Click & Execute OligoWorks RapiZyme Proteinase K Digestion method (Figure 3A) and OligoWorks WAX SPE Microplate method (Figure 3B) from the OneLab Software Methods Library. The complete workflow, from creating plasma calibration curves and QC samples to digesting and extracting the oligonucleotides with the OligoWorks Microplate Kit was fully automated on Andrew+ Pipetting Robot

configured with the Heater-Shaker+ and Extraction+ Connected Devices.

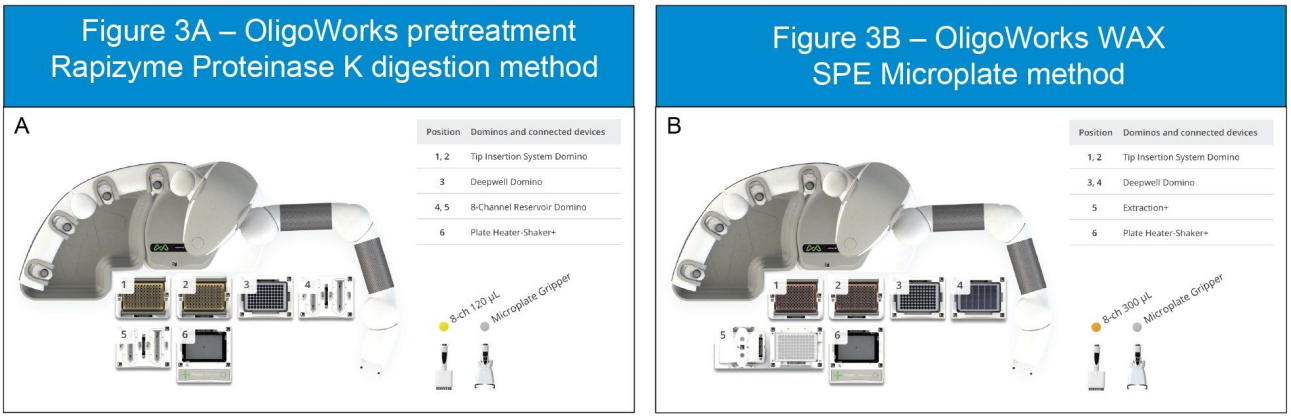

Figure 3. Representative Andrew+ Pipetting Robot Deck Layouts for oligonucleotide sample pretreatment using a Proteinase K Digestion (A) and OligoWorks WAX SPE 96-well Microplate (B). Both layouts illustrate the placement of all dominos, connected devices, and appropriate pipettes required for execution of these methods.

Results and Discussion

Therapeutic Oligonucleotides have proven to be very effective therapies for certain types of genetic or translational dysregulation diseases. With the increase in interest in exploring this therapeutic class for a variety of clinical conditions comes the need for simple, accurate, and robust analytical techniques to analyze and quantify these molecules. Achieving efficient and reproducible extraction of these analytes from complex biological matrices with high recoveries, using relatively simple sample preparation protocols is critically important for LC-MS quantification. Many ADME/DMPK workflows are highly automated for increased efficiency and reproducibility. Liquid-liquid extraction (LLE)-SPE is commonly used for extraction of oligonucleotides from biological matrices. Although effective, LLE is a slow, low-throughput manual process that is not easily automatable or scalable. Other commercially available SPE kits for this workflow use detergent-based reagents, which require extensive washing during SPE to remove these detergents and often require evaporation and reconstitution before injection into LC-MS systems to ensure SPE eluent compatibility. These steps add time, and often increase assay variability with the potential of oligonucleotide loss due to adsorption, solubility, and

potential degradation.

In contrast the OligoWorks Kit-based solution utilizes a simple, detergent-free workflow for LC-MS quantification of ONTs from biofluids that works well across a diverse range of ONTs with little to no method development, and as demonstrated in this study, is easily automated. Sample pretreatment with the RapiZyme Proteinase K Digestion Module effectively disrupts the strong oligonucleotide protein binding that occurs in biological fluids without the use of detergents, thereby removing the need for extensive washing and dry down steps prior to LC-MS analysis. The OligoWorks WAX SPE sorbent is designed to selectively bind oligonucleotides and wash away unwanted matrix components contained within the sample, resulting in a clean SPE eluate that can be directly injected onto an LC-MS system. As described in application note 720008086, the OligoWorks solution demonstrates excellent performance, with high recovery and repeatability across a diverse range of oligonucleotides and with various starting biological sample volumes. The Click and Execute OneLab Software Library Methods for OligoWorks sample pretreatment & SPE enable rapid method deployment, execution, and scalability while lowering risk of human error thus enhancing reproducibility and enabling robust analytical performance. Use of the OligoWorks Kit starting protocol, fully automated on the Andrew+ resulted in excellent oligonucleotide recovery from plasma (>96%) with less than 5% difference seen between manual and automated sample processing as illustrated in Figure 4.

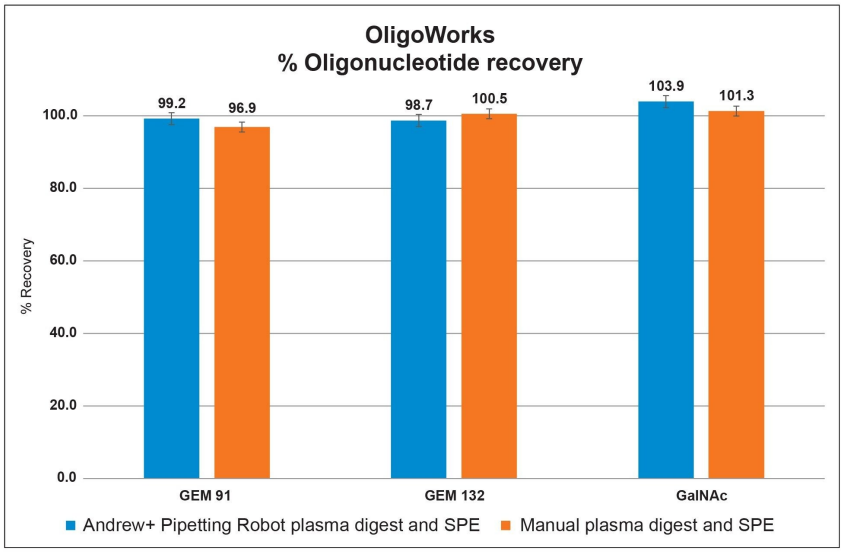

Figure 4. Comparable automated (Andrew+ Pipetting Robot) vs manual sample preparation and extraction performance using the OligoWorks Kits for GEM91, GEM132, and GalNAc oligonucleotides with >96% recovery and <5% difference from manual to automated sample processing ensuring a fit-for-purpose automated OligoWorks sample preparation and extraction solution.

The OligoWorks kit utilized in this study required no method development and facilitated the accurate quantification of four oligonucleotide therapies yielding excellent quantitative performance (no internal standard correction) from 100 µL plasma samples. Automating the workflow on the Andrew+ Pipetting Robot, lower limits of quantification (LLOQ's) of 250 pg/mL for GEM91, GEM132, and GalNAc conjugated siRNA, and 0.50 ng/mL for ssDNA 20-mer oligonucleotides were observed. Calibration curves were linear (r^2>0.99) from 0.25–1000 ng/mL (GEM91, GEM132, and GalNAc-siRNA) and 0.5–1000 ng/mL (ss DNA), with % bias and coefficient of variations (CV's) <15% for all triplicate points at each level achieving the recommended small molecule bioanalytical method validation criteria (as shown in Table 1). Specifically, accuracies and CVs across the calibration curves for GEM91, GEM 132, GalNAc, and ss DNA ranged from 85.2–119.2% and 1.97–13.87%, respectively.

Accuracy and precision for all QC levels across triplicate extractions was also within the bioanalytical method validation guidelines of ±15%. Mean accuracies for QC points for GEM91, GEM132, GalNAc conjugated siRNA, and ssDNA 20-mer oligonucleotides were between 92.30–104.07% with mean CVs between 2.82–6.77%,

respectively (as shown in Table 1). Area response for QC points increased linearly across the concentration range, as illustrated in Figure 5.

Sensitive, linear, accurate and precise

Calibration curve statistics

Analyte	Range	Weighting	Linear regression	% Accuracy range	% CV range
GEM91	0.25–1000 ng/mL	1/x	>0.99	85.4–114.7	2.01–11.43
GalNAc				85.2–114.4	2.01–13.44
GEM132				85.9–119.2*	1.97–9.67
ss DNA (20-mer)	0.50–1000 ng/mL			85.7–112.4	0.99–13.87

*% Accuracy of 119.2 for LLOQ - Acceptable per Bioanalytical method validation guidelines

QC statistics

Analyte	QC level	Expected concentration (ng/mL)	Mean observed concentration (ng/mL) (N=3)	Mean % accuracy (N=3)	Mean % CV (N=3)
GEM91	LQC	0.75	0.74	98.17	6.42
GalNAc			0.69	92.30	2.90
GEM132			0.78	104.07	5.13
ss DNA (20-mer)			0.69	92.63	8.69
GEM91	MQC	50	52.97	105.95	2.82
GalNAc			49.79	99.56	6.42
GEM132			51.72	103.43	7.41
ss DNA (20-mer)			55.15	110.29	0.99
GEM91	HQC	750	756.55	100.87	4.61
GalNAc			733.97	97.87	13.44
GEM132			748.28	99.82	6.77
ss DNA (20-mer)			763.63	101.84	4.66

Table 1. Linear accurate and precise quantitation calibration curve sample (A) and QC sample (B) performance statistics for GEM91, GEM132, GalNAc, and ss-DNA 20-mer oligonucleotides from plasma, using the OligoWorks kit, automated on the Andrew+ Pipetting Robot followed by and subsequent LC-MS/MS analysis.

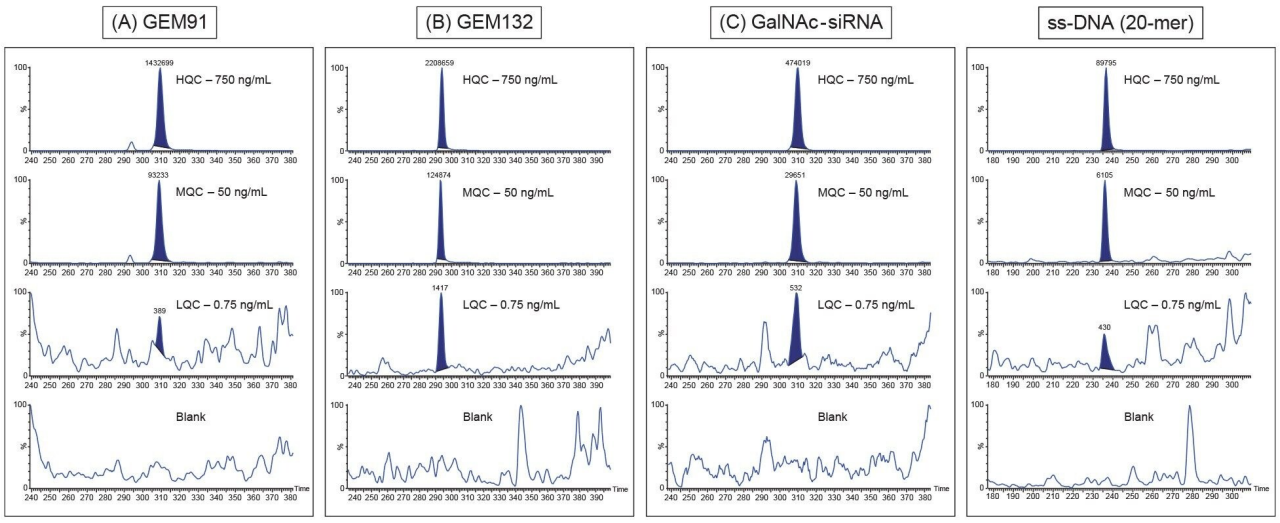

Figure 5. Representative QC chromatograms for GEM91 (A), GEM132(B), GalNAc (C), and ss DNA (D).

Conclusion

Accurate and robust oligonucleotide quantification from plasma was achieved using the OligoWorks SPE Microplate kit (with simple stepwise protocols and standardized, pre-measured, detergent free reagents). This workflow was fully automated on the Andrew+ Pipetting Robot with downloadable OneLab Click & Execute Library Methods to facilitate easy and reproducible execution of the OligoWorks Kit sample preparation and extraction workflow from day-to-day, user-to-user, and lab-to-lab. This fully automated and standardized approach (achieving high oligonucleotide recovery) greatly simplified and streamlined sample extraction, maximized lab productivity, reduced errors, and ensured overall analytical method performance.

References

1. Margot Lee, Nikunj Tanna, Mary Trudeau. Development of a Standardized, Kit-Based Approach for Selective and Reproducible Sample Preparation and Extraction for Therapeutic Oligonucleotides from Biological

Matrices, Waters Application Note 720008086, September 2023.

2. OligoWorks SPE Kits and Components, Waters User Manual, 720008066 <https://www.waters.com/waters/support.htm?lid=135127508> .

Featured Products

ACQUITY Premier System <https://www.waters.com/waters/nav.htm?cid=135077739>

Xevo TQ Absolute Triple Quadrupole Mass Spectrometry <https://www.waters.com/nextgen/global/products/mass-spectrometry-systems/xevo-tq-absolute.html>

MassLynx MS Software <https://www.waters.com/513662>

TargetLynx <https://www.waters.com/513791>

Andrew+ Pipetting Robot with OneLab Software <https://www.andrewalliance.com/>

720008068, September 2023

Quantitative Bioanalysis Revolutionized

Harness the power to transition your bioanalysis capabilities between:

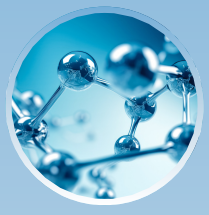

SMALL MOLECULES

Elevated sensitivity across polarity modes.

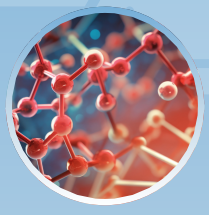

PEPTIDES & PROTEINS

Streamlined method optimization coupled with superior sensitivity.

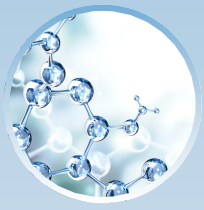

NOVEL MOLECULES

Exceptional sensitivity and quantitative performance. Seamlessly transition to new bioanalysis requirements.

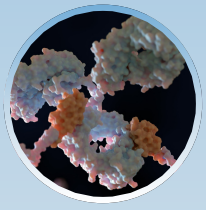

OLIGONUCLEOTIDES

Address nonspecific binding issues head-on, while boosting negative ion performance.

Maximum Versatility with Absolute Performance

Master your quantitation challenges with the ACQUITY™ Premier and Xevo™ TQ Absolute LC-MS/MS bioanalysis solution.

Achieve absolute sensitivity and unparalleled versatility with every sample analyzed.

Waters™

Learn more at waters.com

Research Article

For reprint orders, please contact: reprints@future-science.com

Bioanalysis

Assessing the impact of nonspecific binding on oligonucleotide bioanalysis

Jennifer M Nguyen*[,1,2], Martin Gilar[2], Brooke Koshel[2], Michael Donegan[2], Jason MacLean[2], Zhimin Li[2] & Matthew A Lauber[2]

[1]School of Science, University of Copenhagen, Rolighedsvej 30, 1958 Frederiksberg, Denmark

[2]Waters Corporation, 34 Maple Street, Milford, MA 01757, USA

*Author for correspondence: Jennifer_Nguyen@waters.com

Aim: Accurate and reliable quantification of oligonucleotides can be difficult, which has led to an increased focus on bioanalytical methods for more robust analyses. Recent advances toward mitigating sample losses on liquid chromatography (LC) systems have produced recovery advantages for oligonucleotide separations. **Results & methodology:** LC instruments and columns constructed from MP35N metal alloy and stainless steel columns were compared against LC hardware modified with hybrid inorganic-organic silica surfaces. Designed to minimize metal-analyte adsorption, these surfaces demonstrated a 73% increase in 25-mer phosphorothioate oligonucleotide recovery using ion-pairing reversed-phase LC versus standard LC surfaces, most particularly upon initial use. **Conclusion:** Hybrid silica chromatographic surfaces improve the performance, detection limits and reproducibility of oligonucleotide bioanalytical assays.

First draft submitted: 28 May 2021; Accepted for publication: 18 August 2021; Published online: 2 September 2021

Keywords: bioanalysis • ion-pairing • LC-UV-MS • mass spectrometry • oligonucleotides • pH • phosphorothioate • spectrofluorometric quantitation

An emerging focus on RNA-based therapies in the biopharmaceutical industry has led to an increasing demand for improved bioanalytical technologies to support the development of these complex drugs. Antisense therapy is one form of treatment to address genetic diseases, and it employs the use of synthetic short, single stranded oligodeoxynucleotides called antisense oligonucleotides (ASOs). These ASOs can range in length but typically consist of around 20 nucleotides and bind to RNA through Watson–Crick base pairing. Through this mechanism, an ASO can alter gene expression and inhibit the translation of proteins to achieve a therapeutic effect. While the first publication describing the potential of ASOs as therapeutic agents was released in 1978 by Zamecnik and Stephenson [1], it was not until 1998 that the US FDA approved the first ASO, fomivirsen, for treating cytomegalovirus retinitis [2]. Since 2016, with the prominent release of the personalized RNA therapy, milasen [3], RNA therapies have been subject to a rapid pace of development, which has placed increasing demands on the development of bioanalytical techniques to facilitate *in vitro* cellular studies, pharmacokinetics and pharmacodynamics for not just ASOs, but also for small interfering RNA (siRNA) and other oligonucleotide modalities.

The two most common bioanalytical methods used to quantify therapeutic oligonucleotides from a complex sample matrix are hybridization immunoassays such as enzyme-linked immunosorbent assay (ELISA) and liquid chromatography coupled to mass spectrometry (LC-MS) [4,5]. Similar to developing a protein-based therapy, these methods are required in preclinical development to obtain toxicological, pharmacokinetic and metabolic properties of the oligonucleotide in animal models before beginning human trials. Hybridization-ELISA assays can be used in these preclinical trials for quantification [6]. However, while highly sensitive, hybridization-ELISA lacks specificity to distinguish intact oligonucleotides and its truncated metabolites [4,7]. In general, nucleic acid metabolism occurs through the hydrolysis of the phosphodiester bonds of nucleic acids by endo- and exonucleases [8]. Characterization of these metabolites is extremely important for assessing biotransformation events and to evaluate the pharmacokinetic impact of oligonucleotide therapeutics. Chromatographic assays, especially those paired with MS detection, have the capability of monitoring and characterizing the target oligonucleotide and its related

newlands press

metabolites. Husser and co-workers have shown that LC-MS can be sensitive enough to determine the cleavage points and metabolites of oligonucleotides conjugated with GalNAc, a ligand that can grant greater potency through high affinity liver targeting but also causes changes in the biotransformation of oligonucleotides [9,10]. More recent publications by Kim and co-authors have described the development of an LC-MS method for the 2′-*O*-methyl modified phosphorothioate ASO eluforsen and its metabolites [8], and Kilanowska and co-authors have described the *in vitro* metabolism of various modified and different length ASOs with human liver microsomes using LC-MS [11]. Nevertheless, there remain challenges in using LC-MS for quantitation. Due to the polyanionic properties of oligonucleotides, there can be a propensity toward non-specific binding, not just to biological materials such as proteins or lipids, but also to chromatographic LC hardware [7]. These surfaces are generally made from metals such as stainless steel or titanium, where pronounced sample losses with these metal surfaces can be difficult to contend with [12].

To address this challenge, many different approaches have been applied to reduce adsorption and non-specific binding. Sample passivation and conditioning of the LC system and column is a common method to mask the active sites of metals or materials that would contribute to non-specific binding [12]. Metal ions, which can be found in mobile phase reagents or shed from LC pumps, can also cause problems for an analysis [13]. In addition, metal chelators, such as EDTA or other additives, can also be added to the mobile phase or sample vial [14,15]. These chelators have been shown to improve the peak shape of oligonucleotides by chelating metal ions and preventing adduct formation with sodium and potassium. While additives like EDTA can improve peak shape, they can also cause undesirable effects, most notably ion suppression in MS detection. Therefore, the concentration of these reagents must be carefully optimized in order to ensure desired performance is achieved in terms of sensitivity and lower limits of quantitation (LLOQ) [16,17].

Ultimately, these studies of chelators reveal that there is also a need to improve LC components to minimize adsorption and sample loss. Very little has been published on refining LC system and column components to prevent oligonucleotide adsorption. Typically, systems made of alternative metals such as nickel cobalt MP35N alloy or titanium have been used for biopharmaceutical applications and to prevent corrosion that would otherwise occur with stainless steel systems [18]. These systems can still suffer from adsorptive losses and in the case of titanium, can also contribute to system contamination [19]. Polyether ether ketone (PEEK) tubing and hardware have also been employed as an alternative but lack the mechanical strength to withstand UHPLC operational pressures [20]. Though PEEK-lined steel tubing can allow higher operational pressures, higher variability exists with internal diameters of PEEK tubing versus stainless steel and titanium [20]. Moreover, the hydrophobicity of PEEK can cause issues related to hydrophobic secondary interactions [21,22].

Thus, we have investigated an alternative chromatographic surface to minimize sample losses resulting from metal-ion mediated adsorption. This new technology consists of a highly crosslinked, hybrid organic/inorganic ethylene-bridged siloxane surface that is chemically similar to bridged-ethylene hybrid (BEH) sorbent [23]. This novel surface is more hydrophilic than PEEK and more chemically resilient than fused silica. Previous studies by Tuytten and co-authors have shown that phosphorylated biomolecules adsorb strongly to stainless steel and that the number of phosphate moieties correlate to the strength of adsorption [24]. When analyzing the classes of analytes that are susceptible to metal adsorption, significant improvements in recovery and peak shape have been gained upon using these hybrid surfaces to reduce metal-sensitive analyte interactions with the electron-deficient metallic LC surfaces [23].

Here, we applied hybrid surfaces toward the reversed-phase (RP) LC-MS bioanalysis of oligonucleotides. As modifications to the oligonucleotide backbone are often incorporated to increase nuclease resistance, we examined the impact of hybrid surfaces on the quantitation of a 25-mer phosphorothioate (PS) oligonucleotide and the recoveries of various length oligodeoxythymidines [25]. Additionally, because RPLC-MS of oligonucleotides is primarily performed at neutral to high pH, we evaluated the effect of mobile phase pH on oligonucleotide recovery. Finally, to demonstrate their utility for bioanalytical assays, we compared the linearity of calibration curves generated from columns and LC systems constructed with and without hybrid silica chromatographic surfaces.

Materials & methods

Samples & reagents

Trecovirsen, also known as GEM91®, GEM132, and 39-mer oligodeoxythymidine were acquired from Integrated DNA Technologies, Inc. (IA, USA). Trecovirsen is an antisense phosphorothioate (PS) oligonucleotide (ASO) with an average mass of 7771 g/mol and a sequence of 5′d(CTC TCG CAC CCA TCT CTC TCC TTC T)3′.

GEM132 has an average mass of 6600 g/mol and a sequence of 5′d(U′G′GGGCTTACCTTGCGA'A′C′A′)3′, where the label represents 2′-*O*-methyl modifications. An equimolar mixture of lyophilized 15, 20, 25, 30 and 35-mer oligodeoxythymidines was acquired from Waters Corporation (MA, USA) in the form of the MassPREP OST Standard. LC-MS grade methanol (MeOH), acetonitrile (ACN) and acetic acid were purchased from Thermo Fisher Scientific (MA, USA), and MilliQ water was used. Triethylamine (TEA), N, N-diisopropylethylamine (DIPEA), and hexylamine (HA) were purchased from Millipore Sigma (MA, USA), and 1,1,1,3,3,3-hexafluoro-2-isopropanol (HFIP) was purchased from Acros Organics (NJ, USA).

Recovery of oligomers with conventional & hybrid surface columns

An equimolar mixture of 15, 20, 25, 30 and 35-mer oligodeoxythymidines was reconstituted to a 5 pmol/µl solution and analyzed by LC-UV with an ACQUITY UPLC H-Class Bio system that had been modified with hybrid silica surfaces, as described by DeLano *et al.*, including the injection needle [23]. Comparative separations were performed on unused 2.1 × 150 mm stainless steel columns packed with a 130 Å, 1.7 µm BEH C18 stationary phase and unused columns of the same dimension and stationary phase constructed with hybrid silica hardware. An ion-pairing mobile phase system comprised of 25 mM hexylammonium acetate (mobile phase A) and a 50:50 solution of mobile phase A and acetonitrile (mobile phase B) at a pH of 6 or 7 (only aqueous mobile phase A was pH adjusted using acetic acid). Samples were injected at an injection volume of 2 µl, or a mass load of 10 pmol per oligonucleotide, and run at a temperature of 60°C, flow rate of 0.4 ml/min, and gradient from 50 to 86% B in 12 min. Chromatograms were recorded with an ACQUITY UPLC PDA detector equipped with a 5 µl titanium flow cell at 260 nm using chromatography software Empower 3.0.

Impact of pH on oligonucleotide recovery

Trecovirsen was analyzed by LC-UV in an MISER type experiment with an ACQUITY UPLC H-Class Bio system modified with hybrid silica hardware components. Briefly, MISER (multiple injections in single experimental run) allows numerous injections to be made while a separation is still occurring [26]. For this experiment, the column was removed and a 2.1 mm stainless steel frit was placed in a flow path between the injector and detector. The frit housing outlet was connected to a PDA detector cell using 75 µm i.d. × 40 cm PEEK tubing. Separations were performed at a flow rate of 0.2 ml/min at 30°C and employing isocratic elution using 10 mM aqueous ammonium acetate mobile phase at pH 4.5, 7.0, or 8.5. Fifty injections of a 2 pmol/µl solution of trecovirsen were made in blocks of 10 injections (0.5 minute/injection) using an injection volume of 1 µl and followed by a gap of 0.5 or 2 min after each block of injections, and the resulting peaks of all injections were recorded as a single chromatogram. The recovery of the oligonucleotide was estimated from a control experiment where the frit was replaced with a PEEK union. The signal with the PEEK union is considered to be 100%. Analyses were performed with UV detection at 260 nm using Empower 3.0 for data acquisition and analysis.

Generation of LC-UV calibration curves

A 2.6 pmol/µl solution of trecovirsen was used to run a twofold dilution series with injection volumes of 4 µl until the analyte could no longer be detected. Separations were performed on previously conditioned 2.1 × 50 mm stainless steel or hybrid surface columns packed with a 130 Å, 1.7 µm BEH C18 sorbent using an ion-pairing mobile phase system comprised of 8.6 mM TEA, 100 mM HFIP at pH 8.25 (mobile phase A) and methanol (mobile phase B). An ACQUITY UPLC H-Class PLUS Bio Binary System was used in conjunction with the stainless steel and hybrid surface columns. An equivalent system outfitted with hybrid surface components was employed for testing corresponding hybrid surface columns. Samples were run at a temperature of 60°C, flow rate of 0.2 ml/min, gradient from 14 to 24% B in 10 min, and UV detection at 260. Empower 3.0 software was used for data acquisition and analysis.

Generation of LC-MS calibration curves

Trecovirsen was analyzed by LC-MS with a UPLC and triple quadrupole mass spectrometer (ACQUITY UPLC H-Class Bio equipped with hybrid surfaces hyphenated to a Xevo TQ-XS mass spectrometer; Waters, MA, USA). A 0.75 pmol/µl (5 µg/ml) concentration of GEM132 was added to samples and used as an internal standard to compensate for variability in ionization efficiency from one run to another. Calibration curves were generated from dilutions of a 0.13 pmol/µl (1 µg/ml) concentration of trecovirsen, and the peak area ratio (analyte peak area to internal standard peak area) was used to plot linearity. Separations were performed on unused 2.1 × 50 mm

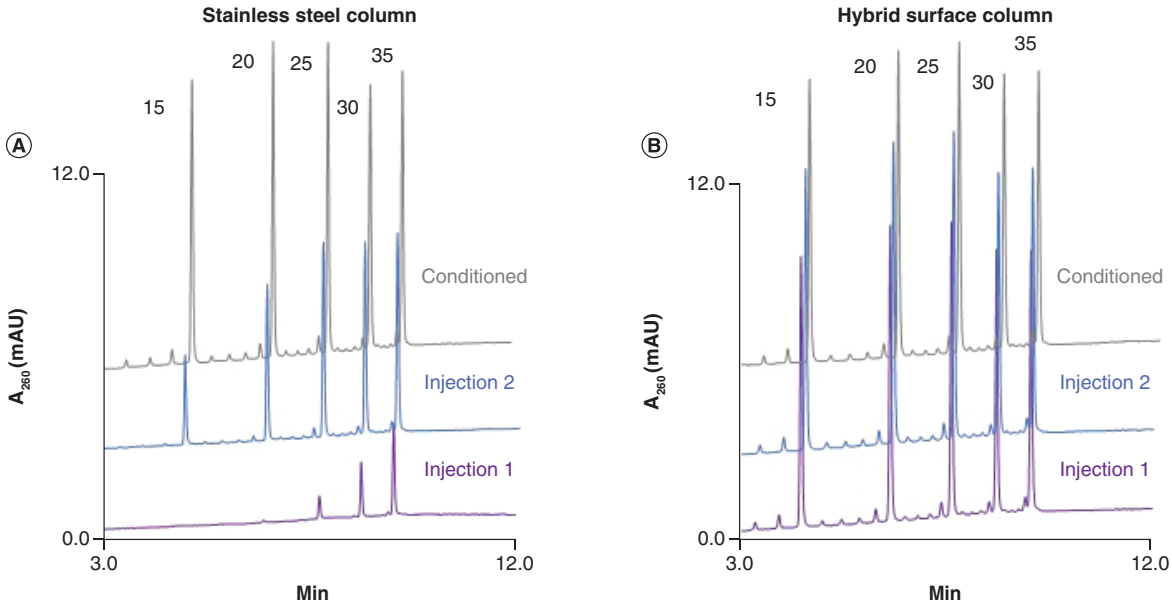

Figure 1. UV chromatograms corresponding to the first use of the columns and runs collected after high mass load conditioning. An equimolar mixture of 15, 20, 25, 30 and 35-mer oligodeoxythymidines was separated using either a 2.1 × 150 mm **(A)** stainless steel column or **(B)** a hybrid surface column and a pH 6 mobile phase.

stainless steel or hybrid surface columns packed with a 130 Å, 1.7 µm BEH C18 sorbent and using an ion-pairing mobile phase system comprised of 5.8 mM (or 0.1%) DIPEA, 98 mM (or 1%) HFIP in water (mobile phase A) and 2.2 mM (0.0375%) DIPEA, 73 mM (0.75%) HFIP in 65% acetonitrile (mobile phase B). Samples were run at a temperature of 60°C, flow rate of 0.3 ml/min, and gradient from 5 to 25% B in 20 min using injection volumes of 5 µl. MS analysis was performed in negative MRM mode using MassLynx 4.1. A capillary voltage of 2.0 kV, sampling cone at 45, source offset at 30, a source temperature of 150°C, a desolvation temperature of 600°C, desolvation gas flow set at 1000 L/h, and a collision energy of 5 eV. The transitions used, in m/z, were 732.80 → 94.90 and 824.50 → 94.96 for GEM132, and 863.10 → 94.96 and 971.03 → 94.96 for trecovirsen.

Results & discussion

Recovery of oligomers by ion pairing reversed phase chromatography

Prior research has shown that acidic analytes with anionic properties interact with electron deficient surfaces such as metals, which results in decreased analyte recovery [24]. Hybrid inorganic-organic silica surfaces based on ethylene bridged siloxane polymer can be applied to metals to mitigate these problematic ionic interactions. We sought to evaluate ethylene bridged siloxane hybrid silica surfaces for oligonucleotide LC-based quantitation by first investigating the recoveries of a sample consisting of 15, 20, 25, 30 and 35-mer oligodeoxythymidines.

Figure 1 shows a comparison of the poly dT oligomers separated with unused stainless steel versus hybrid surface columns. The injection labeled 'conditioned' was executed after an injection of 1 nmol of 39 mer oligodeoxythymidine in a separate injection. This high mass load injection served to 'condition' the columns, where the high load of the oligonucleotide sample served to saturate any potential binding sites within the columns and to therefore help minimize any subsequent analyte losses.

With the stainless steel column, poor initial recovery of each of the five components of the standard was observed. Upon seeing its first injections, this column showed recoveries for the 15, 20, 25 and 30-mer oligodeoxythymidines that were approximated to be under 20%. Meanwhile, the recovery of the 35-mer, while higher, was still less than 40%. Interestingly, problems from secondary interactions seem to lessen in severity according to elution order, which suggests that early eluting peaks encounter and then sacrificially passivate active sites during each chromatographic run. Later eluting peaks therefore stand a chance of being chromatographed with subtly better recovery. To that point, the 15-mer oligomer was not even recovered until the second injection, and it was only after conditioning the column with the 1 nmol injection of 39-mer oligodeoxythymidine that full recovery of oligonucleotide species could be achieved. Improvements in recovery were observed from injection 1 to injection 2 using the stainless steel

column, suggesting that each injection gradually 'conditions' the column, improving the sample recovery for later injection, presumably due to saturation of ionic adsorption sites present in the metal column hardware. In contrast, separations using a hybrid surface column gave nearly full recovery for all oligodeoxythymidines upon even its initial use. In another experiment, a quantitative experiment was performed to confirm that the signal observed with the hybrid surface column was indeed representative of ~90% recovery (see Supplementary Information).

Impact of pH on oligonucleotide recovery

It was hypothesized that the pH of an ion pairing reversed phase separation might affect the magnitude of adsorptive losses for oligonucleotides, as has been previously shown for the small molecule adenosine triphosphate (ATP) [23]. In addition, mass load dependence needed to be investigated further. The previously mentioned results were obtained with a pH 6 mobile phase and with sample loads that were much higher than those found in bioanalytical assays. Oligonucleotide separations are characteristically performed using high pH mobile phases, because DNA and RNA are more stable at neutral to basic pH [27]. A pH above 9 is generally not advised given that it deprotonates ion-pairing agents and thereby compromises ion-pairing based retention mechanisms [28]. Oligonucleotide separations tend to be performed at pH 7 to 9 and with organosilica or polymeric stationary phases for their increased stability over silica [29]. Since our initial investigations using conventional stainless steel and hybrid surface columns were performed at pH 6, we ran the same set of experiments but with pH increased to 7. Interestingly, at pH 7, each oligodeoxythymidine could be partially recovered upon first injection. Nevertheless, the loss of sample onto a stainless steel column could still be observed, even though it was not as pronounced as was seen with pH 6 mobile phase (Supplementary Figure 3).

To explore the impact of pH on sample adsorption and recovery, we used trecovirsen as a model analyte. Trecovirsen is a 25-mer phosphorothioate ASO that has been studied as a treatment for HIV-1 [30–32]. Phosphorothioate is a common backbone modification, where a sulfur atom replaces the non-bridging oxygen of the phosphate linkage to protect against nuclease attack [33]. This modification has been shown to increase the non-specific binding of oligonucleotides to proteins and impact the metal binding of oligonucleotides [34,35]. For this investigation, we employed the use of MISER (Multiple Injections in Single Experimental Run) for pH screening using a single 2.1 mm stainless steel frit for high throughput injections [26]. No chromatographic column was used in this experiment. The rationale of using a frit for the experiments is that highly porous frits (used in LC columns to hold the sorbent in place) represents a significant amount of the surface area that an analyte encounters. In this study, non-metallic LC components were employed to ensure that adsorption events were isolated to the frit being placed into the flow path, and the recovery of the oligonucleotide was normalized to a control experiment where the frit was replaced with a PEEK union (data not shown).

In Figure 2A are MISER chromatograms obtained at pH 4.5, 7 and 8.5. The lowest oligonucleotide recovery was observed at pH 4.5, where the first injections of trecovirsen show nearly complete sample loss. In the subsequent injections, the peaks areas and heights gradually increased, suggesting that the frit surface was progressively conditioned by the oligonucleotide sample. Presumably, the sample was adsorbed onto the metallic frit surfaces, saturating the active adsorptive sites. However, full recovery was never achieved when compared with the control experiment, even after 50 injections of sample. Similar experiments were performed at pH 7 and 8.5, respectively, which are more common pH conditions used for oligonucleotide LC analysis. Sample loss was less pronounced at these higher pH values, and the number of injections needed to condition the frit was reduced. Only at the highest pH – pH 8.5 – was the sample recovery satisfactory and reproducible across 50 injections using a stainless steel frit. In a separate experiment, we performed a study on the recovery of a 30 mer oligodeoxythymidine using a mobile phase system comprised of 25 mM hexylammonium acetate at three different pH values (pH 6, 7 and 8.5) for six previously unused stainless steel columns (Supplementary Material). We observed that elevated pH does help to mitigate sample loss, where recovery at pH 6 to pH 7 improves from 19 to 54%. However, even at pH 8.5, only 75% recovery could be achieved (Supplementary Figure 4). Alternatively, the oligonucleotide was almost fully recovered regardless of the pH when hybrid surface columns were used, with recoveries of over 95% from pH 6 to 8.5. More detail can be found in the Supplementary Material.

Figure 2A also offers an important insight regarding the mechanism of passivating a stainless steel frit as achieved by repetitive injections of oligonucleotide sample. One can notice that the buildup of oligonucleotide on the frit surface was not continuous and did not reach full frit 'saturation' even after 50 injections. In addition, when a gap of 2 min was inserted after each 10 injections, the first injection area in the next series was lower than the preceding injection in the previous injection series. This can be explained by slow bleed of adsorbed oligonucleotide from the

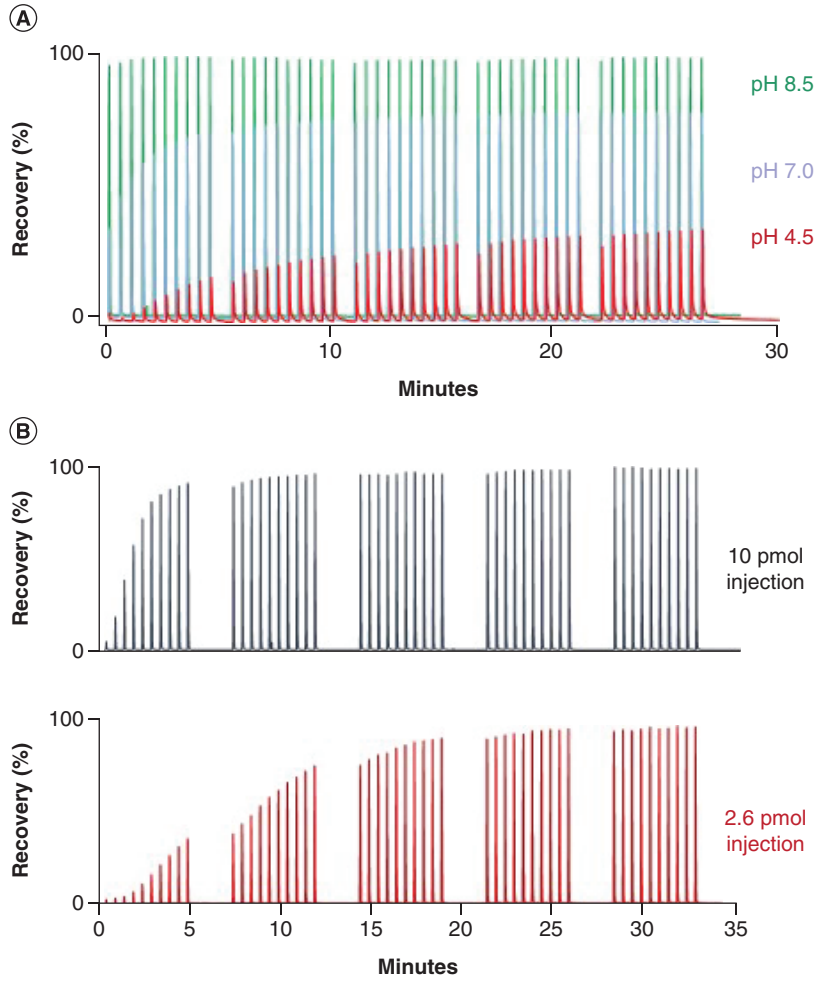

Figure 2. Effect of pH on apparent oligonucleotide adsorption on a 2.1 mm i.d. stainless steel frit. (A) 50 consecutive injections of 2 pmol of 25 mer oligonucleotide was performed at pH 4.5, pH 7.0 or at pH 8.5. **(B)** Compares 50 oligonucleotide injections using a fresh stainless steel frit as performed with 2.6 or 10 pmol sample mass per injection at pH 6.8.

stainless steel frit surface. A similar effect has been observed with other analytes, such as organic acids [36]. These observations have practical implications for the LC analysis. The conditioning of the LC system or column hardware, often practiced by analysts, can be achieved by repetitive sample injections, but the conditioning is transient in nature [37,38]. An inconsistent state of the LC system/column conditioning can have direct consequences toward the assay's accuracy.

Figure 2B further illustrates an important consideration for LC frit (column) conditioning. The available LC surfaces, in our case the 2.1 mm i.d. stainless steel frit, have finite adsorption capacity. Such capacity can be saturated more speedily with an exposure to a higher concentration (mass) of the sample. Nearly complete sample recovery was observed after 10 injections of 10 pmol oligonucleotides, while 30 to 40 injections were required to reach the recovery plateau with 2.6 pmol injections of the sample.

Generation of LC-UV calibration curves

The above experiments, in particular Figure 2B, suggest that quantitative bioanalysis of oligonucleotides performed at low concentrations would be especially challenging on conventional LC hardware. Thus, the application of hybrid surfaces to both the LC and column should prove beneficial in this respect and as demonstrated by De Lano and *et al.* [23]. To that end, we performed a systematic experiment to evaluate improvements in trecovirsen recovery when using LC hardware in three configurations: a stainless steel column with a conventional system, a hybrid surface column with a conventional system, and hybrid surfaces put to use in both the column and LC system. To

Table 1. Average peak areas and corresponding percent RSDs as performed on previously conditioned LC hardware in three configurations: stainless steel column with a conventional system, hybrid surface column with a conventional system and hybrid surfaces used for both the column and system.

Mass load (pmol)	Stainless steel column/conventional LC system		Hybrid surface column/conventional LC system		Hybrid surface column/hybrid surface LC system	
	Log(peak area) (n = 3)	%RSD	Log(peak area) (n = 3)	%RSD	Log(peak area)(n = 3)	%RSD
10.40	5.25	1.3	5.34	0.5	5.41	0.3
5.20	4.93	0.9	5.02	1.3	5.10	0.4
2.60	4.59	2.0	4.71	0.2	4.79	0.7
1.30	4.22	4.1	4.39	1.2	4.48	1.3
0.65	3.90	3.1	4.09	0.6	4.14	1.9
0.32	3.41	7.0	3.76	0.9	3.84	0.1
0.16	3.00	9.2	3.44	1.6	3.47	2.1
0.08	2.54	12.2	3.16	2.4	3.20	0.3
0.04	Not detected		2.78	8.6	2.84	2.3
0.02			Detectable but SNR <3		2.41	2.2
0.01					Detectable but SNR <3	

examine the lower limits of detection for these configurations, mass loads down to 0.01 pmol were investigated for quantitation using LC-UV, which was a 1000-times lower than the mass load used in Figure 1 and a 100-times lower than used in Figure 2.

Prior to data collection over three triplicate injections, the LC system and column were conditioned with multiple injections of trecovirsen. Table 1 lists the average of the peak area (in log) and percent deviation for the three sets of equipment configurations. Here, the stainless steel column and conventional system yielded the lowest recovery (as determined by the log of the peak area) for each injection regardless of mass load. While switching to a hybrid surface column on a conventional system improved recovery, the highest yield resulted from using hybrid surfaces within both the column and the LC hardware. The effect from the hybrid surfaces granted a lower limit of detection and lower percent RSDs throughout the dilution series.

The calibration curves of each dilution series are shown in Figure 3 to make it possible to visually assess dynamic range differences. By plotting each calibration curve in a log-log plot, one can see that different slopes (response factors) were observed for each configuration, which indicates that there are analyte recovery differences even after following sample-based conditioning procedures. Overlaying the data revealed rather significant linear differences especially at low mass data points, despite each curve appearing linear with an R-squared value close to one. Recovery, and thus linearity, was improved by using hybrid surfaces. When employed for both column and LC hardware, hybrid silica surfaces afforded the best linearity throughout the dynamic range, lowest limits of detection, and best repeatability (lowest percent RSD). Dynamic range with optical detection approached three orders of magnitude with the hybrid column and LC hardware, but was only two orders of magnitude with a conventional system and a stainless steel column.

Generation of LC-MS calibration curves

High throughput capabilities and the ability to monitor oligonucleotide drug targets and their related metabolites have made LC-MS an attractive and common alternative to immunoaffinity assays such as ELISA. Additionally, as LC instrumentation continues to be developed, LC-MS assays are becoming increasingly sensitive. Thus, experiments next turned to exploring even lower detection limits based on LC-MS detection with a triple quadrupole mass spectrometer.

In general, LC-MS bioanalysis of oligonucleotides necessitates the use of an internal standard that can be used to correct for run-to-run fluctuations in ionization efficiency [39,40]. We thus included a high concentration of GEM132 as an internal standard to neat solutions of trecovirsen and generated calibration curves from these samples on previously unused stainless steel versus hybrid surface columns (Figure 4). The data is plotted on a log/log plot to better illustrate linearity across the entire calibration range. No weighted regression is applied to this curve.

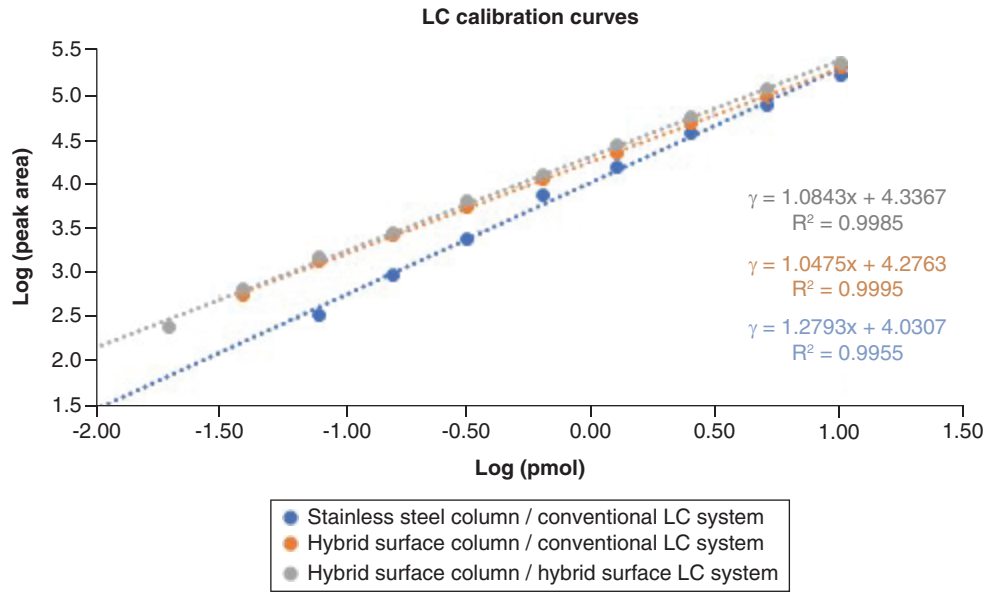

Figure 3. Comparison of the linearity of calibration curves using previously conditioned LC hardware in three configurations: stainless steel column with a conventional system (blue), hybrid surface column with a conventional system (orange), and hybrid surfaces for both column and system (gray). The graph is viewed in log/log mode to better visualize the data trend throughout the calibration range.

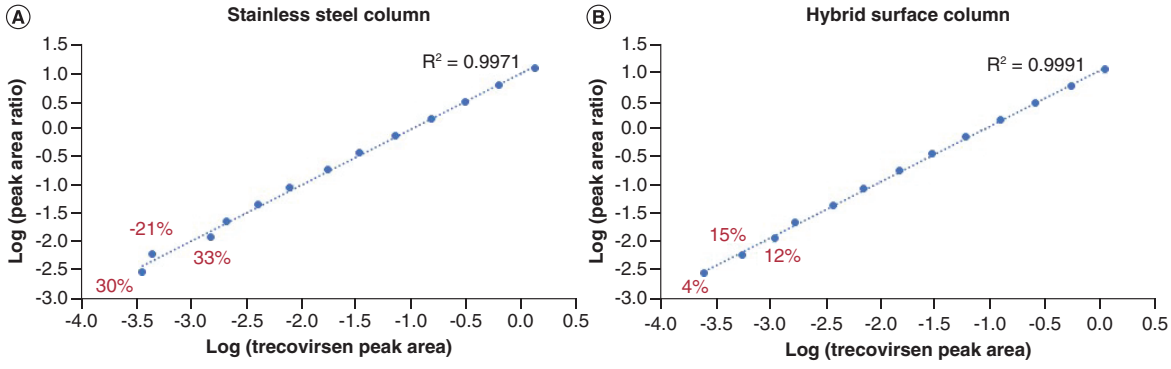

Figure 4. Comparison of the linearity at the low end of the calibration curves as generated through LC-MS separations of trecovirsen using previously unused 2.1 × 50 mm stainless steel versus hybrid surface columns. Graphs are viewed in log/log mode using the peak area ratio of the internal standard to trecovirsen to better visualize the data trend throughout the calibration range.

Much like in Figure 3, although the curves appear linear and have R-squared values close to one, when using the stainless steel column, the three lowest concentrations would fall outside of typical bioanalytical acceptance criteria [41]. Compared with the hybrid surface column, where the lowest concentration in the linear dynamic range was 0.36 fmol/µl (2.8 ng/ml, 1.8 fmol on column), the limit of quantitation for the conventional column was only down to 6.3 fmol/µl (49 ng/ml, 32 fmol on column). The elimination of non-specific binding, which is most pronounced at the low end of the calibration curve, resulted in a 17× improvement in the limit of quantitation observed. Even with the internal standard spiked into the sample, there can be challenges in performing reliable measurements with a stainless steel columns, most particularly when attempting to analyze low sample concentrations.

The non-linearity observed with the stainless steel column is likely due to there being active sites in the column that cannot be passivated with the addition of this quantity of internal standard. It might also be important to consider whether an internal standard elutes before or after the analyte peak. Nevertheless, as seen in Supplementary Figure 5, the initial recoveries from the first injections of the internal standard were poor when using a stainless

steel column, with almost a fourfold decrease upon first injection versus hybrid surface columns. However, they did progressively increase over time, from injection to injection. This can cause analytical problems because the peak area ratio (analyte peak area to internal standard peak area) is variable and changing overtime. The hybrid surface column, in turn, gave reproducible peak area and a peak area ratio from injection 1 to injection 20.

This study demonstrates that the ability to use neat standards is noteworthy for LC-MS applications. While the presence of other biological components in matrix may produce less sizable recovery differences, matrix effects are often calculated for bioanalytical applications, with the reference being the analyte in the absence of the matrix [5,42]. In addition, publications involving the treatment of neat standards of oligonucleotides with nucleases have been demonstrated to provide insight into biotransformation pathways and analysis of metabolites [43]. Appropriate MRM transitions are often chosen by infusing neat standards into the MS to monitor the target analyte, ensuring no overlap with its metabolites. Furthermore, sample matrices such as urine, consisting primarily of water and salt with little plasma proteins, may benefit from hybrid silica surfaces [7].

Conclusion

Our results demonstrate the utility of ethylene-bridged hybrid silica chromatographic surfaces for oligonucleotide bioanalysis. Hybrid surfaces improved the recovery of a metal-sensitive, phosphorothioate oligonucleotide and circumvented the need for column or system conditioning. The data showed that while standard LC and stainless steel column hardware required multiple sample injections to improve recoveries and peak widths, a configuration fully outfitted with hybrid surfaces can achieve these results with high reproducibility upon first injection. In turn, the linear dynamic range and calibration curves generated with bioanalytical assays could be enhanced with the use of alternative chromatographic surfaces, especially at lower mass loads. Based on our experiments, the performance of standard, metal-based LC systems can be improved at elevated pH, but it is only a partial solution. Recovery of oligonucleotides (and in general, acidic analytes) were improved via dynamic system passivation by repetitive injections of sample, but the effect was only transient. Improvements in recovery and reproducibility of oligonucleotides on LC hardware (column and LC system) modified with hybrid silica surfaces can help address these shortcomings and give new options for enhanced bioanalytical approaches for oligonucleotide therapeutics.

Future perspective

With the rise in RNA/DNA-based therapies, new bioanalytical approaches are required to support the development of oligonucleotide biotherapeutics and to understand their biotransformation and pharmacokinetic profiles. Here, ethylene bridged hybrid silica surfaces were employed within both an LC system and the column to improve the recovery and lower limits of detection of phosphorothioate oligonucleotides and oligodeoxythymidines, which is indicative of their potential value for other nucleic acid based analytes. As these nucleic acid therapeutics are becoming more complex, the need for better quantitation and higher reproducibility will be increasingly apparent. It appears that chromatographic surfaces based on hybrid silica will be of value in the pursuit of new approaches for LC-based quantitation.

Supplementary data

To view the supplementary data that accompany this paper please visit the journal website at: www.future-science.com/doi/suppl/10.4155/bio-2021-0115

Acknowledgments

The authors would like to thank M DeLano, M Lame and K Brennan for their expertise, advice and discussions surrounding hardware and oligonucleotide separations.

Financial & competing interests disclosure

All authors are employed by Waters Corporation. The work in this article was financially supported by Waters Corporation, and Waters equipment and consumables were used for this research. The authors have no other relevant affiliations or financial involvement with any organization or entity with a financial interest in or financial conflict with the subject matter or materials discussed in the manuscript apart from those disclosed.

No writing assistance was utilized in the production of this manuscript.

Summary points

- Aim: to investigate the use of ethylene-bridged hybrid silica as a chromatographic surface and its suitability for the quantitation of oligonucleotide biotherapeutics.
- Separations of a 25-mer PS oligonucleotide and various length oligodeoxythymidines were analyzed and quantified through spectrofluorometric detection using systems and columns constructed from standard, metal based versus hybrid silica based LC surfaces.
- Oligonucleotide recoveries at various pH conditions and sample loads were investigated.
- Calibration curves were generated to comparatively assess the dynamic range of LC-UV and LC-MS separations of a PS oligonucleotide.
- Quantitation of nanogram levels of oligonucleotide was possible using hybrid surfaces, including a 73% increase in recovery versus standard, metal based LC surfaces.
- Reproducible and robust performance was observed even upon the first injection and use of a hybrid surface column, eliminating the need for conditioning.
- Ion-pairing separations performed at higher pH can help to mitigate the need for system passivation/conditioning when standard LC surfaces are used.
- Employing hybrid surfaces extends the dynamic range of calibration curves and thus allows for lower limits of detection and improved quantitation for oligonucleotide bioanalysis.
- Hybrid chromatographic surfaces are a viable alternative to metal based LC surfaces, as seen in instances of them improving the recovery and reproducibility of LC-based quantitation of oligonucleotides.

Ethical conduct of research

The authors state that they have obtained appropriate institutional review board approval or have followed the principles outlined in the Declaration of Helsinki for all human or animal experimental investigations. In addition, for investigations involving human subjects, informed consent has been obtained from the participants involved.

References

Papers of special note have been highlighted as: • of interest; •• of considerable interest

1. Zamecnik PC, Stephenson ML. Inhibition of Rous sarcoma virus replication and cell transformation by a specific oligodeoxynucleotide. *Proc. Natl Acad. Sci. USA* 75(1), 280–284 (1978).
2. Verma A. Recent advances in antisense oligonucleotide therapy in genetic neuromuscular diseases. *Ann. Indian Acad. Neurol.* 21(1), 3–8 (2018).
3. Amariles P, Madrigal-Cadavid J. Ethical, economic, societal, clinical, and pharmacology uncertainties associated with milasen and other personalized drugs. *Ann. Pharmacother.* 54(9), 937–938 (2020).
4. Basiri B, Bartlett MG. LC-MS of oligonucleotides: applications in biomedical research. *Bioanalysis* 6(11), 1525–1542 (2014).
5. Li P, Gong Y, Kim J *et al.* Hybridization liquid chromatography-tandem mass spectrometry: an alternative bioanalytical method for antisense oligonucleotide quantitation in plasma and tissue samples. *Anal. Chem.* 92(15), 10548–10559 (2020).

• **Demonstrates LC-MS as used for the bioanalysis of antisense oligos.**

6. Tremblay G, Khalafaghian G, Legault J, Nielsen P, Bartlett A. Dual ligation hybridization assay for the specific determination of oligonucleotide therapeutics. *Bioanalysis* 3(5), 499–508 (2011).
7. Wang L. Oligonucleotide bioanalysis: sensitivity versus specificity. *Bioanalysis* 3(12), 1299–1303 (2011).

• **Review of oligo bioanalysis.**

8. Kim J, Basiri B, Hassan C *et al.* Metabolite profiling of the antisense oligonucleotide eluforsen using liquid chromatography-mass spectrometry. *Mol. Ther. Nucleic Acids* 17, 714–725 (2019).
9. Husser C, Brink A, Zell M, Muller MB, Koller E, Schadt S. Identification of GalNAc-conjugated antisense oligonucleotide metabolites using an untargeted and generic approach based on high resolution mass spectrometry. *Anal. Chem.* 89(12), 6821–6826 (2017).
10. Sewing S, Gubler M, Gerard R *et al.* GalNAc conjugation attenuates the cytotoxicity of antisense oligonucleotide drugs in renal tubular cells. *Mol. Ther. Nucleic Acids.* 14, 67–79 (2019).
11. Kilanowska A, Nuckowski L, Studzinska S. Studying *in vitro* metabolism of the first and second generation of antisense oligonucleotides with the use of ultra-high-performance liquid chromatography coupled with quadrupole time-of-flight mass spectrometry. *Anal. Bioanal. Chem.* 412(27), 7453–7467 (2020).

12. Lauber M, Walter TH, Gilar M *et al.* Low adsorption HPLC columns based on MaxPeak high performance surfaces. *Waters White Paper 720006930EN* (2020).
13. Birdsall RE, Gilar M, Shion H, Yu YQ, Chen W. Reduction of metal adducts in oligonucleotide mass spectra in ion-pair reversed-phase chromatography/mass spectrometry analysis. *Rapid Commun. Mass Spectrom.* 30(14), 1667–1679 (2016).
14. Hsiao JJ, Potter OG, Chu TW, Yin H. Improved LC/MS methods for the analysis of metal-sensitive analytes using Medronic acid as a mobile phase additive. *Anal. Chem.* 90(15), 9457–9464 (2018).
15. Pesek JJ, Matyska MT, Fischer SM. Improvement of peak shape in aqueous normal phase analysis of anionic metabolites. *J. Sep. Sci.* 34(24), 3509–3516 (2011).
16. Liu J, Li J, Tran C *et al.* Oligonucleotide quantification and metabolite profiling by high-resolution and accurate mass spectrometry. *Bioanalysis* 11(21), 1967–1980 (2019).
17. Basiri B, Sutton JM, Hooshfar S, Byrnes CC, Murph MM, Bartlett MG. Direct identification of microribonucleic acid miR-451 from plasma using liquid chromatography mass spectrometry. *J. Chromatogr. A* 1584, 97–105 (2019).
18. In: *The HPLC Expert II.*Kromidas S (Ed.). Wiley-VCH, Weinheim, Germany (2017).
19. De Pra M, Greco G, Krajewski MP *et al.* Effects of titanium contamination caused by iron-free high-performance liquid chromatography systems on peak shape and retention of drugs with chelating properties. *J. Chromatogr. A* 1611, 460619 (2020).
20. Rao S, Rivera B, Anspach JA. Bioinert versus biocompatible: the benefits of different column materials in liquid chromatography separations. *LC GC N Am.* 36(6), 24–29 (2018).
21. Lough J, Mills MJ, Maltas J. Analyte adsorption in liquid chromatography valve injectors for samples in non-eluting solvents. *J. Chromatogr. A* 726, 67–75 (1996).
22. Hambleton P, Lough WJ, Maltas J, Mills M. Unusual analyte adsorption effects on inert LC components. *J. Liq. Chromat. Rel. Tech.* 18, 3205–3217 (1995).
23. DeLano M, Walter TH, Lauber MA *et al.* Using hybrid organic-inorganic surface technology to mitigate analyte interactions with metal surfaces in UHPLC. *Anal. Chem.* 93(14), 5773–5781 (2021).

•• **Description of the properties of hybrid surfaces.**

24. Tuytten R, Lemiere F, Witters E *et al.* Stainless steel electrospray probe: a dead end for phosphorylated organic compounds? *J. Chromatogr. A* 1104(1–2), 209–221 (2006).
25. Monia BP, Johnston JF, Sasmor H, Cummins LL. Nuclease resistance and antisense activity of modified oligonucleotides targeted to Ha-ras. *J. Biol. Chem.* 271(24), 14533–14540 (1996).
26. Welch CJ, Gong X, Schafer W *et al.* MISER chromatography (multiple injections in a single experimental run): the chromatogram is the graph. *Tetrahedron: Asymmetry* 21, 1674–1681 (2010).
27. Gilar M, Bouvier ESP. Purification of crude DNA oligonucleotides by solid-phase extraction and reversed-phase high-performance liquid chromatography. *J. Chromatogr. A* 890(1), 167–177 (2000).
28. Fountain KJ, Gilar M, Gebler JC. Analysis of native and chemically modified oligonucleotides by tandem ion-pair reversed-phase high-performance liquid chromatography/electrospray ionization mass spectrometry. *Rapid Commun. Mass Spectrom.* 17(7), 646–653 (2003).
29. Wyndham KD, O'gara JE, Walter TH *et al.* Characterization and evaluation of C18 HPLC stationary phases based on ethyl-bridged hybrid organic/inorganic particles. *Anal. Chem.* 75(24), 6781–6788 (2003).
30. Lisziewicz J, Sun D, Weichold FF *et al.* Antisense oligodeoxynucleotide phosphorothioate complementary to Gag mRNA blocks replication of human immunodeficiency virus type 1 in human peripheral blood cells. *Proc. Natl Acad. Sci. USA* 91(17), 7942–7946 (1994).
31. Sereni D, Tubiana R, Lascoux C *et al.* Pharmacokinetics and tolerability of intravenous trecovirsen (GEM 91), an antisense phosphorothioate oligonucleotide, in HIV-positive subjects. *J. Clin. Pharmacol.* 39(1), 47–54 (1999).
32. Veal GJ, Agrawal S, Byrn RA. Synergistic inhibition of HIV-1 by an antisense oligonucleotide and nucleoside analog reverse transcriptase inhibitors. *Antiviral Res.* 38(1), 63–73 (1998).
33. Gan R, Wu X, He W *et al.* DNA phosphorothioate modifications influence the global transcriptional response and protect DNA from double-stranded breaks. *Sci. Rep.* 4, 6642 (2014).
34. Zhou W, Saran R, Liu J. Metal sensing by DNA. *Chem. Rev.* 117(12), 8272–8325 (2017).
35. Saran R, Huang Z, Liu J. Phosphorothioate nucleic acids for probing metal binding, biosensing and nanotechnology. *Coord. Chem. Rev.* 428, 1–17 (2020).
36. Smith KM, Wilson ID, Rainville PD. Sensitive and reproducible mass spectrometry-compatible RP-UHPLC analysis of tricarboxylic acid cycle and related metabolites in biological fluids: application to human urine. *Anal. Chem.* 93(2), 1009–1015 (2020).
37. Stoll DR, Hsiao JJ, Staples GO. Troubleshooting LC separations of biomolecules, part I: background, and the meaning of inertness. *LC GC N Am.* 38(3), 146–150 (2020).

38. Hsiao JJ, Chu TW, Potter OG, Staples GO, Stoll D. Troubleshooting LC separations of biomolecules, part 2: passivation and mobile-phase additives. *LC GC Eur.* 33(8), 388–392 (2020).
39. Zhang G, Lin J, Srinivasan K, Kavetskaia O, Duncan JN. Strategies for bioanalysis of an oligonucleotide class macromolecule from rat plasma using liquid chromatography-tandem mass spectrometry. *Anal. Chem.* 79(9), 3416–3424 (2007).
40. Chen B, Bartlett M. A one-step solid phase extraction method for bioanalysis of a phosphorothioate oligonucleotide and its 3′ n-1 metabolite from rat plasma by uHPLC-MS/MS. *AAPS J.* 14(4), 772–780 (2012).
41. Kadian N, Raju KS, Rashid M, Malik MY, Taneja I, Wahajuddin M. Comparative assessment of bioanalytical method validation guidelines for pharmaceutical industry. *J. Pharm. Biomed. Anal.* 126, 83–97 (2016).
42. Ramanathan L, Shen H. LC-TOF-MS methods to quantify siRNAs and major metabolite in plasma, urine and tissues. *Bioanalysis* 11(21), 1983–1992 (2019).
43. Shemesh CS, Yu RZ, Gaus HJ *et al.* Elucidation of the biotransformation pathways of a galnac3-conjugated antisense oligonucleotide in rats and monkeys. *Mol. Ther. Nucleic Acids* 5, e319 (2016).

Xenobiotica
the fate of foreign compounds in biological systems

ISSN: (Print) (Online) Journal homepage: www.tandfonline.com/journals/ixen20

Rapid determination of the pharmacokinetics and metabolic fate of gefitinib in the mouse using a combination of UPLC/MS/MS, UPLC/QToF/MS, and ion mobility (IM)-enabled UPLC/QToF/MS

Billy J. Molloy, Adam King, Lauren G. Mullin, Lee A. Gethings, Robert Riley, Robert S. Plumb & Ian D. Wilson

To cite this article: Billy J. Molloy, Adam King, Lauren G. Mullin, Lee A. Gethings, Robert Riley, Robert S. Plumb & Ian D. Wilson (2021) Rapid determination of the pharmacokinetics and metabolic fate of gefitinib in the mouse using a combination of UPLC/MS/MS, UPLC/QToF/MS, and ion mobility (IM)-enabled UPLC/QToF/MS, Xenobiotica, 51:4, 434-446, DOI: 10.1080/00498254.2020.1859643

To link to this article: https://doi.org/10.1080/00498254.2020.1859643

XENOBIOTICA
2021, VOL. 51, NO. 4, 434–446
https://doi.org/10.1080/00498254.2020.1859643

Taylor & Francis
Taylor & Francis Group

RESEARCH ARTICLE

Rapid determination of the pharmacokinetics and metabolic fate of gefitinib in the mouse using a combination of UPLC/MS/MS, UPLC/QToF/MS, and ion mobility (IM)-enabled UPLC/QToF/MS

Billy J. Molloy[a], Adam King[a], Lauren G. Mullin[a], Lee A. Gethings[a], Robert Riley[b], Robert S. Plumb[c] and Ian D. Wilson[d]

[a]Waters Corporation, Wilmslow, UK; [b]Evotec (UK), Ltd., Abingdon, UK; [c]Waters Corporation, Milford, MA, USA; [d]Computational and Systems Medicine, Department of Metabolism, Digestion and Reproduction, Imperial College London, London, UK

ABSTRACT

1. The metabolism and pharmacokinetics of gefitinib (Iressa®, N-(3-chloro-4-fluorophenyl)-7-methoxy-6-(3-morpholino-propoxy)quinazolin-4-amine), a selective thymidylate kinase inhibitor for the epidermal growth factor receptor (EGFR), was studied after IV and PO administration to male C57BL6 mice at 10 and 50 mg/kg respectively.
2. The pharmacokinetics and metabolism of gefitinib were investigated using a range of rapid UHPLC-MS and UHPLC-IM-HRMS methods, using both reversed-phase (RP) and hydrophilic interaction liquid chromatography (HILIC), to rapidly determine the drugs pharmacokinetics and metabolic fate.
3. Rapid oral absorption resulted in peak plasma concentrations at 1 h of ca. 7 μg/mL, that declined with a half-life of 3.8 h (2.6 h for the IV route), and providing an estimated oral bioavailability of 53%. Gefitinib itself was the major circulating drug-related compound in plasma extracts, with a total of 11 metabolites identified.
4. The urinary profiles determined using both HILIC and RP-UPLC-IM-MS detected gefitinib and 10 metabolites or 15 metabolites respectively including the detection of a number of novel glucuronide conjugates.
5. Despite rapid, sub 5 min, LC profiling methods being employed metabolite coverage was shown to be high and compared well with that of previous studies.

ARTICLE HISTORY
Received 30 October 2020
Revised 30 November 2020
Accepted 1 December 2020

KEYWORDS
Gefitinib; pharmacokinetics; metabolite profiling; novel conjugates; ion mobility

Introduction

The anilinoquinazoline drug gefitinib (Iressa®, N-(3-chloro-4-fluorophenyl)-7-methoxy-6-(3-morpholino-propoxy)quinazolin-4-amine Figure 1) is a thymidylate kinase inhibitor that is selective against the epidermal growth factor receptor (EGFR). Gefitinib was developed for the treatment of cancer and has been shown to be active against non-small cell lung cancer (NSCLC) in patients with sensitive mutations of EGFR (e.g. Cohen *et al*. 2004, Maemondo *et al*. 2010, Dhillon 2015). Previous studies have shown that gefitinib is well absorbed following oral administration, with good bioavailability, but undergoes extensive metabolism. Metabolism is complex, *in vitro* and *in vivo*, involving multiple oxidations by CYPs 3A4, 3A5 and 2D6 (primarily 3A4) (McKillop *et al*. 2004c, 2005), with metabolism occurring at many sites on the molecule. These biotransformations include oxidation of the morpholine ring, defluorination and O-demethylation (McKillop *et al*. 2004c, 2005, Liu *et al*. 2015, Wang *et al*. 2020). *In vitro* studies have shown that CYP3A4 was involved in the biotransformation of gefitinib to produce metabolites of M537194, M608236 and M387783, while CYP2D6 has been shown to be responsible for the reaction leading to the formation of the major O-desmethyl metabolite (M523595) (McKillop *et al*. 2004c, 2005; Li *et al*. 2007). Numerous validated methods for the quantification of gefitinib and M523595, as well as other metabolites, have been reported (e.g. Jones *et al*. 2002, McKillop *et al*. 2004a, Zhao *et al*. 2005, Wang *et al*. 2011, Sparidans *et al*. 2016, Zheng *et al*. 2016, Guan *et al*. 2019). In addition, a number of metabolic profiling studies undertaken used chromatographic methods of 15 (e.g. Wang *et al*. 2020) to 55 min (McKillop *et al*. 2004b) duration to generate the MS and MS/MS spectral quality for confident drug metabolite identification. However, continuing developments in chromatography and mass spectrometry, combined with the introduction of novel technologies such as ion mobility spectrometry, offer significant opportunities to improve throughput to and increase the efficiency of modern drug discovery.

CONTACT Lauren Mullin lauren_mullin@waters.com Waters Corporation, Stamford Avenue, Altrincham Road, Wilmslow SK9 4AX, UK; Ian D. Wilson i.wilson@imperial.ac.uk Computational and Systems Medicine, Department of Metabolism, Digestion and Reproduction, Imperial College London, South Kensington Campus, London, SW7 2AZ, UK

Supplemental data for this article can be accessed here.

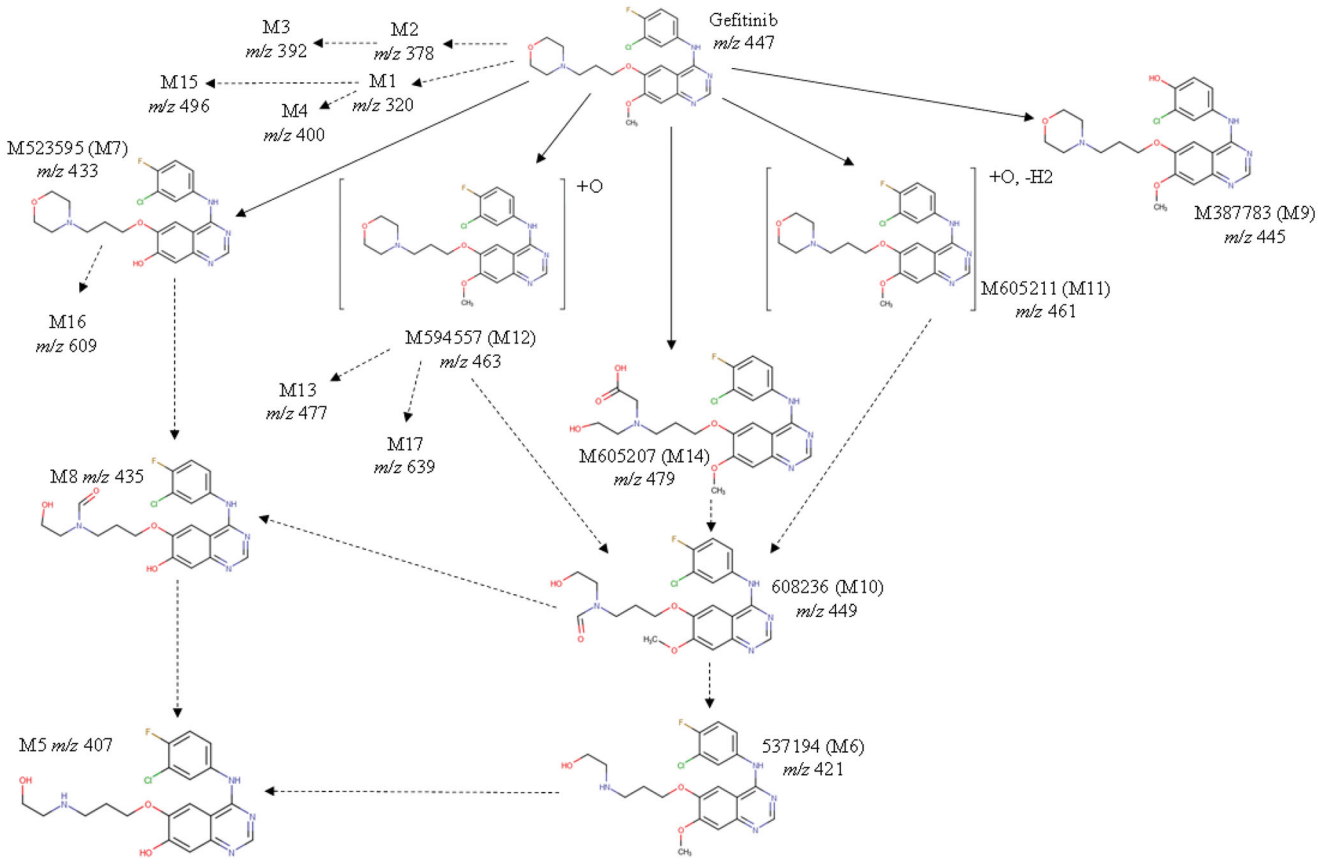

Figure 1. Metabolites of gefitinib previously identified by McKillop *et al.* (2004a, 2004b, 2004c) and others (Liu *et al.* 2015, Wang *et al.* 2020), as well as novel structures identified in this study. Structures not illustrated can be found in Figure S2.

Here we describe studies on the pharmacokinetics and metabolism of gefitinib, designed to evaluate the potential of short (sub 5 min) gradient UPLC/MS/MS, UPLC/QToF/MS and UPLC/IM/HRMS as a means of rapidly and efficiently defining the pharmacokinetics and metabolic fate of compounds.

Materials and methods

Solvents and chemicals

Solvents and chemicals including LC/MS grade water, methanol, acetonitrile, ammonium acetate, formic acid were all obtained from Sigma Aldrich (Dorset, UK). Instrument calibration used the 'Waters Major Mix IMS/ToF Calibration Kit for IMS' (Waters Corp., Milford, USA). Leucine-enkephalin (Sigma Aldrich) was used as the lock mass. Gefitinib drug substance, gefitinib-d6 (internal standard) and O-desmethyl gefitinib (M523595) were purchased from Toronto Research Chemicals (Toronto, Canada).

Study conduct

The study was performed using 30 male C57Bl/6JRj mice, aged 9 weeks and weighing between 20.3 and 26.5 g at Evotec SAS (Toulouse, France) after management review and in accordance with National and EU guidelines. Doses were chosen based on those used in published studies (e.g. Zheng *et al.* 2016, Barzi *et al.* 2017). The study was carried out using oral (PO) and intravenous (IV) administration. For IV dosing the drug was administered as a clear solution in HPBCD/pH 4.0 50 mM acetate buffer (10%/90% w/v). PO Administration was as a homogeneous white suspension formulated in hydroxypropylmethyl cellulose (HPMC)/polysorbate80/water (0.5%/0.1%/99.4%; w/w/v). Samples were transferred from the study site to Waters Corp. (Wilmslow, UK) on solid carbon dioxide.

IV administration of gefitinib (10 mg/kg)

For IV administration gefitinib was dosed, formulated at a 1 mg/mL, to 10 male C57Bl/6JRj mice, divided into 2 groups of 5. All animals received a single 10 mg/kg (10 mL/kg) dose of gefitinib via the tail vein. The mice were housed, in 2 groups of 5, in meta

bowls for the collection of urine and faeces. Blood samples (50 µL) were obtained at pre-dose, 0.10, 0.25, 0.5, 0.75, 1, 2, 3, 8, and 24 h post-dose, or 100 µL at termination (1 animal at each of 0.5, 1, 2, 3, and 24 h post-dose) with 2 mice sampled at each sampling time (each mouse was sampled twice during the course of the study). Blood was collected from the tail vein into Minivette POCT HeLi coated capillaries. Plasma samples were prepared by centrifugation at 2500 *g* with the samples transferred to Eppendorf vials and stored at −80 °C until analysis.

In addition to blood, urine was collected at Predose (overnight before dosing) and over the periods 0–3, 3–8 and 8–24 h post-administration. Faeces were collected at Predose (overnight before dosing) and 0–8 and 8–24 h post-dosing. All samples were stored on receipt at −80 °C until analysis as described below.

Oral (PO) administration of gefitinib (50 mg/kg)

For PO administration 20 male C57Bl/6JRj mice were divided into a gefitinib dosed group ($n = 10$) and a vehicle dose group ($n = 10$) which were each subdivided divided into 2 groups of 5. Mice were housed in two meta bowls for collection of urine and faeces. Gefitinib was administered at 50 mg/kg formulated at 5 mg/mL (10 mL/kg) by gavage. Samples (plasma, urine, faeces, organs etc.) were collected, prepared and stored as described for the IV arm of the study above.

Plasma sample preparation for pharmacokinetic analysis

Mouse plasma samples (10 μL) were prepared by protein precipitation with 40 μL of methanol containing 30 ng/mL of internal standard (gefitinib-d6). After vortex mixing the samples were centrifuged at 25 000 *g* for 5 min. For ULPC/MS/MS analysis an aliquot of 10 μL of the resulting supernatant was diluted with 490 μL of 1:1 v/v methanol:water. A combined calibration curve was constructed in control C57Bl mouse plasma, containing both gefitinib and the O-desmethyl metabolite (M523595), covering the range 0 to 7500 ng/mL. This comprised a solvent blank (1:1 v/v methanol:water), double blank (extracted matrix with no internal standard), matrix blank (extracted matrix with internal standard) and 7 concentrations of the two analytes (0, 15, 75, 300, 750, 1500, 3000, and 7500 ng/mL). In addition to the standard curve, combined quality control samples were prepared containing both gefitinib and its O-desmethyl metabolite (M523595) at 30, 1000 and 6000 ng/mL. Following column equilibration and pre-analytical system checks, the run order used for analysis was as follows. Solvent blank; double blank; matrix blank; QCs (30, 1000, and 6000 ng/mL); matrix blank; calibration curve samples (0, 15, 300, 1500, and 7500 ng/mL), matrix blank; extracted plasma samples; matrix blank; the remaining calibration samples (0, 75, 750, and 3000 ng/mL); matrix blank; another set of QCs (30, 1000, and 6000 ng/mL); and finally another matrix blank. For batch acceptance, the QC samples had to be within ±15% of the nominal value, with at least 2/3 achieving this, with no more than one failure at each level.

UPLC/MS/MS sample analysis for PK determination

Plasma extracts (2 μL) were analysed using an Acquity I-Class UPLC system connected to a Xevo TQ-S Micro tandem quadrupole mass spectrometer (Waters Corporation, Wilmslow, UK). UPLC separation was performed using a 2.1 × 100 mm BEH C18 1.7 μm column (Waters Corporation, Milford, USA) maintained at 60 °C at a flow rate of 650 μL/min. The linear reversed-phase gradient used was composed of 0.1% formic acid (v/v) in 10 mM aqueous ammonium acetate (solvent A) and 0.1% formic acid (v/v) in acetonitrile (solvent B). The gradient profile started at a composition of 5% solvent B and increased to 50% solvent B over 2.9 min. This was followed by a 1.5 min column flush step of 95% solvent B, and then re-equilibration (0.6 min) to the starting conditions before the next injection. MS analysis was performed at unit mass resolution using positive electrospray ionisation (+ve ESI) at a capillary voltage of 2.0 kV, collision energy of 33 eV, a cone voltage of 30 V with the source temperature set to 150 °C. The cone gas flow was 50 L/h and the gas used was nitrogen. The desolvation gas temperature was 650 °C, the desolvation gas flow was 1000 L/h. The data were collected using MassLynx V 4.1 (Waters Corp., Milford, USA). MRM (Multiple Reaction Monitoring) transitions monitored for the MS detection of gefitinib and its metabolites were as follows. Gefitinib (446.62 => 128.23); gefitinib-d6 [IS] (452.62 => 134.23); O-desmethyl gefitinib (432.62 => 128.23); M537194 (421.62 => 320.33); M37783 (444.62 => 128.23) and finally M605211 (460.62 => 142.23).

Metabolite profiling and identification of gefitinib metabolites in plasma

Samples for metabolite detection and identification were prepared by pooling equal amounts (2 μL/sample) for the period 45–120 min for the PO and 30–60 min for the IV routes, respectively, corresponding to the observed C_{max} time points for each route. These samples were then mixed with 4 volumes of methanol to precipitate proteins. After vortex mixing and centrifugation at 25 000 *g* for 5 min, 10 μL of the resulting supernatant was diluted to 500 μL with 490 μL of 1:1 v/v methanol:water to provide a sample suitable for analysis. Chromatographic profiling was performed using the Acquity I-Class UPLC system connected to a Synapt XS MS (Waters Corporation, Wilmslow, UK). The separation was performed using a 2.1 × 100 mm BEH C18 1.7 μm UPLC column maintained at 60 °C at a flow rate of 650 μL/min using the same chromatographic separation as that used to perform the quantitative determinations described above. For sample analysis, an injection volume of 2 μL was used.

IM and MS data were acquired in positive electrospray ionisation (+ve ESI) mode with a capillary voltage of 3.0 kV and a source temperature set at 100 °C. The cone gas flow was 50 L/h and the gas used was nitrogen. The desolvation gas temperature was 300 °C, the desolvation gas flow was 600 L/h and the nebuliser gas flow was 6 bar. Following ionisation, the ions were passed into the ion mobility cell. The helium cell (situated at the front of the drift cell) gas flow was fixed at 180 mL/min, and the IMS gas was nitrogen with a flow fixed at 90 mL/min. A wave velocity of 650 m/s, a wave height of 40 V, an EDC delay coefficient of 1.54 V, a bias of 3, a mobility RF offset of 250, an RF offset of 300, an IMS wave delay of 1000 μs and a DC entrance of 20 were applied. The IMS was calibrated using the Waters Major Mix IMS/ToF Calibration Kit for IMS. Following IM the ions were

subjected to MS^E acquired over the *m/z* range 50-1200. Continuum model was applied to the experiment with a low collision energy of 20 eV and an elevation for the high collision energy of 40 eV. Leucine enKcephalin (MW = 555.62) was used as lock mass with a scan collected every 30 s and a cone voltage fixed at 40 V. The data were collected using MassLynx vs.4.2 software (Waters Corp., Wilmslow, UK) and processed using UNIFI Scientific Information System V 1.9.4 (Waters Corp., Milford, USA).

Metabolite profiling and identification for gefitinib metabolites in urine

Metabolite profiling of urine was performed using both reversed-phase (RP) and hydrophilic liquid interaction chromatography (HILIC). For analysis by both modes of LC 20 μL of each urine sample was mixed with 20 μL of LCMS grade water in 1.5 mL centrifuge tubes then 350 μL of LCMS grade ACN. The samples were vortex mixed and left at 2-8 °C for 10 min and then centrifuged at 13 000 rcf for 10 min and 150 μL of the supernatant was removed for HILIC analysis.

For analysis by RP-UPLC 100 μL of the supernatant was further diluted 1:1 with LCMS grade water to increase the aqueous composition of the sample prior to the analysis.

Urine samples prepared for HILIC analysis were analysed as described by Spagou *et al*. (2011) using an I-Class ACQUITY PLUS UPLC comprised of a binary solvent manager, sample manager and column oven (Waters Corp., MA, USA). Chromatography was performed using a 2.1 × 100 mm, 1.7 μm BEH HILIC ACQUITY column (Waters Corp., MA, USA) with mobile phases consisting of 0.1% (v/v) formic acid and 10 mM ammonium acetate in 95:5, ACN:Water (solvent A) and 0.1% (v/v) formic acid with 10 mM ammonium acetate in 50:50, ACN:Water (solvent B). The separation was performed at 40 °C and 0.4 mL/min and 3 μL of each sample were injected. Profiling was performed using a solvent gradient starting at 1% solvent B (1 min), followed by a linear increase to 100% (11 min) then returning to the initial conditions (0.1 min) for re-equilibration (4 min) before the next injection.

Similarly, the RP-profiling of urine also took place on an I-Class ACQUITY PLUS UPLC as described above, with separation on a 2.1 × 100 mm, 1.8 μm HSS T3 ACQUITY column (Waters Corp., Milford, USA). The mobile phases consisted of 0.1% (v/v) formic acid in water (solvent A) and 0.1% (v/v) formic acid in ACN (solvent B). The separation was performed at 40 °C and 0.5 mL/min. Samples of 3 μL were analysed via a solvent starting at 1% solvent B (1 min), increasing in a series of linear gradients, first to 15% (3 min), then 50% (6 min) and finally 95% (9 min) which was held for 1 min and then returned to 0.1% B (0.1 min) for re-equilibration (2 min) (Want *et al*. 2010).

For HILIC profiling the MS data were collected using ESI positive (ESI+) mode using a SYNAPT XS mass spectrometer (Waters Corp., Wilmslow, UK). Data were collected in continuum mode using $HDMS^E$ over the *m/z* range 50–1200 with a scan time of 0.1 s (Rodriguez-Suarez *et al*. 2013, Rainville *et al*. 2017). Low energy (MS1) utilised low collision energy of 4 eV, whilst elevated energy (MS2) provided fragment ion data using a linear collision energy ramp of 19–45 eV. Leucine enkephalin at a concentration of 200 pg/μL was infused at a flow rate of 20 μL/min via the lock spray interface and acquired every 30 s as lock mass to ensure mass accuracy. The capillary voltage was 1.0 kV (ESI+), cone voltage was 25 V, source temperature was set at 120 °C with a cone gas (nitrogen) flow rate of 50 L/h, desolvation gas temperature of 600 °C and nebulisation gas (nitrogen) flow of 800 L/h. Ion mobility settings consisted of the ion mobility T-wave velocity at 650 m/s and pulse height of 40 V. Nitrogen was implemented as the drift gas and set to a flow rate of 180 mL/min. The ion mobility device was calibrated (CCS range = 130–306 $Å^2$) using the Major Mix IMS calibration kit (Waters Corp., Wilmslow, UK) to allow for CCS values to be determined in nitrogen. The TOF was also calibrated over the acquisition mass range prior to analysis using 0.5 mM sodium formate. Data were collected using MassLynx vs.4.2 software (Waters Corp., Wilmslow, UK).

For RP-LC profiling of urine, the MS data were also collected using an SYNAPT XS mass spectrometer (Waters Corp., Wilmslow, UK) within positive ESI. The instrument was operated in resolution (V optics) mode with ion mobility enabled for all experiments. Data were collected in continuum mode using $HDMS^E$ over the *m/z* range 50–1200 with a scan time of 0.1 s (Rodriguez-Suarez *et al*. 2013, Rainville *et al*. 2017). Low energy (MS1) utilised low collision energy of 4 eV, whilst elevated energy (MS2) provided fragment ion data using a linear collision energy ramp of 19–45 eV. Leucine enkephalin at a concentration of 200 pg/μL was infused at a flow rate of 20 μL/min via the lock spray interface and acquired every 30 s as lock mass to ensure mass accuracy. The capillary voltage was 1.0 kV (ESI+), cone voltage was 25 V, source temperature was set at 120 °C with a cone gas (nitrogen) flow rate of 50 L/h, desolvation gas temperature of 600 °C and nebulisation gas (nitrogen) flow of 800 L/h. Ion mobility settings consisted of the ion mobility T-wave velocity at 650 m/s and pulse height of 40 V. Nitrogen was implemented as the drift gas and set to a flow rate of 180 mL/min. The ion mobility device was calibrated (CCS range = 130–306 $Å^2$) using the Major Mix IMS calibration kit (Waters Corp., Wilmslow, UK) to allow for CCS values to be determined in nitrogen (reported as $^{TW}CCS_{N2)}$. The TOF was also calibrated over the acquisition mass range prior to analysis using 0.5 mM sodium formate. Data were collected and visualised using MassLynx vs.4.2 software (Waters Corp., Wilmslow, UK).

Data analysis for metabolite identification

Gefitinib and its metabolites we identified by a combination of the presence of the Cl isotope pattern, authentic standards and the use of accurate mass MS, MS/MS values for common fragment ions of gefitinib. Measured CCS values for putative metabolite structures were also compared with theoretically derived CCS values using an in house machine learning program (see Nye *et al*. 2019).

Results and discussion

As has been amply demonstrated in several studies, starting with the original publications by McKillop *et al.* (2004c, 2005, 2006), the metabolism of gefitinib results in the production of a variety of structures (Figure 1), and has led to several different naming schemes for these metabolites in different publications. In order not to cause further confusion we have, in general, adopted the long-established numbering system used by McKillop *et al.* (2004a, 2004b, 2004c) for naming known metabolites. However, for convenience, have also used (with suitable cross-referencing) a numbering system within this manuscript, based on increasing mass, to annotate metabolite peaks in, for example, Figures and Tables, etc.

Drug and metabolite bioanalysis

Since its discovery, numerous methods have been described for the bioanalysis of gefitinib in plasma from a variety of species (e.g. Jones *et al.* 2002, McKillop *et al.* 2004b, Zhao *et al.* 2005, Wang *et al.* 2011, Sparidans *et al.* 2016; Zheng *et al.* 2016, Guan *et al.* 2019). For this study, the pharmacokinetic determination of gefitinib and its major circulating metabolites (the O-desmethyl (M523595) and the morpholino carbonyl compound (M605211)), a rapid 4.4 min UPLC-MS/MS method was used. The concentrations of these analytes in mouse plasma were determined by means of a 'fit for purpose' assay using 10 µL of mouse plasma/sample. Gefitinib, which was quantified via the use of a d6 internal standard, eluted with a retention time of 1.88 min whilst the major O-desmethyl metabolite, which was quantified against a standard curve produced with an authentic standard, eluted slightly earlier at 1.76 min (Figure 2). The morpholino carbonyl compound (M605211), which eluted at 2.45 min, and for which no standard was available, was semi-quantified using the gefitinb-d6 and assuming a similar relative response to gefitinib. Similarly, two further, less abundant, gefitinib metabolites, the desfluoro-phenol (M387783) and M537194 (resulting from the ring-opening and partial degradation of the morpholine ring, see Figure 1), for which no authentic standards were available, were semi-quantified (when detected) using the gefitinb-d6 and assuming a similar relative response to gefitinib. The method, based on protein precipitation with 4 volumes of methanol and dilution, was found to be linear for gefitinib ($R^2 = 0.9994$) and its O-desmethyl metabolite over the range 5–7500 ng/mL using $1/\times$ weighting and internal standard calibration. Following PO administration gefitinib, and its various metabolites noted above, were detectable in the samples from dosed animals over much, or all, of the time course of the study. In the case of IV dosing, gefitinib was detectable in plasma only up to 6 h post dose but not in the terminal 24 h sample. The drug was not detected in samples from the vehicle dosed controls. All of the QC samples used to monitor the assay were within the acceptance criteria of ±15% of their nominal values.

Pharmacokinetic analysis

Following IV administration at 10 mg/kg, gefitinib plasma concentrations as determined by UPLC/MS/MS, declined bi-exponentially with an estimated clearance of 14.4 mL/min/kg. The volume of distribution at steady-state was calculated as 2.8 L/kg and the terminal half-life was 2.6 h. These parameters are broadly consistent with data reported in previous mouse PK studies (Zhou *et al.* 2012, Bi *et al.* 2016, Zheng *et al.* 2016). Gefitinib was rapidly and extensively metabolised to the O-demethylated metabolite (M523595) while plasma concentrations of the morpholino carbonyl metabolite (M605211) rose more steadily. The T_{max} for both of these metabolites was 0.75 h with exposures ($AUC_{0\text{-inf}}$) of 917 and 812 ng/mL h (approximately 8 and 7% of the parent compound, respectively). The M387783 and M537194 metabolites were not detectable after IV dosing of gefitinib at this level.

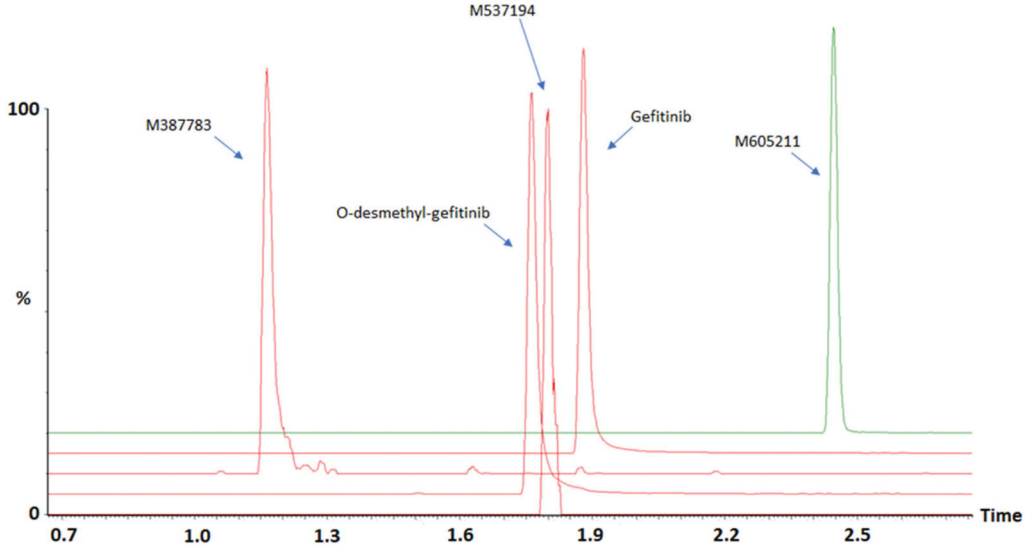

Figure 2. Multiple reaction monitoring mass chromatograms for the UPLC-MS of gefitinib and its O-desmethyl metabolite (M523595) together with the morpholino carbonyl metabolite (M605211), M387783, and M537194 in plasma extracts. Metabolite numbering refers to those in the original McKillop *et al.* (2004a, 2004b, 2004c) publications.

Table 1. Summary of PK parameters for gefitinib and selected metabolites.

	Gefitinib		O-demethylated M523595		Morpholino carbonyl M605211		Desfluoro-phenol M387783	
Parameter	IV	PO	IV	PO	IV	PO	IV	PO
AUC_{0-t} (ng/mL × h)	10 421	43 488	801	5760	714	1808		64
AUC_{0-inf} (ng/mL × h)	11 604	43 984	917	5894	812	2522		128
Cl (mL/min/kg)	14.4							
V_{ss} (L/kg)	2.8							
V_z (L/kg)	3.2							
$T^1/_2$ (h)	2.6	3.8	2.8	4.8	2.6	4.7		2.9
C_{max} (ng/mL)		7031		1153		520		31
T_{max} (h)		1		0.75		1		0.75
Bioavailability (%)		53						

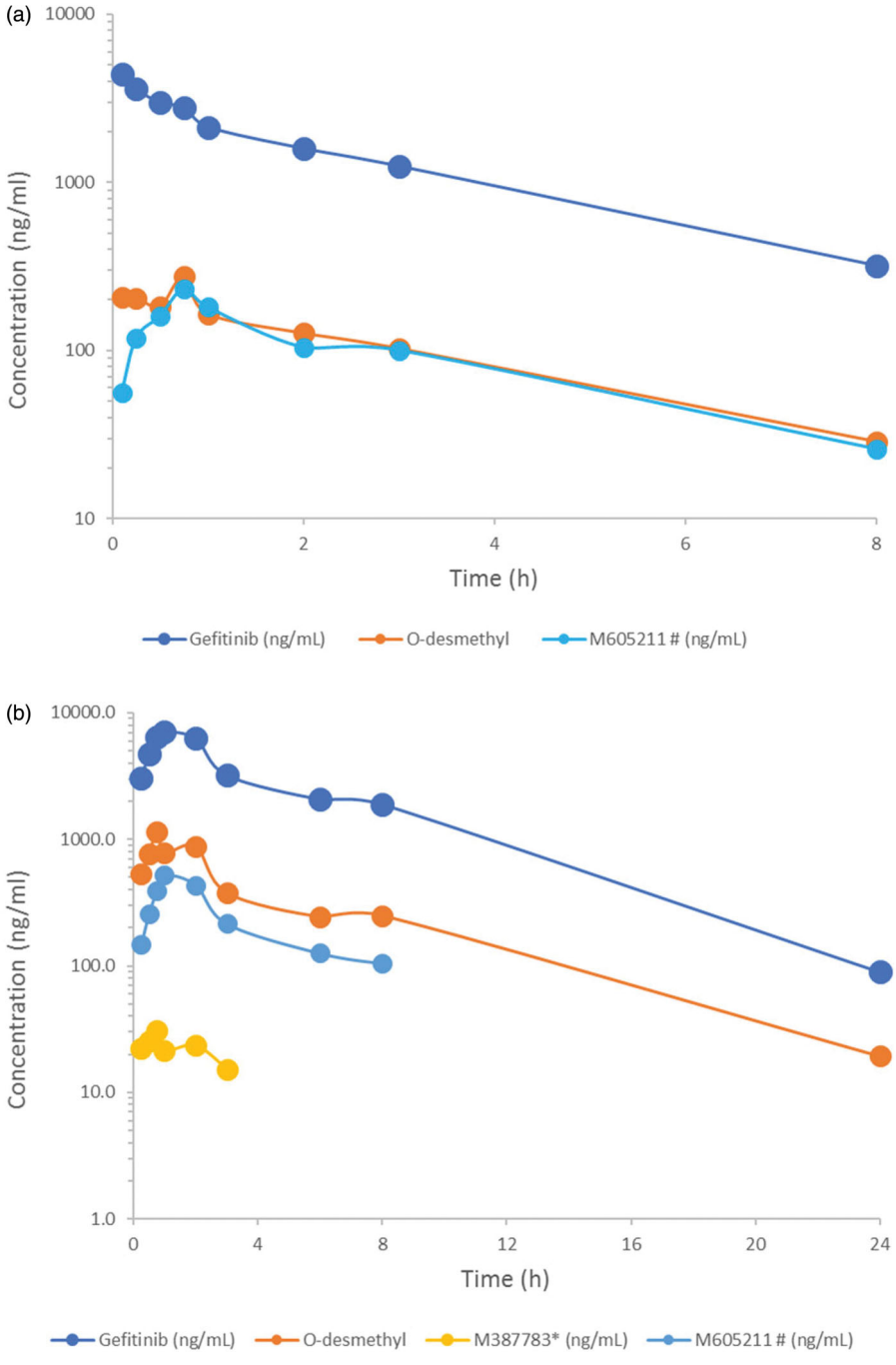

Figure 3. Plasma concentrations of gefitinib and selected metabolites. IV (10 mg/kg) (upper) and PO (50 mg/kg) (lower).

Table 2. Gefitinib and metabolites in pooled mouse plasma extracts prepared from samples taken from animals from both IV and oral doses.

Compound	Expected *m/z**	Description	Obs. RT plasma (min.)	Obs. CCS (Å^2) avg. plasma	Obs. fragments *m/z*
Gefitinib	447.1594	Drug substance	1.93	204.9	100.0757, 128.1070, 320.0597
M1	320.0597	Cleavage of ether group resulting in loss of alkane chain and morpholine group	2.19	167.8	304.0284
M2	378.1015	Cleavage of morpholine group followed by hydroxylation	2.36	186.1	305.0362, 304.0284
M3	392.0808	Cleavage of morpholine group followed by carboxylic acid formation	2.33	187.91	318.0440
M5	407.1281	O-desmethylation followed by morpholine ring cleavage resulting in loss of C_2H_4	1.72	197.6	306.0425
M6 (M537194)	421.1437	Morpholine ring cleavage resulting in loss of C_2H_4	1.82	197.7	320.0597
M7 (M523595)	433.1437	O-desmethylation	1.82	202.4	100.0570, 128.107, 305.0362, 346.0753
M10 (M608236)	449.1392	Morpholine ring cleavage resulting in loss of CH_2 and aldehyde formation	2.26	207.6	130.0863, 320.0597
M11 (M605211)	461.1386	Addition of oxygen and loss of two hydrogens on morpholine ring	2.51	205.6	142.0862, 320.0597, 86.0600
M12 (M594577)	463.1543	Hydroxylation	1.98	203.44	144.1019
M13	477.1336	Dihydroxylation	2.31	209.2	158.0812, 320.0597

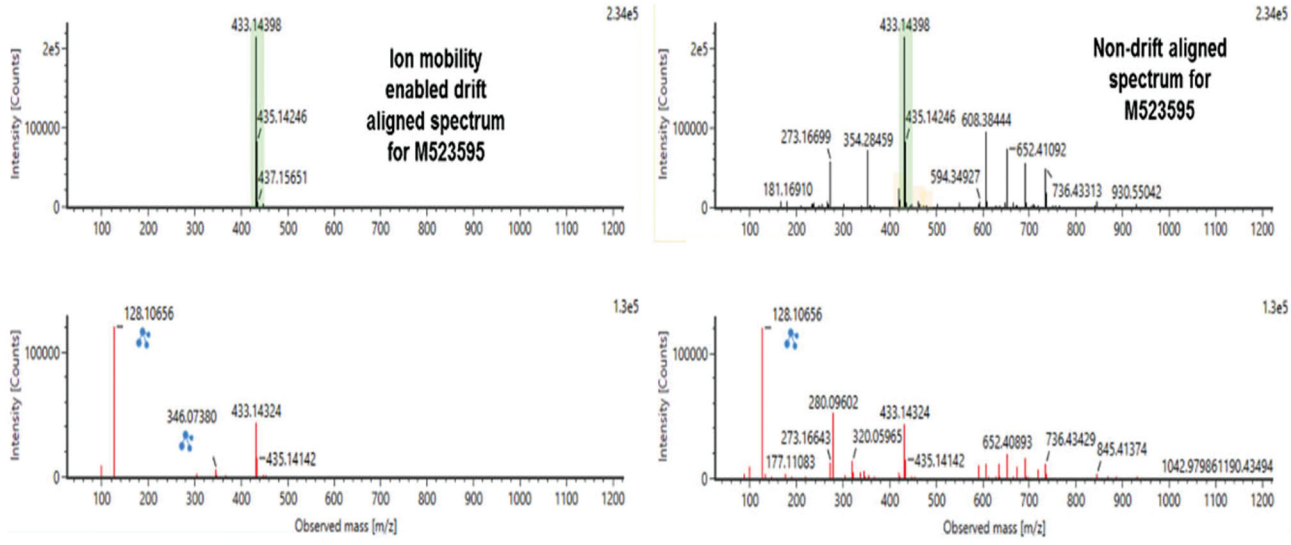

Figure 4. HDMS^E mass spectra for the O-desmethyl metabolite (M523595 (M7)) obtained either with IM enabled mobility generated drift-aligned precursor and product ion spectra (left panels, upper: MS; lower: MS^E) or without IM filtering (right panels, upper: MS; lower: MS^E). The improvement in spectral quality for the IM-enabled data is clear.

The O-demethylated metabolite (M523595) and the morpholino carbonyl metabolite (M605211) were also detected in blood following IV dosing (T_{max} 0.75 h) with exposures ($AUC_{0\text{-}inf}$) of 917 and 812 ng/mL x h (approximately 8 and 7% of the parent compound, respectively). The M387783 and M537194 metabolites were not detectable after IV dosing of gefitinib at this level.

Maximal observed blood concentrations of gefitinib after PO dosing (50 mg/kg) of 7031 ng/mL were reached after 1 h. Bioavailability was estimated at 53% (using AUC_{0-t}) and the oral half-life was estimated at 3.8 h. Circulating concentrations of the O-demethylated metabolite and M605211 were again detectable along with the desfluoro phenolic metabolite M387783 (relative exposures to these metabolites were 2–13% of the parent compound). Peak blood concentrations of these metabolites were observed 0.75–1 h after dosing. M537194 was not detected. Interestingly, the concentration-time profiles following PO dosing at this level suggested the presence of a minor second peak at around 8 h for gefitinib and the O-demethylated metabolite as reported previously (Zheng *et al*. 2016). While several phenomena (e.g. enterohepatic circulation) could contribute to such an effect, care should be exercised so as to not over-interpret this observation.

These results are summarised in Table 1, and illustrated in Figure 3 (dose normalised profiles are provided in the Supplementary information, Figure S1).

Gefitinib metabolite profiling and identification in plasma

In order to obtain metabolite profiles pooled plasma extracts were prepared for the 2–6 h time point samples (corresponding to the peak oral plasma concentrations of gefitinib) for

analysis by LC combined with IM-enabled MS. The chromatographic separation was the same as that used for gefitinib bioanalysis in plasma with the addition of an IM-separation prior to MS. This IM step was done in order to improve mass spectral quality as the IM step provides additional separation of co-eluting contaminants or unrelated ions from those of the drug-related metabolites. In addition, the use of a travelling wave (TW) IM device also provides collision cross-section (CCS) data which can be of value in structural characterisation. Gefitinib itself has, because of its atomic composition ($C_{22}H_{24}ClFN_4O_3$) a monoisotopic molecular mass of 446.1524 Da and its MS spectrum is characterised by a distinctive chlorine isotope pattern, greatly facilitating the detection of drug-related compounds. The drug had a base peak at *m/z* 447.1594 in positive ESI corresponding to the $[M+H]^+$ ion and an observed CCS value of 204.9 Å^2 (Table 2). When fragmented gefitinib produced two major product ions at *m/z* 320.0597 and *m/z* 128.1070 (Table 2 and Figure S2) corresponding to the loss of the 3-morpholinopropoxy-side chain substituent and the corresponding N-(3-chloro-4-fluorophenyl)-7-methoxy-6) quinazolin-4-amine fragment. The data obtained from the metabolite profiling of the plasma extracts were searched and the metabolites identified on the basis of, for example, of precursor and product ions and the possession of an isotope distribution pattern consistent with a single chlorine atom (which of course would exclude metabolites where dechlorination had occurred). By this means, in addition to gefitinib itself (which was seen as by far the major drug-related signal in plasma extracts) the O-desmethyl metabolite (M523595, *m/z* 433.1439 (M14), denoted as M7 in Figure 1) was identified as a major circulating metabolite, showing a prominent fragment ion at *m/z* 128.107 (Figure 4). The other known major circulating metabolite M605211 ('M11' in Figure 1, Table 2), a morpholino carbonyl biotransformation product showed, in addition to its expected $[M+H]^+$ ion at *m/z* 461.1386, three main product ions at *m/z* 320.0597 amu, providing an atomic composition of $C_{15}H_{12}ClFN_3O_2$ (mass error 0.9mDa) corresponding to the 4-quinazolinamine, N-(3-chloro-4-flurophenyl)-7-methoxy portion of the molecule, another at *m/z* 142.861, $C_7H_{12}NO_2$ (mass error 0.1 mDa) and *m/z* 86.0595, C_4H_8NO (mass error 0.5 mDa) (Figure S2(c)). In addition to these compounds, 10 previously documented metabolites (McKillop *et al.* 2005, Liu *et al.* 2015), showing a range of oxidative biotransformations, were also identified as indicated in the mass chromatogram shown in Figure 5. These metabolites are listed in Table 2. Support for these identifications, as well as partial localisation of metabolic transformation, was provided by the observed fragment ions and accurate mass measurement of all ions. This information was used to produce structures for the identifications described below and shown in Figure 1 (representative mass spectra are provided in Supplementary Figures S2(b–s)).

LC-IM-MS-based metabolite characterization

A particular challenge, in both 'manual' and automated, software-driven metabolite identification, is in obtaining interference-free MS spectra for interpretation. As is becoming more

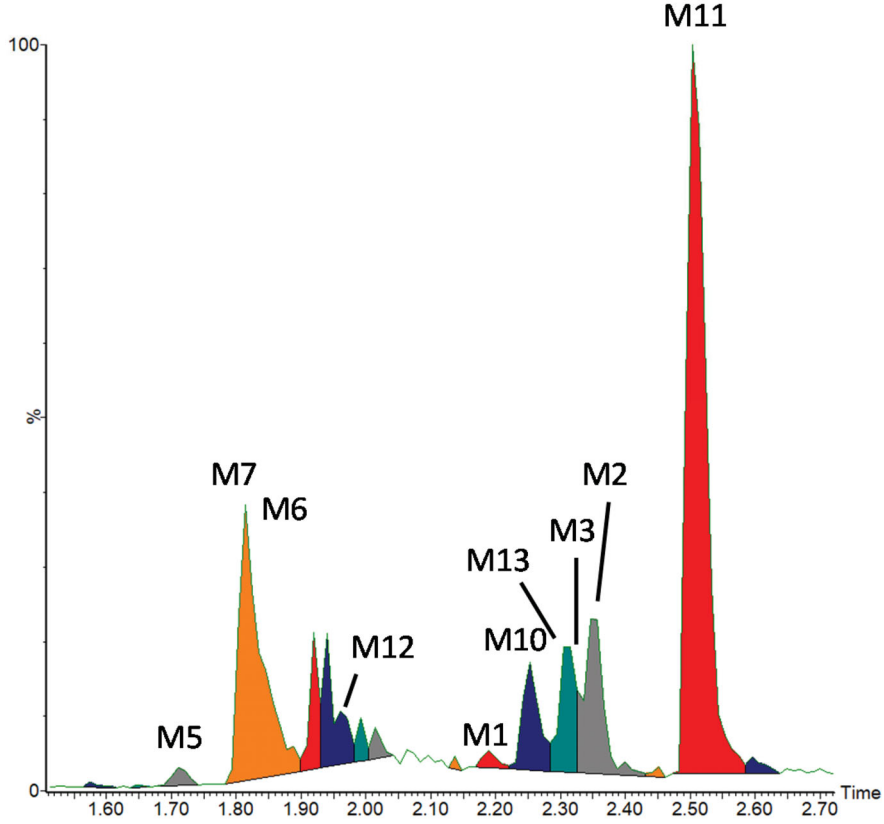

Figure 5. Reconstructed ion chromatogram showing the gefitinib metabolite profile for pooled protein-precipitated plasma extracts obtained for PO-dosed male C57Bl6 mice (for key to peak identities see Table 2).

Table 3. Gefitinib and metabolites in pooled mouse urine samples prepared from samples taken from animals from both IV and oral doses.

Compound	Expected *m/z*	Description	Obs. RT urine RP (min.)	Obs. RT urine HILIC (min.)	Obs. CCS (Å^2) avg. urine RP method	Obs. CCS (Å^2) avg. urine HILIC method	Obs. fragments *m/z*
Gefitinib	447.1594	Drug substance	4.5	1.27	205.9	206.4	100.0757, 128.1070
M1	320.0597	Cleavage of ether group resulting in loss of alkane chain and morpholine group	5.20	0.39	169.5	171.0	304.0284, 305.0362
M2	378.1015	Cleavage of morpholine group followed by hydroxylation	5.31	ND in POOL	187.5	ND in POOL	
M4	400.0165	M1 followed by sulphate formation	5.34	0.38	185.3	187.7	320.0597
M6 (M537194)	421.1437	Morpholine ring cleavage resulting in loss of C_2H_4	4.43	2.22	198.5	199.1	102.9130, 320.0597
M7 (M523595)	433.1437	O-desmethylation	4.46	3.79	203.5	202.4	
M8	435.1230	O-desmethylation and morpholine ring cleavage resulting in loss of CH_2 and aldehyde formation	5.14	ND in POOL	201.4	ND in POOL	
M9 (M387783)	445.1637	Oxidative defluorination	3.88	1.73	206.72	206.4	128.1070, 271.0588
M10 (M608236)	449.1392	Morpholine ring cleavage resulting in loss of CH_2 and aldehyde formation	5.18	0.57	207.6	207.5	130.0863, 320.0597
M11 (M605211)	461.1386	Addition of oxygen and loss of two hydrogens on morpholine ring	5.50	0.54	207.5	206.4	142.0862
M12 (M594577)	463.1543	Hydroxylation	4.60/4.79	2.10/2.39	204.7/210.3	204.4/209.6	144.1019/128.1070
M13	477.1336	Dihydroxylation	5.26	0.54	210.9	210.4	158.0812, 142.0862
M14 (M605207)	479.1492	Morpholine ring opening and carboxylic acid formation	4.66	3.34	212.7	214.3	160.0968
M15	496.0918	M1 followed by glucuronidation	4.48	2.51	211.2	211.8	320.0597
M16	609.1758	O-desmethylation and glucuronidation	4.28	3.78	232.4	231.94	433.1443
M17	639.1864	Hydroxylation and glucuronidation	4.15	3.19	246.0	245.6	463.1542

widely appreciated the incorporation of IM into the analytical workflow provides an extra, orthogonal, dimension of separation that complements that obtained from LC/MS. This separation (the 'drift time', or arrival time distribution (ATD)) is based on size, shape and charge and can be used to separate the ions of interest from co-eluting interferences, allowing it to be used as a 'filter' that removes unrelated signals in the resulting mass spectrum. An example of this enhanced spectral quality is shown in Figure 4, for the analysis of the O-desmethyl metabolite (M523595 (M7)). This clearly shows the presence of many coeluting ions in the 'unfiltered' MS and MS/MS data and the very significant improvement in the quality of the spectra obtained as a result of the use of IM-mobility generated drift-aligned precursor and product ion spectra. The drug metabolite-related *m/z* 346.0738 fragment peak was obscured in the conventional MS data shown in Table 3 but, in contrast, was easily observed in the IMS drift aligned data (Figure 4). This improved spectral quality clearly makes the task of confident metabolite identification simpler and hence faster.

Gefitinb metabolite profiling and identification in urine

As indicated in the experimental methods, metabolite profiling for urine was undertaken using both RP- and HILIC-based separations with IM-MS detection. The use of two different modes of LC was done with the aim of maximising the detection of gefitinib metabolites by exploiting their different retention mechanisms. Thus, whilst the expectation would be that metabolism generally results in compounds having a lower Log D than the parent drug, which will therefore mean that they elute earlier than the parent in an RP-LC separation this is not always the case. Indeed, this is well illustrated for the metabolites of gefitinib profiled in plasma where a similar number eluted after the drug as before it. On the other hand, in RP-based separations very polar conjugates are quite likely to elute at, or near, the solvent front, in areas where ion suppression is high and interfering contaminants are present that complicate both detection and interpretation of mass spectra. We conjectured that for these types of polar metabolite HILIC may provide a useful alternative to RP-separations as well as providing increased sensitivity, due to the more favourable ionisation properties of the high-organic eluents used for HILIC separation, when using ESI.

The reconstructed mass chromatograms obtained for both RP- and HILIC separations are illustrated in Figure 6(A,B). This profiling resulted in the detection of small amounts of gefitinib together with 15 metabolites in the case of RP and 13 for HILIC. The different chromatographic selectivities of the two systems are evident from both Figure 6(A,B) and Table 3 and, in our view, provides support for the concept of using both modes to ensure maximum metabolite coverage.

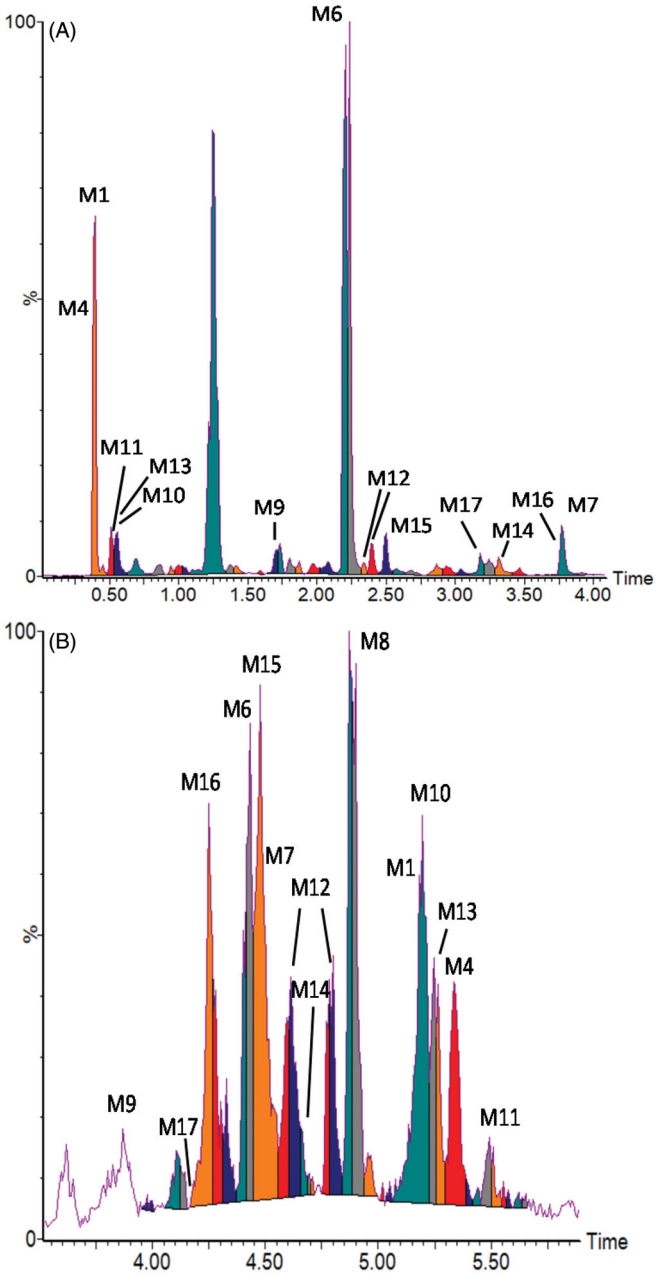

Figure 6. Reconstructed ion chromatogram of identified mouse metabolites of gefitinib in a urinary pool sample (both IV and PO dosed animals) obtained from the RPLC (A) and HILIC (B) profiling methods.

Of note is that, whilst many of the detected metabolites were also found in the plasma extracts a number of conjugated metabolites were detected which were unique to urine. These comprised 3 glucuronides and one sulphate conjugate and were characterised based on MS fragmentation, with suggested structures shown in Figure S2(q–s) for the glucuronides M15–17 and Figure 7 for the sulphate M4.

The application of IM-derived CCS values in metabolite profiling

In this work, as described above, we evaluated the use of ion mobility (IM) in metabolite profiling from the point of view of improving spectral quality via an enhanced resolution from co-eluting contaminants. In addition, we also examined the use of the $^{TW}CCS_{N2}$ value of metabolites as an aid to structure elucidation and metabolite identification. As indicated above the improvements to the spectral quality provided by the additional IM dimension of separation were of clear value for metabolite identification due to the removal of unrelated ions. In addition, and perhaps not unexpectedly, the measurements for the $^{TW}CCS_{N2}$ values of individual metabolites (which ranged from 169.5 to 246.0 Å) were conserved between both of the RP separations employed for profiling. In a similar fashion, the $^{TW}CCS_{N2}$ values were also conserved between the RP and HILIC methods, and both UPLC-QToF/MS and UPLC-IM-HRMS detected the same metabolites. This may be of value insofar as both MS and $^{TW}CCS_{N2}$ data can be combined to 'track' metabolites across different LC systems, and indeed laboratories. However, we were also interested in knowing if the $^{TW}CCS_{N2}$ values obtained here could be useful in helping to confirm, or discount, potential metabolite structures by aiding discrimination between different possible sites of metabolism (e.g. hydroxylation etc.). Obviously, it is often possible to pinpoint sites of metabolism such as hydroxylation, conjugation etc., based on mass spectrometric data, but this can be difficult where fragmentation is limited. If such is the case for any of the metabolites detected that are considered important, then their isolation (e.g. for NMR spectroscopy), or the synthesis of possible candidates, to enable unambiguous structural elucidation may be required. Both isolation or synthesis may represent complex or resource-intensive alternatives and a method that allowed an easier way to provide an answer would clearly be preferable. CCS Values can now be calculated *de novo* using a variety of approaches (Zhou *et al.* 2016, Nye *et al.* 2019) for metabolically plausible structures allowing their estimation in the absence of synthetic standards. If such an approach can be shown to be sufficiently accurate this information could be employed in support of putative structural identifications in the same way as calculated accurate mass and predicted fragmentation data are currently employed. Here we used an in-house program (see Nye *et al.* 2019) to calculate the CCS_{N2} values of the known metabolites of gefitinib, and then compared these values against those determined from those detected in the samples. The comparison of calculated vs measured $^{TW}CCS_{N2}$ values obtained is shown in Figure 8. As this figure shows, for most of the metabolites the correspondence for the calculated and measured $^{TW}CCS_{N2}$ values obtained provides an excellent fit to the line of unity ($R^2 = 0.96$). Clearly, this comparison indicated reasonable agreement between experimental and calculated CCS_{N2} values varying between −4.1 and +1.2% (mean absolute error = 1.4%) (see also the CCS_{N2} and observed $^{TW}CCS_{N2}$ in Table 3). As such it might be taken as a strong indication of the value of CCS in confirmation of metabolite structure. However, as we have suggested above, calculated CCS_{N2} values can also be obtained for plausible alternative metabolite structures that are nevertheless consistent with the mass of the molecular ion from the MS data. Therefore, in addition to the values for the known

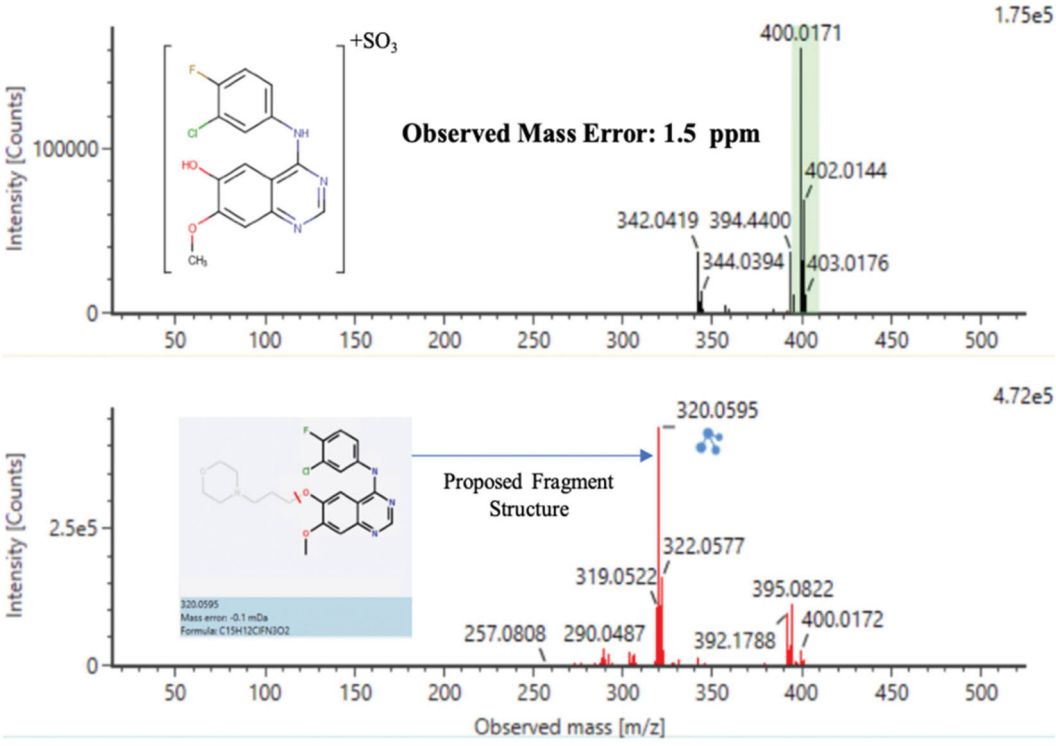

Figure 7. Mass spectral data for the sulphate conjugate (M4). The high energy fragment mass is composed of the neutral loss of the SO_3 group. The precursor and product ions are shown in the upper and lower spectra respectively.

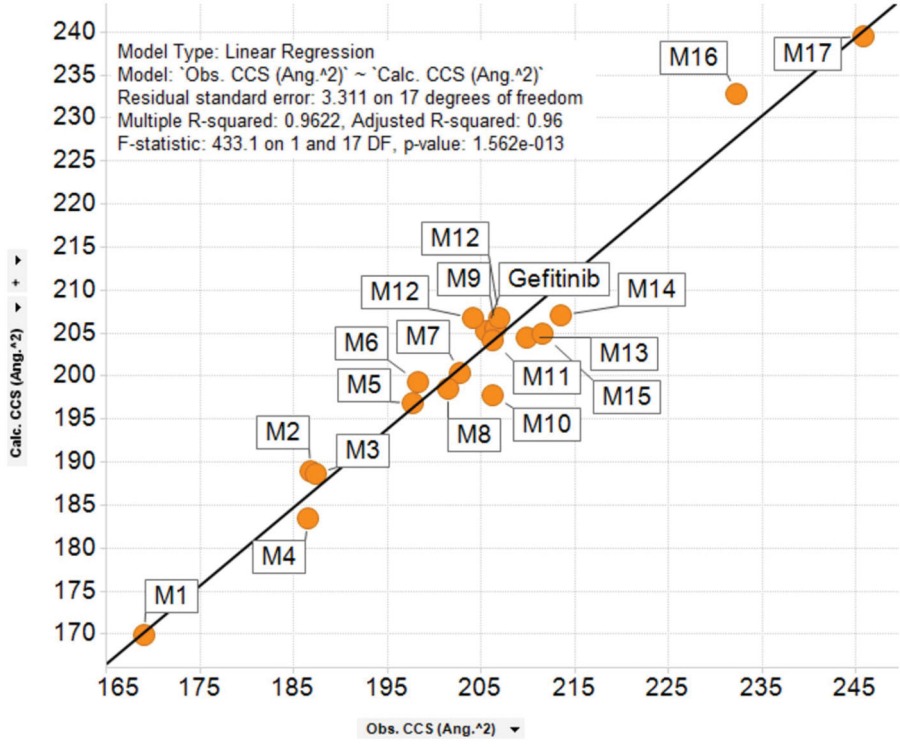

Figure 8. Regression analysis of predicted vs. experimentally observed $^{TW}CCS_{N2}$ values (as averaged across both plasma and urine sample measurements).

metabolites, for metabolically plausible structures that changed the proposed site of metabolism (e.g. hydroxylation) CCS_{N2} values were also calculated for e.g., all potential sites of hydroxylation. The values for both presumably correct identifications (with the site structurally localised by observed mass shifts evidenced in fragment ion formation) and the various alternative structures were then compared to see if their calculated CCS values could be used to discriminate between the actual and potential gefitinib metabolites. The results of this exercise are displayed in Figure S3 and were somewhat disappointing as no significant differentiation was afforded by the calculated CCS_{N2} values across

the possible sites of hydroxylation. Thus the calculated CCS_{N2} values were all within 2% relative error of one another, a cut-off that has been employed elsewhere (e.g. D'Atri *et al*. 2018, Righetti *et al*. 2018, Letertre *et al*. 2020). indicating that the calculation of CCS_{N2} values currently would not successfully distinguish outside of the measured CCS tolerance the different hydroxylation positions. However, progress in both instrumentation and calculation of CCS values is progressing rapidly and we are confident that in the near future both will be able to provide useful input into structure determination, even for complex situations such a described for gefitinib.

Conclusion

Currently, routine metabolite profiling and identification in the context of drug discovery employs LC-MS with extended analysis times (up to an hour in some cases). However, the mass spectral properties of gefitinib, combined with the knowledge of common metabolic routes of functionalisation and conjugation enabled the circulating metabolites of the drug to be profiled using the same, relatively rapid, separation employed for drug bioanalysis. For urine, to ensure that coverage was as comprehensive as possible, and mindful of the possibility that more polar metabolites than those detected in plasma might be present slightly longer separations, employing both RP- and HILIC-based profiling, were used. However, even with this combination of modes of chromatography the time taken to profile urine samples was still only 20 min. The added value, and current limitations, of IM, have also usefully been highlighted in this study and there can be no doubt that the application of this technology will increasingly become routine in metabolite profiling, first for enhancing both separations and the quality of MS data. With advancements in both IM technology and our ability to calculate CCS values with greater accuracy and precision IM may also contribute significantly to metabolite characterisation.

Disclosure statement

The authors report no declarations of interest.

ORCID

Adam King http://orcid.org/0000-0002-0819-2874
Lauren G. Mullin http://orcid.org/0000-0001-5560-933X
Lee A. Gethings http://orcid.org/0000-0003-3513-364X
Robert S. Plumb http://orcid.org/0000-0002-1380-9285
Ian D. Wilson http://orcid.org/0000-0002-8558-7394

References

Barzi, M., *et al.* 2017. A novel humanized mouse lacking murine P450 oxidoreductase for studying human drug metabolism. *Nature communications*, 8 (1), 39.

Bi, Y., *et al.* 2016. A whole-body physiologically based pharmacokinetic model of gefitinib in mice and scale-up to humans. *The AAPS journal*, 18 (1), 228–238.

Cohen, M.A., *et al.* 2004. United States Food and Drug Administration drug approval summary: gefitinib (ZD1839; Iressa) tablets. *Clinical cancer research*, 10 (4), 1212–1218.

D'Atri, V., *et al.* 2018. Adding a new separation dimension to MS and LC-MS: what is the utility of ion mobility spectrometry? *Journal of separation science*, 41, 20–67.

Dhillon, S., 2015. Gefitinib: a review of its use in adults with advanced non-small cell lung cancer. *Targeted oncology*, 10 (1), 153–170.

Guan, S., *et al.* 2019. Development and validation of a sensitive LC-MS/MS method for determination of gefitinib and its major metabolites in human plasma and its application in non-small cell lung cancer patients. *Journal of pharmaceutical and biomedical analysis*, 172, 364–371.

Jones, H.K., *et al.* 2002. A sensitive assay for ZD1839 (Iressa1) in human plasma by liquid–liquid extraction and high performance liquid chromatography with mass spectrometric detection: validation and use in Phase I clinical trials. *Journal of pharmaceutical and biomedical analysis*, 29 (1–2), 221–228.

Letertre, M., *et al.* 2020. Metabolic phenotyping using UPLC–MS and rapid microbore UPLC–IM–MS: determination of the effect of different dietary regimes on the urinary metabolome of the rat. *Chromatographia*, 83 (7), 853–861.

Li, J., *et al.* 2007. Differential metabolism of gefitinib and erlotinib by human cytochrome P450 enzymes. *Clinical cancer research*, 13 (12), 3731–3737.

Liu, X., *et al.* 2015. Metabolomics reveals the formation of aldehydes and iminium in gefitinib metabolism. *Biochemical pharmacology*, 97 (1), 111–121.

Maemondo, M., *et al.* 2010. Gefitinib or chemotherapy for non-small-cell lung cancer with mutated EGFR. *New England journal of medicine*, 362 (25), 2380–2388.

McKillop, D., *et al.* 2004a. Pharmacokinetics of gefitinib, an epidermal growth factor receptor tyrosine kinase inhibitor, in rat and dog. *Xenobiotica; the fate of foreign compounds in biological systems*, 34 (10), 901–915.

McKillop, D., *et al.* 2004b. Metabolic disposition of gefitinib, an epidermal growth factor receptor tyrosine kinase inhibitor, in rat, dog and man. *Xenobiotica*, 34 (10), 917–934.

McKillop, D., *et al.* 2004c. In vitro metabolism of gefitinib in human liver microsomes. *Xenobiotica; the fate of foreign compounds in biological systems*, 34 (11–12), 983–1000.

Mckillop, D., *et al.* 2005. Cytochrome P450-dependent metabolism of gefitinib. *Xenobiotica; the fate of foreign compounds in biological systems*, 35 (1), 39–50.

McKillop, D., *et al.* 2006. Minimal contribution of desmethyl-gefitinib, the major human plasma metabolite of gefitinib, to epidermal growth factor receptor (EGFR)-mediated tumour growth inhibition. *Xenobiotica; the fate of foreign compounds in biological systems*, 36 (1), 29–39.

Nye, L.C., *et al.* 2019. A comparison of collision cross section values obtained via travelling wave ion mobility-mass spectrometry and ultra high performance liquid chromatography-ion mobility-mass spectrometry: application to the characterisation of metabolites in rat urine. *Journal of chromatography A*, 1602, 386–396.

Rainville, P.D., *et al.* 2017. Ion mobility spectrometry combined with ultra performance liquid chromatography/mass spectrometry for metabolic phenotyping of urine: effects of column length, gradient duration and ion mobility spectrometry on metabolite detection. *Analytica chimica acta*, 982, 1–8.

Righetti, L., *et al.* 2018. Ion mobility collision cross section database: application to mycotoxin analysis. *Analytica chimica acta*, 1014, 50–57.

Rodriguez-Suarez, E., *et al.* 2013. An ion mobility assisted data independent LC-MS strategy for the analysis of complex biological samples. *Current analytical chemistry*, 9 (2), 199–211.

Spagou, K., *et al.* 2011. HILIC-UPLC-MS for exploratory urinary metabolic profiling in toxicological studies. *Analytical chemistry*, 83 (1), 382–390.

Sparidans, R.W., *et al.* 2016. Liquid chromatography-tandem mass spectrometric assay for therapeutic drug monitoring of the B-Raf inhibitor encorafenib, the EGFR inhibitors afatinib, erlotinib and gefitinib and the O-desmethyl metabolites of erlotinib and gefitinib in human

plasma. *Journal of chromatography. B, analytical technologies in the biomedical and life sciences*, 1033–1034, 390–398.

Wang, C., *et al.* 2020. Tentative identification of gefitinib metabolites in non-small-cell lung cancer patient plasma using ultra-performance liquid chromatography coupled with triple quadrupole time-of-flight mass spectrometry. *PLoS One*, 15 (7), e0236523.

Wang, L.Z., *et al.* 2011. Rapid determination of gefitinib and its main metabolite, O-desmethyl gefitinib in human plasma using liquid chromatography-tandem mass spectrometry. *Journal of chromatography. B, analytical technologies in the biomedical and life sciences*, 879 (22), 2155–2161.

Want, E.J., *et al.* 2010. Global metabolic profiling procedures for urine using UPLC-MS. *Nature protocols*, 5 (6), 1005–1018.

Zhao, M., *et al.* 2005. Specific method for determination of gefitinib in human plasma, mouse plasma and tissues using high performance liquid chromatography coupled to tandem mass spectrometry. *Journal of chromatography B*, 819 (1), 73–80.

Zheng, N., *et al.* 2016. Simultaneous determination of gefitinib and its major metabolites in mouse plasma by HPLC-MS/MS and its application to a pharmacokinetics study. *Journal of chromatography. B, analytical technologies in the biomedical and life sciences*, 1011, 215–222.

Zhou, X., *et al.* 2012. Novel liposomal gefitinib (L-GEF) formulations. *Anticancer research*, 32 (7), 2919–2924.

Zhou, Z., *et al.* 2016. Large-scale prediction of collision cross-section values for metabolites in ion mobility mass spectrometry. *Analytical chemistry*, 88 (22), 11084–11091.

Waters™

Application Note

Rapid High Sensitivity LC-MS/MS Bioanalytical Method for the Simultaneous Quantification of Gefitinib Based PROTACs – 3 and Gefitinib in Rat Plasma to Support Discovery DMPK Studies

Robert S. Plumb

Waters Corporation

This is an Application Brief and does not contain a detailed Experimental section.

Abstract

PROTACs molecules represent a new approach to candidate drug design that can overcome the drug resistance experienced by many small molecule therapies and increase access to previously undruggable proteins, whilst reducing the manufacturing costs, scale-up issues, shelf-life, stability, and storage issues associated with protein biotherapeutics. The accurate quantification of these PROTACs molecules in blood derived fluids is critical to support discovery and development DMPK packages. A rapid (4-minute) LC-MS/MS bioanalytical assay for the quantification of PROTACs-3-gefitinib and gefitinib in rat plasma was developed. The limit of detection (LOD) was determined to be 20 pg/mL for gefitinib PROTACs-3 from 10 µL sample, with a linear dynamic range of 20 pg/mL–1,000 ng/mL. The assay was subjected to a 3-day validation with CV of 5% at the LOD.

Benefits

PROTACs quantification in plasma, LC-MS/MS, DMPK, Bioanalysis.

Introduction

Proteolysis Targeting Chimeras (PROTACs) are a new class of drug molecules which work by mobilizing the ubiquitin–proteasome system to achieve proteasome-mediated degradation of the target protein via the cell machinery. PROTACs consist of three main components i) target binding moiety, ii) linker, and iii) ubiquitin E3 ligase binding moiety, Figure 1. These heterobifunctional molecules function via the binding of the target moiety to the protein of interest (POI) while E3 ubiquitin ligase is simultaneously bound by the other end of the PROTACs molecule. Binding of the POI and the ligase causes ubiquitination of the POI which is then degraded by the cellular ubiquitin-proteosome system, during which the PROTACs molecule is regenerated. These PROTACs can be considered "large small molecules" and as such share many of the attributes of small molecules, such as synthesis scale up, cost of manufacture, shelf life, stability, and route of administration. PROTACs eliminate all functions of the target protein via degradation, hence providing differentiated pharmacology, and do not require target binding moieties that inhibit protein function. They also significantly increase the number of "druggable" proteins, opening up the possibility for new safer medicines.[1,2]

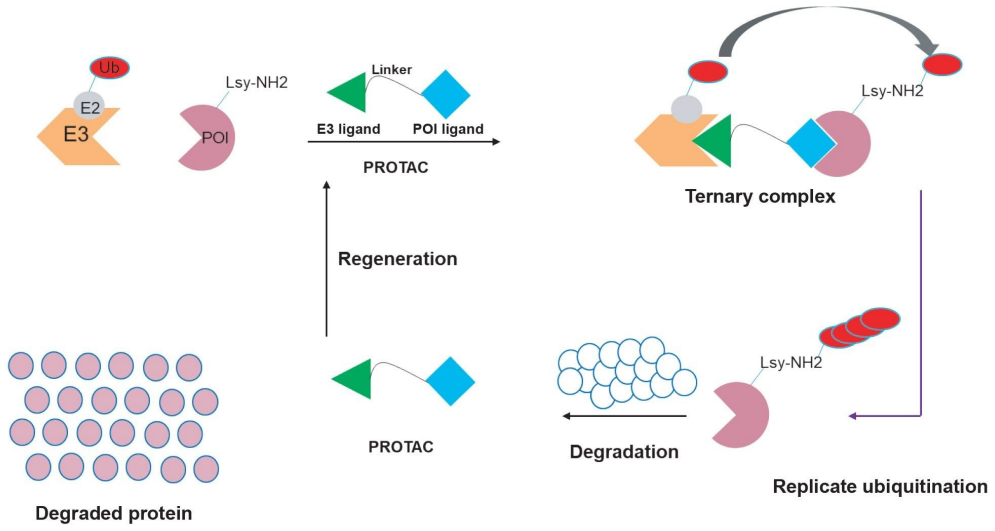

Figure 1. PROTACs catalysed protein degradation.

Gefitinib is a tyrosine kinase inhibitor for the treatment of non-small cell lung cancer, it is a potent epidermal growth factor receptor (EGFR) inhibitor which operates by interrupting cell signalling.[3] The pharmacokinetics and in vivo metabolism of gefitinib in the rat and mouse have been previously reported and showed that the compound was well absorbed with peak concentrations occurring at 1 hour, with an estimated oral bioavailability of 50–60%, and a half-life of 3.8 hours (2.6 hours for the IV route).[3,4] Previous publications have demonstrated that PROTACs molecules have a long half-life (11–15 hours) with measurable concentrations 48 hours post dose. To facilitate the determination of the pharmacokinetics of gefitinib based PROTACs-3 a high sensitivity bioanalytical method was developed for the simultaneous determination of gefitinib and gefitinib based PROTACs-3 in rat plasma over the concentration range of 20 pg/mL to 1000 ng/mL.

Experimental

Sample Description

Calibration lines were prepared by the dilution of authentic standard of gefitinib and gefitinib based PROTACs-3, Figure 2, in control Wistar rat plasma over the range of 10 pg/mL to 1,000 ng/mL. The methodology was developed and validated in accordance with the FDA Bioanalytical Method Validation Guidance for Industry, May 2018.[5] As such the volume of organic solvent from the authentic standard spiking solution was kept below 5% (v/v). Quality control samples (QCs) were prepared in a similar manner from a separate weighing of authentic standards. The plasma samples were prepared by mixing 20 µL plasma with 60 µL acetonitrile containing gefitinib-d6 as the internal standard at a concentration of 50 ng/mL in a 1.5 mL microcentrifuge tubes. The solution was vortex mixed and stored at -20 °C for 1 hour, the sample was then vortex mixed again before centrifugation at 25,000 g for 5 minutes at 4 °C. The resulting sample was transferred to an autosampler vial for analysis. Back calculated standard and QC concentrations were estimated by internal standard quantification using linear regression with a 1/x weighing.

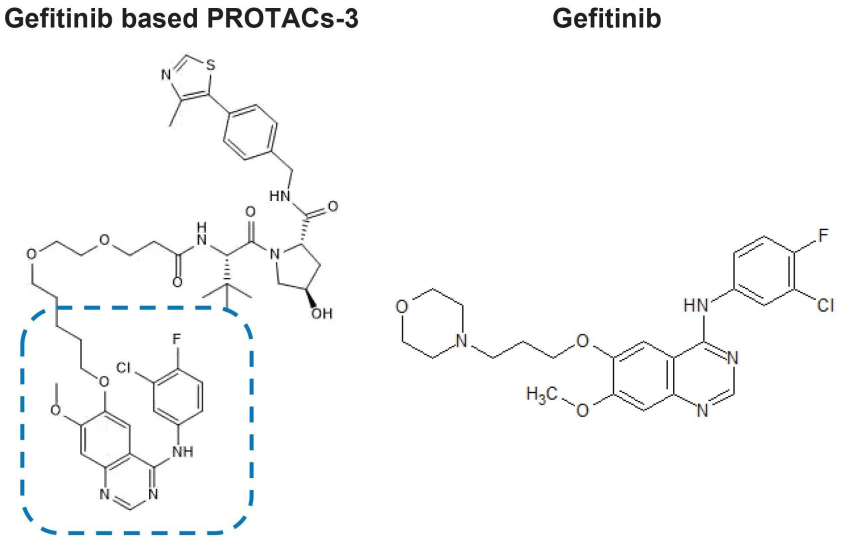

Figure 2. PROTACs-3 Gefitinib (Gefitinib component in dotted line section) and Gefitinib.

Method Conditions

Plasma extracts (2 µL) were analysed using an ACQUITY™ UPLC™ I-Class System connected to a Xevo™ TQ-XS tandem quadrupole mass spectrometer (Waters Corp., Wilmslow, UK). See Tables below for chromatographic, mass spectrometry condition, and informatics employed in this study.

LC Conditions

LC system:	ACQUITY UPLC I-Class
Vials:	TruView LCMS Certified Clear Glass Screw Neck Total Recovery Vial p/n: 186005669CV
Column(s):	ACQUITY HSS T3™ C_{18} 2.1 x 50 mm 1.7 µm Column p/n: 186009467
Column temperature:	60 °C

Sample temperature:	10 °C
Injection volume:	2 µL
Flow rate:	600 µL/min
Mobile phase A:	0.1% FA (v/v) in 1 mM aqueous ammonium formate
Mobile phase B:	0.1% FA (v/v) in ACN containing 1 mM aqueous ammonium formate
Gradient:	See below

Gradient Table

Time (min)	Flow (mL/min)	%A	%B	Curve
0	0.6	95	5	6
0.2	0.6	95	5	6
2	0.6	5	95	6
4	0.6	5	95	6
4.1	0.6	95	5	6

MS Conditions

MS system:	Xevo TQ-XS Triple Quadrupole Mass Spectrometry
Ionization mode:	positive electrospray ionisation (ESI+)
MRM transitions:	
Gefitinib based PROTACs-3:	*m/z*=934.33 > 617.34 (CV=60 V, CE=34 eV)

Gefitinib:	*m/z*=447.25 > 128.20 (CV=36 V, CE=30 eV)
Gefitinib-d6:	*m/z*=453.16 > 134.2 (CV=50 V, CE=48 eV)
Capillary voltage:	2 kV

Data Management

Acquisition software:	MassLynx™ V 4.2
Processing software:	TargetLynx™ XS

Results and Discussion

The bioanalytical method was developed for the simultaneous quantification of Gefitinib ($C_{22}H_{24}ClFN_4O_3$) and Gefitinib based PROTACs-3 ($C_{47}H_{57}ClFN_7O_8S$). The chromatographic separation was optimised to allow for the detection of the dosed compounds and the metabolites of gefitinib and gefitinib based PROTACs-3. The calibration range was evaluated from 10 pg/mL to 1,000 ng/mL in rat plasma.

Mass Spectrometry

The mass spectrometry MRM method parameters for each analyte were evaluated using the MassLynx Intellistart™ software. A 100 nL/mL solution of each analyte (50:50 acetonitrile : water, 0.1% formic acid) was infused, separately, at a flow rate of 10 µL/min (using the on board fluidics of the mass spectrometer). The precursor, productions, cone voltage, and collision energy were evaluated in both ESI+ and ESI- modes. All three analytes gave the strongest response in ESI+ mode, an example of IntelliStart optimisation report for the gefitinib based PROTACs-3 analyte is given below in Figure 3. The results show that the analyte gave rise to a protonated precursor ion with a mass to charge ratio of *m/z*=934.33, and major fragment ions were detected at *m/z*=617.34 and 182.06. The cone voltage profile for both analytes was fairly flat optimizing at 88 V for the *m/z*=617.34 ion, the optimal collision energies were determined to be 34 and 58 eV respectively. The transition *m/z*=934.17–617.34 was selected for quantification of gefitinib based PROTACs-3 due to its more intense response, gefitinib was

monitored using the transitions *m/z*=447.25–128.20 (CV=36 V and CE=30 eV) and gefitinib-d6 was monitored using the transitions *m/z*=453.29 to 134.25 (CV=50 V and CE=48 eV). The mass spectrometry acquisition conditions for gefitinib previously reported by Molly ***et-al***., using tandem quadrupole mass spectrometer were employed in the acquisition of the gefitinib concentrations and are listed above in the methodology section.[4]

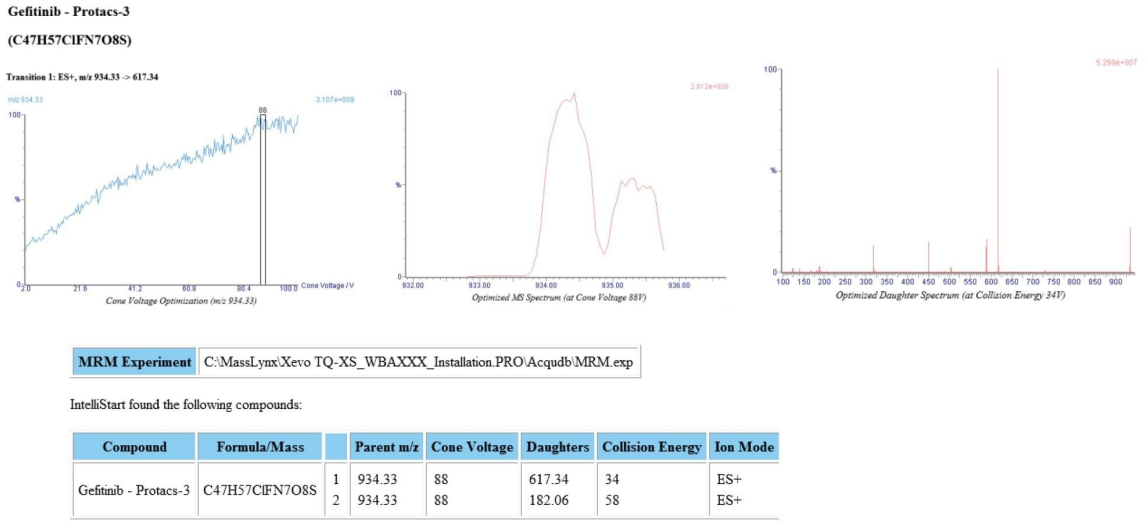

Figure 3. Intellistart Positive ion ESI MRM optimization of Gefitinib based PROTACs-3.

Chromatography

Previous investigation into the *in vivo* metabolism of gefitinib identified several polar metabolites which required the use of a reversed – phase gradient starting at a low organic composition to prevent co-elution with gefitinib. [3,4] Gefitinib based PROTACs-3, however required a high organic concentration in the mobile phase to effect elution. Thus, the chromatography was optimized for the separation of gefitinib, gefitinib based PROTACs-3 and any potential biotransformation's. The final conditions employed a ACQUITY UPLC HSS T3 Column operated at temperature 60 °C with a gradient of 5–95% acetonitrile – aqueous gradient over 2 minutes with a 2 minute hold at 95% acetonitrile, before returning to the initial conditions at 4.1 minutes, using a flow rate of 600 µL/min. Under these conditions gefitinib and gefitinib based PROTACs-3 eluted with retention times of t_R=1.40 and 1.86 min respectively. Figure 4.

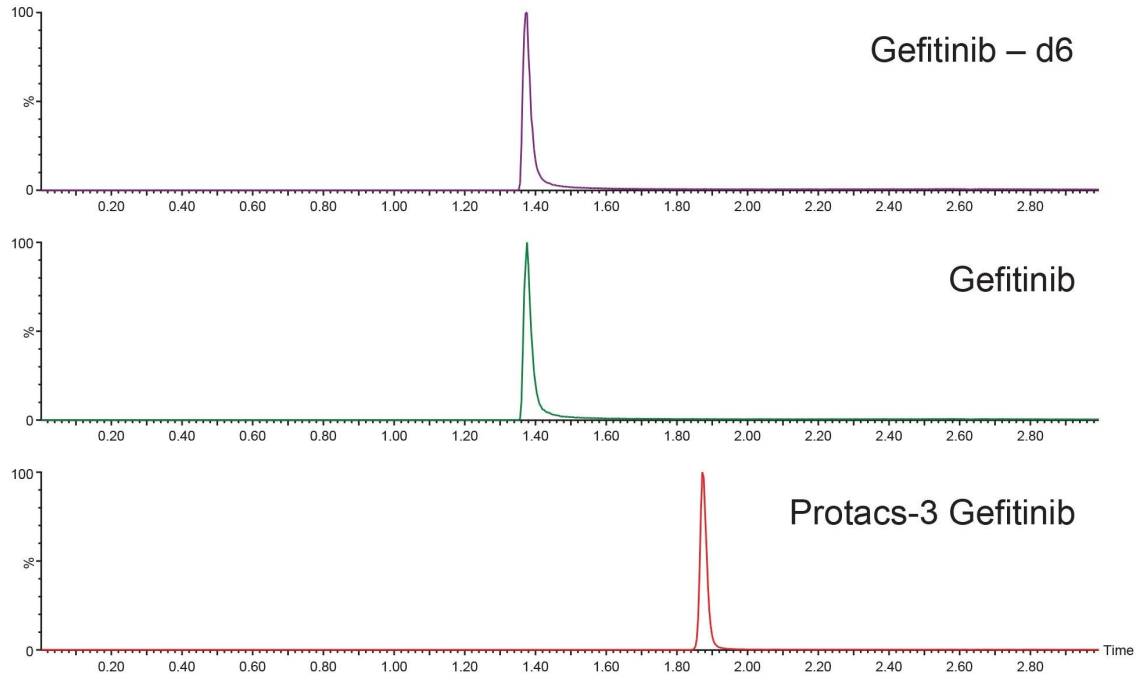

Figure 4. Positive ion LC-MS/MS analysis of gefitinib based PROTACs-3, gefitinib-d6 and gefitinib using a 2.1 x 50 mm ACQUITY HSS T3 1.7 µm C_{18} Column, maintained at 60 °C and eluted with a 5–95% aqueous – acetonitrile 1 mM ammonium formate, 0.1% formic acid gradient over 2 minutes with a 2 minute hold.

Sample Preparation

The plasma samples were prepared by protein precipitation using 1:3 ratio of sample (20 µL) to organic solvent, as detailed above.

Calibration Range

The lower limit of detection (LLoD) and usable linear dynamic range of the gefitinib based PROTACs-3 method was evaluated over the range of 10 pg/mL to 1,000 ng/mL. The limit of detection in rat plasma was determined to be 20 pg/mL (2.5 fg on column), a representative chromatogram is given in Figure 5. The calibration line was determined to be linear over approximately 5 orders of magnitude (20 pg/mL–1,000 ng/mL) using internal standard quantification and 1/x weighting. A representative calibration line is presented in Figure 6, the correlation coefficient was determined to be r^2=0.998, with a negative intercept of -152.165.

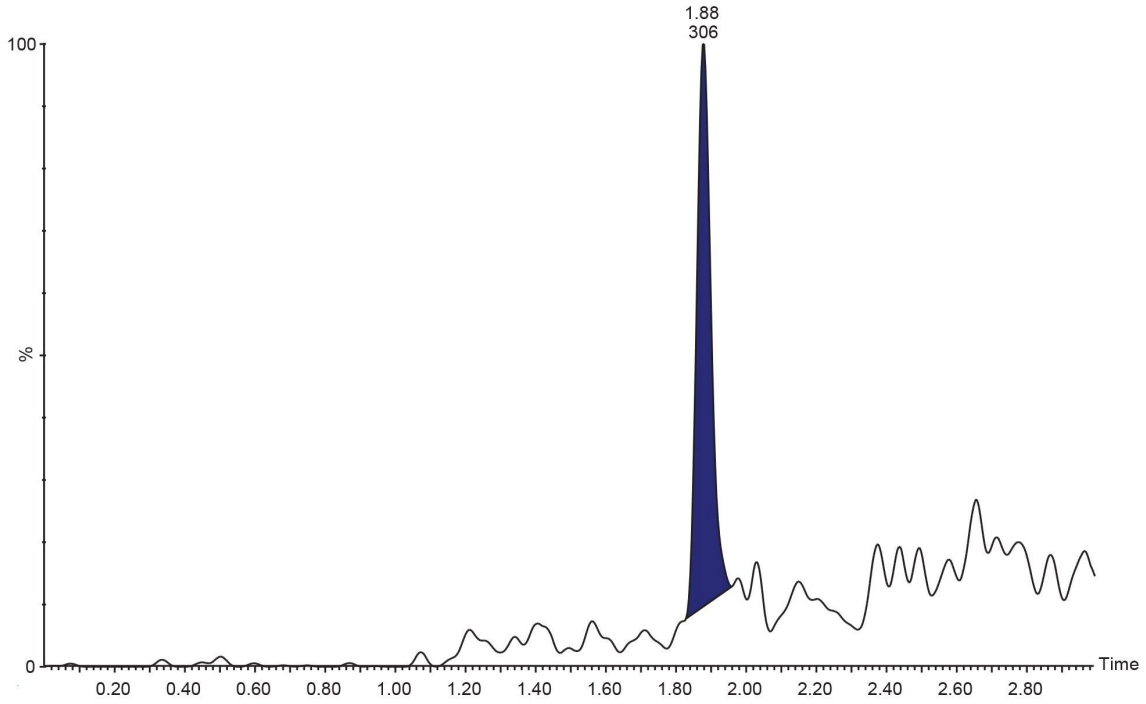

Figure 5. Positive ion LC-MS/MS analysis of gefitinib based PROTACs-3 20 pg/mL standard using a 2.1 x 50 mm ACQUITY HSS T3 1.7 µm C_{18} Column, maintained at 60 °C and eluted with a 5–95% aqueous – acetonitrile 1 mM ammonium formate, 0.1% formic acid gradient over 2 minutes with a 2 minute hold.

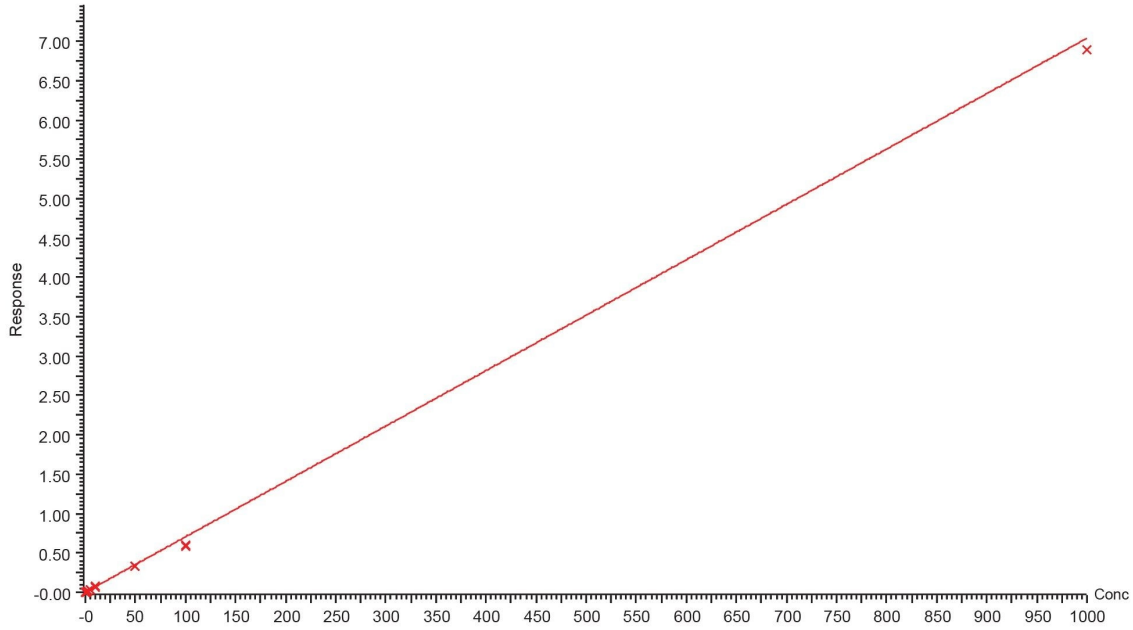

Figure 6. Gefitinib based PROTACs–3 calibration line from 20 pg/mL to 1000 ng/mL.

The limit of detection for gefitinib was determined to be 0.05 ng/mL, with a correlation coefficient of 0.997, a typical calibration line and LOQ standard for gefitinib in rat plasma extract are given in Figure 7.

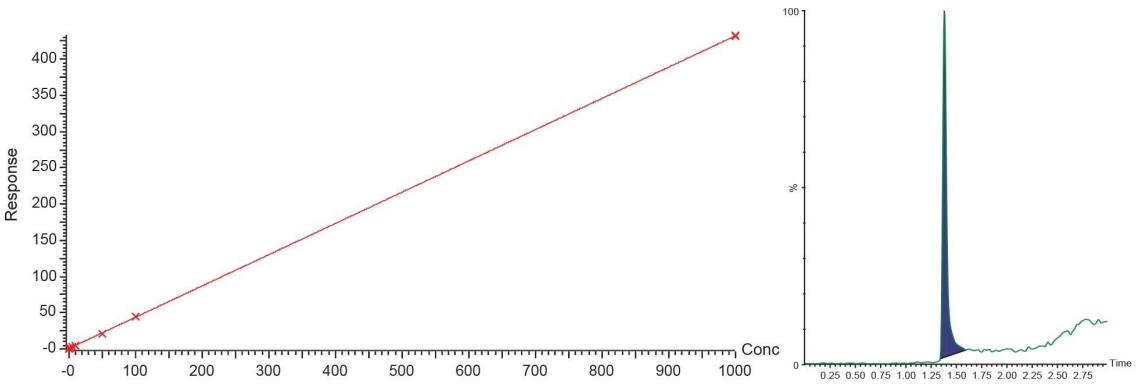

Figure 7. Gefitinib calibration line from 0.5 to 1000 ng/mL and LOQ standard (0.5 ng/mL).

3-Day Validation

Previous studies have shown that gefitinib is well absorbed following PO administration (mouse and rat) with peak plasma concentration being observed at the 1-h time point, with maximum concentration values of 7 µg/mL were obtained for 50 mg/kg dose to the mouse.[4] Plasma concentrations rapidly decline with a half-life 3.8-h with virtually no drug being detectable after 24-h post dose. Thus, for a typical pre-clinical safety assessment study where dose levels typically vary from 1–10 mg/kg an analytical concentration range of 0.5–1000 ng/mL was selected for validation, the bioanalytical method for both gefitinib and gefitinib based PROTACs-3 was subject to a 3 day validation. Samples were analysed in three batches over three days in the following order; solvent blank; blank; calibration curve (0, 0.5, 1, 2, 5, 10, 20, 50, 100, 500, and 1000 ng/mL); matrix blank; QCs (3, 75, 800 ng/mL) samples; blank; extracted plasma samples; QCs (3, 75, 800 ng/mL); blank; calibration curve (0, 0.5, 1, 2, 5, 10, 20, 50, 100, 500, and 1000 ng/mL); blank. The three-day validation showed excellent reproducibility and accuracy for both compounds, Tables 1 and 2.

Sample (ng/mL)	Mean	Standard deviation	%CV
Std 0.5	0.57	0.05	16.1
Std 1	1.05	0.14	12.5
Std 2	1.93	0.16	4.37
Std 5	5.00	0.72	2.90
Std 10	9.23	1.47	1.72
Std 50	48.0	6.34	0.28
Std 100	83.1	8.06	0.12
Std 1000	1020	131	0.01
QC 3	2.95	0.33	11.2
QC 75	67.6	7.34	10.9
QC 800	780	110	14.1

Table 1. Summary of gefitinib based PROTACs-3 quantification in 3-day validation (in total 6 analysis of each standard and QC).

Sample (ng/mL)	Mean	Standard deviation	%CV
Std 0.5	0.53	0.08	15.3
Std 1	0.97	0.05	5.34
Std 2	1.87	0.08	4.37
Std 5	4.95	0.15	3.06
Std 10	9.55	0.24	2.46
Std 50	49.5	1.24	2.51
Std 100	105	4.40	4.21
Std 1000	997	22.5	2.25
QC 3	3.59	0.24	6.74
QC 75	76.1	5.02	6.60
QC 800	812	26.8	3.30

Table 2. Summary of gefitinib quantification in 3-day validation for all data (in total six analysis of each standard and QC).

The freeze-thaw stability of both gefitinib and gefitinib based PROTACs-3 was determined by the analysis of QC samples 3, 75, and 800 ng/mL, the samples were analysed directly following preparation and then following three freeze-thaw cycles at -20°C. The results showed that the measured concentrations % accuracy ranged from 102.9–108.1 for gefitinib to 69.7–109.1% for gefitinib based PROTACs-3.

Conclusion

Proteolysis Targeting Chimeras (PROTACs) use protein targeting ligand linked to a ubiquitin E3 ligase binding

moiety to effect proteasome mediated degradation of a target protein and have molecular weights in the 700–1000 Da range. As part of drug discovery and development, the DMPK characteristics of process PROTACs molecules needs to be determined, in a similar manner to all small molecules and biologics; thus a high sensitivity bioanalytical assay is needed. A reversed – phase gradient LC-MS/MS bioanalytical method was developed and validated for the quantification of gefitinib based PROTACs-3 in rat plasma, using the Waters tandem quadrupole mass spectrometer. The limit of detection was determined to be 20 pg/mL (2.5 fg on column) with a dynamic range on 0.02–100 ng/mL. The method was subject to a three day validation over the range of 1–1,000 ng/mL.

References

1. Bhole RP, Kute PR, Chikhale RV, Bonde CG, Pant A, Gurav SS. PROTACs: A Comprehensive Review of Protein Degradation Strategies in Disease Therapy. ***Bioorg Chem***. 2023;139:106720. doi: 10.1016/j.bioorg.2023.106720.
2. Békés M, Langley DR, Crews CM. PROTAC Targeted Protein Degraders: The Past Is Prologue. ***Nat Rev Drug Discov***. 2022;21(3):181–200. doi: 10.1038/s41573-021-00371-6.
3. McKillop D, Hutchison M, Partridge EA, Bushby N, Cooper CM, Clarkson-Jones JA, Herron W, Swaisland HC. Metabolic Disposition of Gefitinib, an Epidermal Growth Factor Receptor Tyrosine Kinase Inhibitor, in Rat, Dog and Man. ***Xenobiotica***. 2004;34(10):917–34. doi: 10.1080/00498250400009171.
4. Molloy B, Mullin L, King A, Gethings LA, Plumb RS, Wilson ID. The Pharmacometabodynamics of Gefitinib After Intravenous Administration to Mice: A Preliminary UPLC-IM-MS Study. ***Metabolites***. 2021 11;11(6):379. doi: 10.3390/metabo11060379.
5. https://www.fda.gov/files/drugs/published/Bioanalytical-Method-Validation-Guidance-for-Industry.pdf < https://www.fda.gov/files/drugs/published/Bioanalytical-Method-Validation-Guidance-for-Industry.pdf>

Featured Products

ACQUITY UPLC I-Class PLUS System <https://www.waters.com/134613317>

Xevo TQ-XS Triple Quadrupole Mass Spectrometry <https://www.waters.com/134889751>

MassLynx MS Software <https://www.waters.com/513662>

TargetLynx <https://www.waters.com/513791>

720008229, January 2024

Contact us

Editorial Department

editor@bioanalysis-zone.com

Business Development and Support

advertising@future-science-group.com

This supplement is brought to you by Bioanalysis Zone in association with

Waters™